DEPARTEMENT DE PHYSIQUE
DEPARTMENT OF PHYSICS

ATTESTATION DE CORRECTION DE LA THESE DE DOCTORAT/PhD

Nous, Professeurs **NDJAKA Jean Marie Bienvenu, BEN-BOLIE Germain Hubert, DJUIDJE KENMOE Germaine épse ALOYEM, NDONTCHUENG MOYO Maurice** et Professeur **OWONO OWONO Luc Clavin**, respectivement Examinateurs et Président du jury de la thèse de Doctorat/PhD de Monsieur **HAMADOU Issa** Matricule **09W0552**, préparée sous la co-direction du Professeur **SAÏDOU** et du Professeur **OUMAROU BOUBA,** intitulée : « **DOSIMETRIE INTERNE DU ^{219}Rn UTILISANT LA MODELISATION BIOCINETIQUE**», soutenue le mercredi, 05 janvier 2022, en vue de l'obtention du grade de Docteur/Ph.D en Physique, Spécialité **Physique des Rayonnements et Biophysique**, attestons que toutes les corrections demandées par le Jury de soutenance ont été effectuées.

En foi de quoi, la présente attestation lui est délivrée pour servir et valoir ce que de droit.

Fait à Yaoundé le ……1 2 JAN 2022…….

Examinateurs

Le Président du Jury

Pr. NDJAKA J. M. B.

Pr. BEN-BOLIE G. H.

Pr. OWONO OWONO L. C.

Pr. DJUIDJE KENMOE G. A.

Pr. NDONTCHUENG MOYO M.

Le Chef de Département de Physique

UNIVERSITE DE YAOUNDE I
******
CENTRE DE RECHERCHE ET DE FORMATION DOCTORALE EN SCIENCES TECHNOLOGIES ET GEOSCIENCES
******
Unité de Recherche et de Formation Doctorale en Physique et Applications

UNIVERSITY OF YAOUNDE I
******
POSTGRADUATE SCHOOL OF SCIENCE, TECHNOLOGY, AND GEOSCIENCES
******
Research and Training Unit for Doctorate in Physics and Applications

DEPARTMENT OF PHYSICS
DEPARTEMENT DE PHYSIQUE

Laboratory of Nuclear, Atomic, Molecular Physics and Biophysics
Laboratoire de Physique Nucléaire, Atomique, Moléculaire et Biophysique

---

Internal dosimetry of ^{219}Rn using biokinetic modelling

Thesis Submitted in Partial Fulfillment of the Requirements for the award of the Degree of Doctorate/Ph.D. in Physics

Option: Nuclear Physics, Dosimetry and Radiation Protection
***Option** : Physique Nucléaire, Dosimétrie et Radioprotection*

By:

HAMADOU Issa
Registration number: **09W0552**
M.Sc. in Physics

Directors:

SAÏDOU

Associate Professor

University of Yaounde I

OUMAROU Bouba

Associate Professor

University of Yaounde I

Year 2021

This thesis is dedicated to my parents.

For their endless love, support and encouragement.

ACKNOWLEDGEMENTS

- I also thank Professor VONDOU DERBETINI APPOLINAIRE and Doctor ABDOURAHIMI for their teaching, encouragement and their moral support.

- I specially express my acknowledgement to the staff of the Department of Physics, Faculty of Science, University of Yaounde I for their lectures during my higher education. My sincere thanks also go to the Postgraduate School of Science, Technology and Geosciences.

- I would like to thank Professor ALIM, Head of the Department of Physics at the Higher Teachers' Training College of the University of Maroua, for his support and encouragement and all teachers of this department, namely Professor NSANGOU MAMA, Professor MAHAMAT SALEH, Professor EMA'A EMA'A JEAN MARIE, Professor DIFFO TCHINDA JAURÈS, Doctor BACHIROU BOGNO, Doctor BOUBA APOLLINAIRE, Doctor FOTSING TALLA CYRILLE, Doctor MIBAILE JUSTIN and M. BOUBAKARY ABDOU for their warm welcome (as ATER), sympathy and endless support.

- For his moral support and encouragement during my PhD studies I am grateful to my Academic elder M. ATANGANA BINGANA MARTIN SERGE with whom I work.

- I thank Doctor TAKOUKAM SOH SERGE DIDIER, Doctor BINENG GUILLAUME SAMUEL, Doctor NGA ONGODO and M. MBIDA SERGE my academic elders for their encouragement during my thesis.

- My sincere thanks go to the editors and referees of Journal of Radiation Research, for their detailed review, constructive criticism and excellent advice during the preparation of my publication

- This work could not have been possible without the participation and assistance of so many people whose names may not all be enumerated their contributions are sincerely appreciated and gratefully acknowledged. However, I would like to express the deep appreciation particularly to the following: M. MANY MANDA BERTIN, M. NNOMO MANGA RICHARD, M. YIA ETOLO DIDIER, M. WAGOUM DJOUSSI RUFFIN CHRYSAL, M. GUEPSI MBOUDJE MERLIN, M. SEINI YAOUBA and M. DOMGNO KUIPOU WILLIAM for their support.

- I would like to show my gratitude and my love to my family for their support and love through the duration of my Ph.D. cycle. One of the most important motivations to achieve

my Ph.D. has been to make you proud.

• To all relatives, friends and others who in one way or another shared their support, either morally, financially and physically, thank you.

Table of Contents

List of Tables

List of Figures

ABSTRACT

During cancer treatment with isotope of ^{223}Ra, the short-lived radioactive radon isotope ^{219}Rn may be exhaled by the patient. Hospital employees and member of the public may inhale this radionuclide and its decay products. Therefore, it is important to quantify organ doses of actinon progeny exposure. The purpose of this study is to use biokinetics and dosimetric models to assess dose coefficients for actinon progeny. The methodology, the biokinetics and dosimetric models used for calculation of the inhalation doses to actinon progeny were described. The effective dose coefficients were calculated separately for three modes. Those three modes are: the unattached mode which concerned the Activity Median Thermodynamic Diameter (AMTD) of 1 nm, the nucleation and accumulation modes which are represented by the Activity Median Aerodynamic Diameter (AMAD) of 60 nm and 500 nm respectively. The recent biokinetic models of actinon progeny developed in the Occupational Intakes of Radionuclides (OIR) publications series of the International Commission of Radiological Protection (ICRP) were implemented on BIOKMOD (Biokinetic Modeling) to calculate the number of nuclear transformations per activity intake of actinon progeny. The organ equivalent and effective dose coefficients were determined using the dosimetric approach of the ICRP. The inhalation dose coefficients of actinon progeny are dominated by the contribution of lung dose. The dose coefficients of ^{211}Pb and ^{211}Bi calculated are 5.78×10^{-8} Sv.Bq^{-1} and 4.84×10^{-9} Sv.Bq^{-1} for unattached particles (AMTD=1nm) and, 1.4×10^{-8} Sv.Bq^{-1} and 3.55×10^{-9}Sv.Bq^{-1} for attached particles (AMAD=60 nm), and 7.37×10^{-9}Sv.Bq^{-1} and 1.91×10^{-9}Sv.Bq^{-1} for attached particles (AMAD=500 nm). These values are much closer to those of the recently published ICRP-137.

Keywords: Actinon, Internal dosimetry, ^{211}Pb; ^{211}Bi; inhalation; biokinetic models; dosimetric models; dose coefficient

RESUME

Lors du traitement de la metastase osseuse du cancer de la prostate utilisant le ^{223}Ra, l'isotope radioactif du radon ^{219}Rn de courte demi-vie peut être expiré par le patient. Les employés de l'hôpital et les membres du public peuvent inhaler ce radionucléide et ses descendants. Par conséquent, il est important de quantifier les doses suite à l'inhalation des descendants de l'actinon. Le but de cette étude est d'utiliser les modèles biocinétiques et dosimétriques pour évaluer les coefficients de dose des descendants de l'actinon. La méthodologie, les modèles biocinétiques et dosimétriques utilisés pour le calcul des doses par inhalation des descendants de l'actinon ont été décrits. Les coefficients de dose ont été calculés séparement pour trois modes. Ces trois modes sont: le mode des particules non attachées qui concerne le diamètre thermodynamique médian d'activité (DTMA) de 1 nm, les modes de nucléation et accumulation qui sont representés par le diamètre aérodynamique médian d"activité (DAMA) de 60 nm et 500 nm respectivement. Les modèles biocinétiques du plomb et bismuth récemment développés et publiés dans la série de publications intitulée "Occupational Intakes of Radionuclides" de la CIPR ont été implementés sur BIOKMOD pour calculer le nombre de transformations nucléaires par activité incorporée des descendants de l'actinon. Les doses equivalentes et les coefficients de dose ont été déterminés en utilisant l'approche dosimétrique de la CIPR. Les coefficients de dose par inhalation des descendants de l'actinon sont tous dominés par la contribution de la dose pulmonaire. Les coefficients de dose du ^{211}Pb and ^{211}Bi calculés sont de $5{,}78 \times 10^{-8}$ Sv.Bq^{-1} et $4{,}84 \times 10^{-9}$ Sv.Bq^{-1} pour les particules non attachées (DTMA=1 nm), $1{,}4 \times 10^{-8}$ Sv.Bq^{-1} et de $3{,}55 \times 10^{-9}$Sv.Bq^{-1} pour les particules attachées (DAMA=60 nm), et de $7{,}37 \times 10^{-9}$Sv.Bq^{-1} et $1{,}91 \times 10^{-9}$Sv.Bq^{-1} pour les particules de DAMA= 500 nm. Ces valeurs sont très proches de celles récemment publiées par la CIPR-137.

Mots clés: Actinon, Dosimétrie interne, ^{211}Pb; ^{211}Bi; inhalation; modèles biocinétiques; modèles dosimétriques; coefficient de dose

General introduction

According to the World Health Organization (WHO), the second largest cause of lung cancer is radon. Among non-smokers, radon is the largest cause of lung cancer. People exposed to radon have an increased risk of lung cancer. Radon was identified as a health problem since miners from the underground uranium who were exposed to it died of lung cancer at high rates [1]. It is almost present in all air. Everyone breathes in radon every day, usually at very low levels. There are three natural isotopes of radon, namely: radon (^{222}Rn), thoron (^{220}Rn) and actinon (^{219}Rn). In contrast to ^{222}Rn (3.8 days) and ^{220}Rn (55.6 s), which leave the soil and building materials and enter the atmosphere, ^{219}Rn due to its very short half-life (3.96 s) is generally less able to emanate from mineral matrices. Because of typically very low concentrations in the ambient air exposure to ^{219}Rn and its progeny are usually neglected. Thus, the measurement of ^{219}Rn has not been described in standards such as ICRP and ICRU [2, 3]. Recently in hospitals the cancer treatment with ^{223}Ra (Xofigo) was introduced [4]. ^{223}Ra is injected to the patient to fight against bone metastasis of prostate cancer. In the decay chain the radon isotope ^{219}Rn occurs which may be exhaled by the patient [5]. Secondary exposure of care-takes in the hospital and at home may happen by inhalation of ^{219}Rn and its decay products. Actinon is a radioactive noble gas and a decay product of ^{223}Ra in the ^{235}U decay chain. ^{219}Rn decay through the short-lived progeny ^{215}Po, ^{211}Pb, ^{211}Bi and ^{207}Tl to the stable nuclide ^{207}Pb.

The inhaled and deposited radionuclide can damage the respiratory epithelium through the alpha-particle emissions [6, 7]. The damage to the epithelial cells of the lung occurs when radiation damages either directly DNA in the cell nucleus or indirectly through the attack of the free radicals [8]. Instruments and techniques exist to measure fields of penetrating radiation such as, X-rays or gamma rays, that are external to the body and provide a mean for directly quantifying the amount of energy deposited per unit mass of material (air, tissue, and water). These measurements can then be related to a person present in the radiation field and the radiation dose that person would receive. In the case of internally deposited radionuclide, however, direct measurement of the energy emitted from the radionuclide is rarely, if ever, possible. Therefore,

one must rely on dosimetric models to obtain estimates of the spatial and temporal patterns of energy deposition in tissues and organs of the body. In the simplest case, when the radionuclide is uniformly distributed throughout the volume of a tissue, which is large compared with the range of the particulate emissions of the radionuclide, then the dose rate within the tissue is also uniform and calculation of absorbed dose can proceed without complication. However, if nonuniformities in the spatial and temporal distributions of radionuclide are coupled with heterogeneous tissue composition, then calculation of absorbed radiation dose becomes complex and uncertain [3].

Internal and external exposure of workers and members of the public are commonly estimated in terms of the protection quantity, effective dose. Nevertheless, after intake of radionuclides, organs and tissues receive extended doses; whereas, equivalent and effective dose are multiplied over time. The resulting quantities form committed doses. Internal exposure of workers and members of the public is therefore determined in terms of committed effective dose [9].

Whereas many papers have been published on dosimetric studies of radon, thoron and their decay products, the ICRP has published inhalation dose coefficients of actinon progeny (^{211}Pb and ^{211}Bi) using the size characteristic of radon progeny [2]. Stabin et al. have also assessed dose coefficients for actinon progeny in a particular situation of exposure and for one particles size mode (AMAD 5 μm) [10]. The purpose of this study is to determine the inhalation dose coefficients for actinon progeny. Furthermore, this approach could be used to also determine the dose conversion coefficient of actinon progeny for a real situation of secondary exposures of nurses at hospitals or the members of public at home.

There are several piece of software for internal dose assessment. However, most of them are commercialized. In the present work, the models for inhalation of actinon progeny have been mathematically implemented using a freely available package ICRP130Models on the recent version of BIOKMOD (version 5.4), and a dosimetric method is established to evaluate inhalation dose of actinon progeny using Microsoft Excel [11]. To make it effective, effective doses and organ equivalent doses in lung and in other organs of inhaled ^{219}Rn progeny such as ^{211}Pb and ^{211}Bi were determined separately as a function of particle size distribution of three modes, using human respiratory tract model (HRTM), human alimentary tract model (HATM) and systemic models developed by ICRP [2, 7, 12].

This research thesis is set up in three chapters. The first chapter briefly presents some important phenomena which are fundamental to internal exposure, the second chapter presents materials and methods used for internal dose assessment following inhalation of actinon progeny and the

third chapter presents some results and the discussion of those results.

Chapter 1

Literature review

Introduction

Radiation is energy, in the form of particles or electromagnetic rays, released generally from radioactive atoms. The three most common types of radiation are alpha particles, beta particles and gamma rays. Radiation is classified in two types; ionizing and non ionizing radiations. This study is focused on ionizing radiation. In contrast to non ionizing, ionizing radiation has enough energy to produce ions by removing an electron from an atom. The exposure to radiation is called irradiation. Irradiation occurs when all or part of the body is exposed to radiation from a source. Irradiation can lead to gene mutations and increases the risk of cancer (long term exposure) or radiation sickness depending on the amounts of radiation. This chapter briefly describes some important phenomenona and quantites which explain radiation exposure.

1.1 Radioactivity

Radioactivity could be defined by the phenomenon of the emission of ionizing radiation or particles caused by spontaneous disintegration of atomic nuclei or is the process by which an unstable atomic nucleus loses energy by emitting radiation. Radioactive material is usually not described in terms of its mass or volume. Instead, the amount of radioactive material present is communicated in terms of how quickly the material decays, or its activity. In the International System of Units (SI), the units of activity is the Becquerel (Bq). One Becquerel is defined to be one decay or disintegration per second. The Curie (Ci) is another common unit of radioactivity. It is defined as 3.7×10^{10} disintegrations per second. Suppose N is the size of a population of radioactive atoms at a given time t and dN is the amount by which the population decreases in

time dt; then the rate of change is given by the equation below[13]:

$$A(t) = -\frac{dN(t)}{dt} = \lambda \times N(t) \tag{1.1}$$

where λ is the decay constant (s^{-1}) and $A(t)$ is the activity at the time t of the size of a population of radioactive atoms (Bq). The solution of this differential equation is given by:

$$N = N_0 exp(-\lambda t) \tag{1.2}$$

where N_0 is the size of an initial population of radioactive atoms at time $t = 0$. The time required for half of the original population of radioactive atoms to decay is called the half-life, denoted $T_{1/2}$ (s). The relation between $T_{1/2}$ and λ is given by:

$$T_{1/2} = ln2/\lambda \tag{1.3}$$

Each unstable radioactive atom decays by emitting ionizing radiation. There are four major types of radiations; alpha (α), beta (β) electromagnetic waves such as gamma rays (γ) and neutrons. They differ in mass, energy and how they penetrate matter.

1.1.1   Alpha particles (α)

Alpha particles come from the decay of heavy nuclei, whose atomic number is greater than 82 [14].These particles consist of two protons and two neutrons and are the heaviest type of radiation particle. The naturally occurring radioactive materials in the environement, like uranium and thorium, emit alpha particles. The most common alpha emitter in our homes is radon. The general equation describing the decay of a parent nuclei $_Z^A X$ (A: mass number and Z: atomic number) to a nuclei $_{Z'}^{A'} Y$ by emitting alpha particle is given by [13]:

$$_Z^A X \rightarrow _{Z-2}^{A-4} Y + _2^4 He \tag{1.4}$$

where $_2^4 He$ represents the helium atom which is the α particle. α travels a very short distance through air and is not able to penetrate skin. Alpha-emitting materials can be harmful to human if the materials are inhaled, ingested or injected through open wounds.

1.1.2 Beta particles (β)

Beta particles (β) are high energy, high speed electrons (β^-) or positrons (β^+) that are ejected from the nucleus by some radionuclides during a form of radioactive decay called beta decay [15]. Beta particles are much less ionizing than alpha particles and generally do less damage for a given amount of energy deposition. They typically have ranges of tens of centimetres in air (energy dependent) and a few millimetres in the matter. In electron emission also called negative beta decay (symbolized β^- decay), an unstable nucleus emits an energetic electron and an antineutrino, and a neutron in the nucleus becomes a proton that remains in the products nucleus. Thus, negative beta decay results in a daughter nucleus, the proton number (atomic number) of which is one more than its parent but mass number is the same. The energy lost by the nucleus is shared by the electron and the antineutrino. In positive emission called positve beta decay (β^+ decay), a proton in the parent nucleus decays into a neutron that remains in the daughter nucleus, and the nucleus emits a neutrino and a positron, which is a positive particle like electron in mass but of opposite charge. Thus, positive beta decay produces a daughter nucleus, the atomic number of which is one less than its parent and the mass number is the same. The equations describing beta decays are given below [13]:

$$\ _Z^A X \rightarrow\ _{Z+1}^A Y +\ _{-1}^0 e + \overline{\nu}_e \tag{1.5}$$

$$\ _Z^A X \rightarrow\ _{Z-1}^A Y +\ _1^0 e + \nu_e \tag{1.6}$$

where equations 1.5 and 1.6 represent respectively negative beta (β^-) and positive beta (β^+), and $\overline{\nu}_e$ and ν_e are antineutrino and neutrino respectively.In comparison with other forms of radioactivity such as gamma or alpha, beta decay is a relatively slow process. Half-lives for beta decay are never shoter than a few milliseconds.

1.1.3 gamma rays (γ)

A third type of natural radiation, gamma radiation, usually accompanies alpha or beta decay. Gamma radiation and X-rays are electromagnetic radiation like visible light radio waves and ultra violet light. These electromagnetic radiations differ only in the amount of energy they have. Gamma rays are the most energetic of these. This radiation is able to travel many meters in air and many centimeters in human tissue. It readily penetrates most materials. Gamma

emission may occur as the excited states transform to lower energy states of the same nucleus. In some cases an excited nucleus may transform to a lower energy state by ejecting an electron from the cloud surrounding the nucleus. This orbital electron ejection is known as internal conversion and gives rise to an energetic electron and often an X-rays as the atomic cloud falls in the empty orbital of the ejected electron [14]. The general equation describing gamma decay of a nucleus $_Z^A Y$ is given by [15]:

$$_Z^A Y^* \rightarrow _Z^A Y + \gamma \tag{1.7}$$

1.2   Natural decay chains

Radioactive series consist of four independent sets of unstable heavy radionuclides that decay through alpha and beta decays processes until a stable nucleus achieved. The consecutive parents and daughters nuclei begin and end among elements with atomic numbers around 93 and 81 [13]. The three of the sets are the thorium (Th) series, uranium (U) and actinium series, called natural series [13]. They are headed by naturally occuring species of unstable nuclei that have half-lives comparable to the age of the element. The fourth series is the neptunium (Np) chain which is headed by neptunium-237 has a half-life of 2,000,000 years. Its progenies are produced artificially by nuclear reactions and do not occur naturally. In each radioactive chain the decay processes are alpha and beta emissions (sometimes gamma), causing sometimes changes or not of four units in the mass number. The mass numbers of all the members of each series are divisible by four, with a constant remainder [14]. Therefore, the mass number of the members may be expressed as four times an appropriate integer (n) plus the constant for that series. The thorium series is sometimes called the $4n$ series, the neptinunium series, $4n + 1$; the uranium series $4n + 2$ and the actinium series $4n + 3$ series. The thorium series starts with thorium-232 and ends with the stable nuclide lead-208 [13]. The first element in the neptunium series is neptunium-237 and the series ends up with bismuth-209. The uranium series starts with uranium-238 and ends with stable lead-206. The name actinium series was given because actinium-227 was the first discovered element in this series. It begins with uranium-235 and ends with stable lead-207. Figures 1, 2 and 3 present thorium, uranium and actinium series respectively. According to ICRU radon is a ubiquitous natural radionuclide which can be found everywhere [3]. It is the most common element found in our houses.
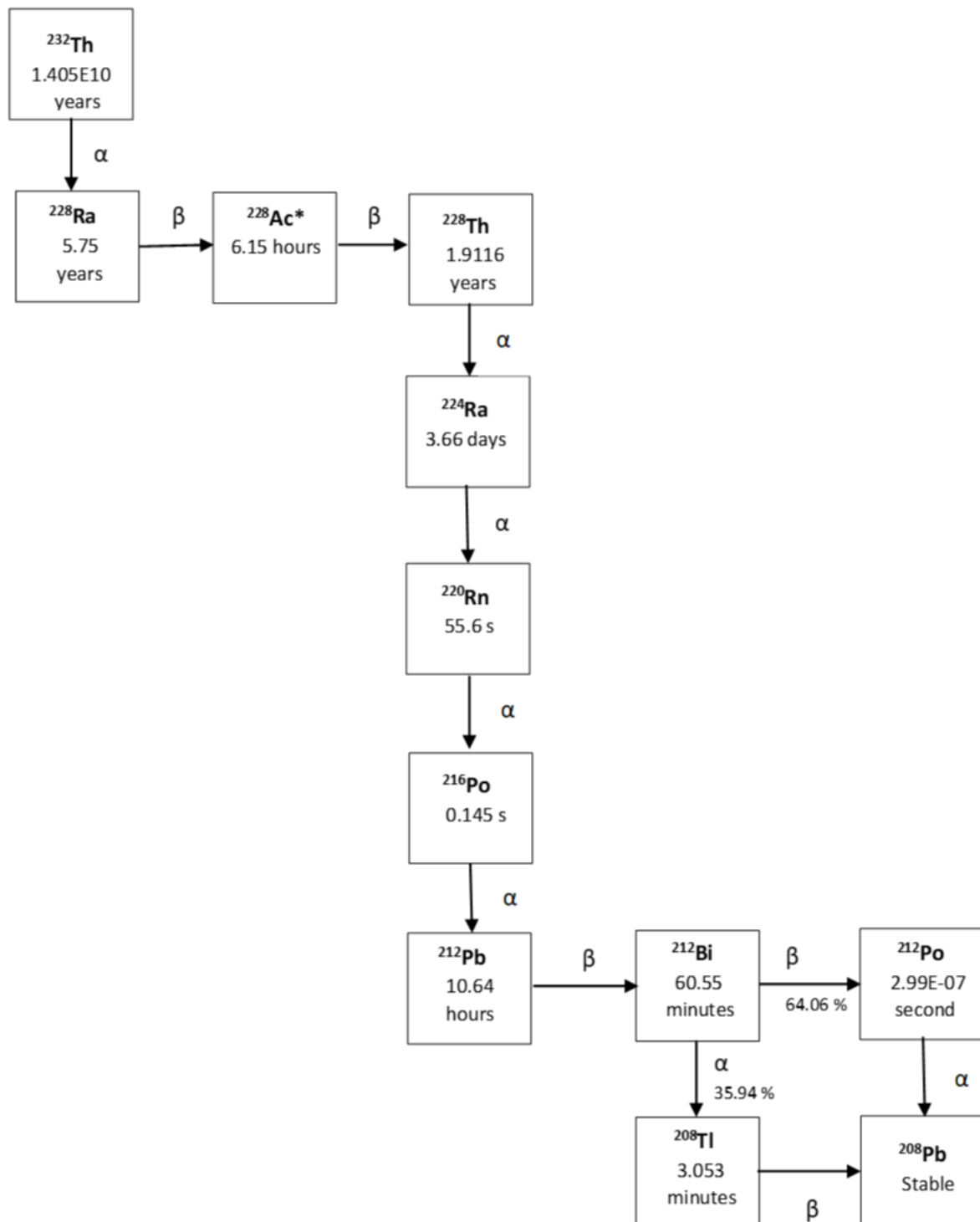
Figure 1.1: Thorium decay chain. symbols α and β indicate alpha and beta decay, and the times shown half-lives. An asterisk (*) indicates that the isotope is also a significant gamma emitter [2, 16].
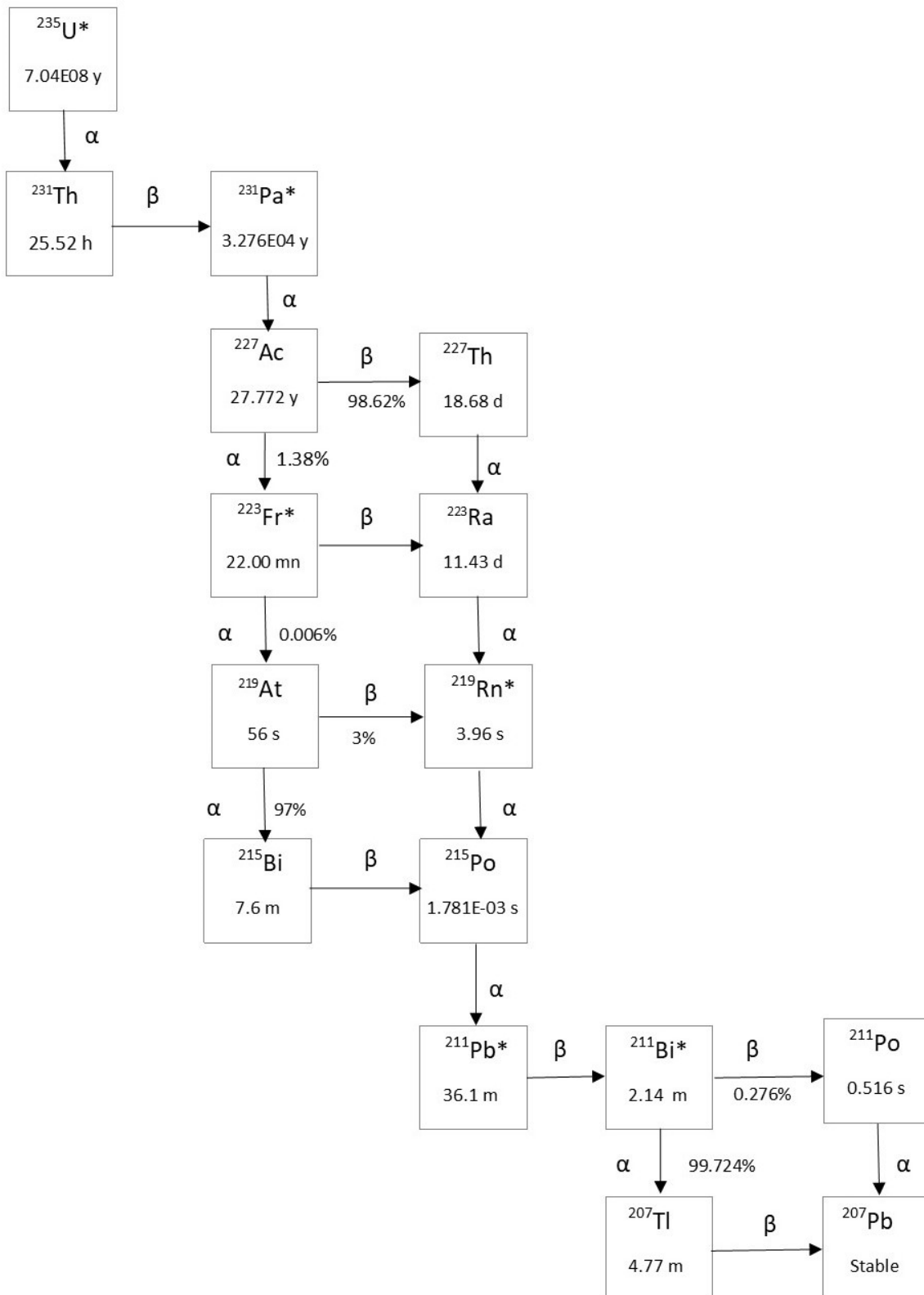
Figure 1.2: Actinium series.symbols α and β indicate alpha and beta decay, and the times shown half-lives. An asterisk (*) indicates that the isotope is also a significant gamma emitter [2, 16]
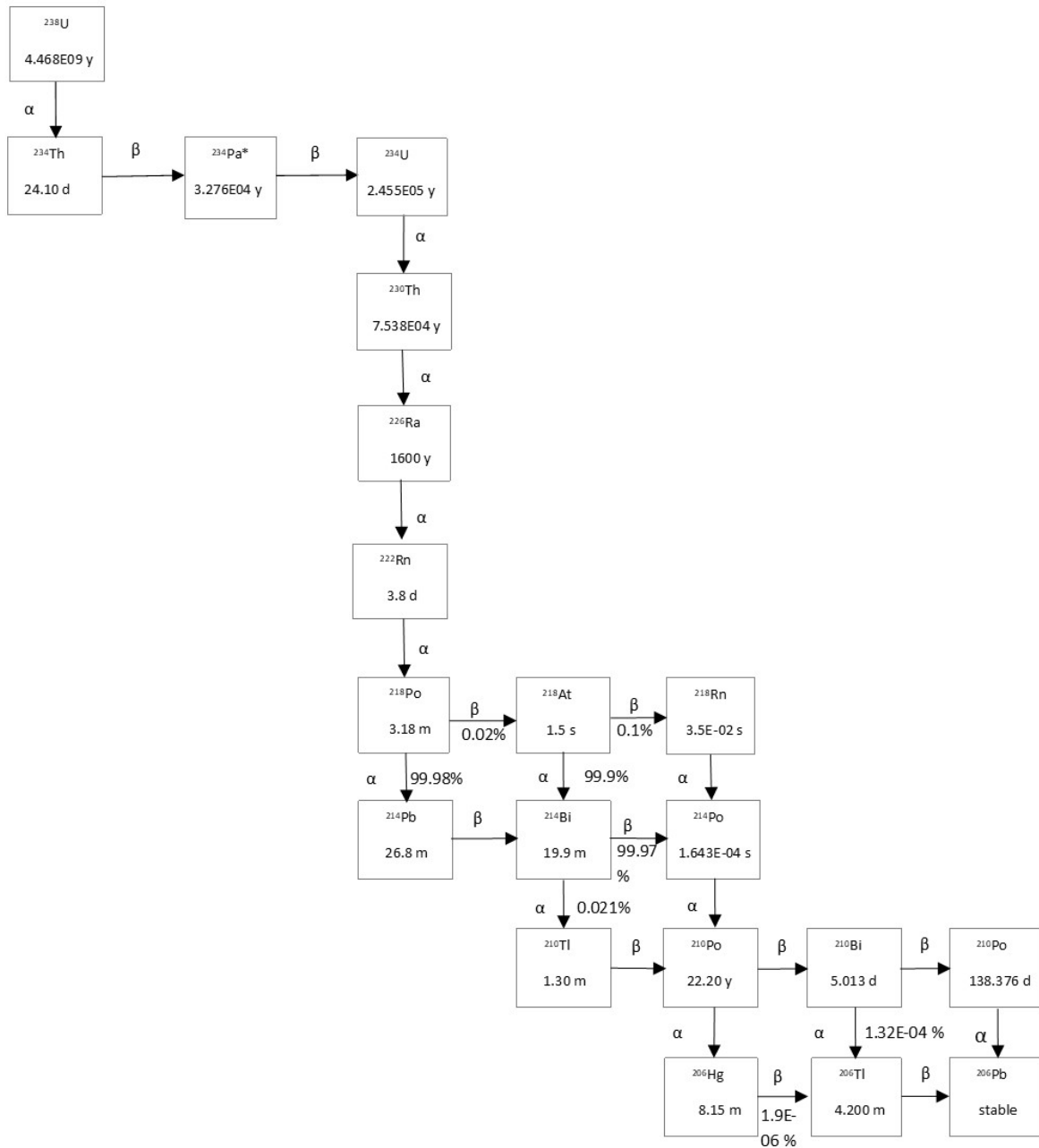
Figure 1.3: Uranium chain. symbols α and β indicate alpha and beta decay, and the times shown half-lives. An asterisk (*) indicates that the isotope is also a significant gamma emitter [2, 16].

1.2.1   Radon ($_{86}$Rn)

There are three natural isotopes of radon, namely: radon (^{222}Rn), thoron (^{220}Rn) and actinon (^{219}Rn) arising from the radioactive decay of the uranium, thorium and the actinium series. ^{222}Rn is a decay product of ^{226}Ra in the ^{238}U series while ^{220}Rn is a decay of ^{224}Ra a member of the ^{232}Th series. Actinon is a direct progeny of ^{223}Ra in the ^{235}U decay chain. The main radiation dose received by the population comes from radon, thoron and their decay products [17]. Therefore, there exist already approaches to assess the inhalation doses for radon ^{222}Rn, ^{220}Rn and their decay products (table 1.1). These approaches have been considerably improved using the recently updated biokinetic and dosimetric models [2, 18]. Table 1.1 shows some values of effective dose per unit exposure to radon progeny and thoron progeny (mSv per WLM) found in the literature.

Table 1.1: Summary of the calculated dose conversion factors for radon and thoron progenies using biokinetic and dosimetric models .

Reference (Radon isotope)	Model type	Exposure scenario	Dose (mSv per WLM^a)
[19] (^{222}Rn Progeny)	HRTM [7]	Home	12.9
		Mine	12.5
[20] (^{222}Rn Progeny)	HRTM [7]	Home	21.1
		Mine	20.9
[2] (^{222}Rn Progeny)	HRTM [2]	Mine	20
		Indoor workplace	18
[21] (^{222}Rn Progeny)	HRTM [7]	Indoor	11
[22] (^{220}Rn Progeny)	HRTM [7]	Indoors	5.4
[23] (^{220}Rn Progeny)	HRTM [7]	Indoors	5.7
[24] (^{220}Rn Progeny)	HRTM [7]	Indoor	13.8
[2] (^{220}Rn Progeny)	HRTM [2]	Mine	4.8
	HRTM [2]	Indoor workplace	5.6

^{a} Working Level Month; HRTM= Human Respiratory Tract Model.

In contrast to ^{222}Rn and ^{220}Rn which leave the soil and building materials and enter the atmosphere. Actinon due to its very short half-life (3.96 s) is generally less able to emanate from mineral matrices. Because of typically very low concentrations in the ambient air, exposure to ^{219}Rn and its decay products are usually neglected. Thus the measurement of ^{219}Rn has not been described in standard such as ICRP or ICRU [2, 3]. Due to this lack of measurements, it is almost impossible to calculate dose conversion coefficient (effective dose per unit exposure) for

actinon progeny. Dosimetry for each actinon progeny could be study instead. Recently, in hospitals cancer treatment with ^{223}Ra (Xofigo) was introduced [4]. ^{223}Ra is injected into patients to fight against bone metastasis of prostate cancer [5]. In the decay chain, ^{219}Rn occurs which may be exhaled by the patient. Secondary exposure of care-takers in the hospital and at home may happen by inhalation of actinon and its decay products. Stabin et al have calculated dose coefficients of actinon progeny for a particular situation of exposure and for particles size of 5 μm using the Activity and Internal Dose Estimates (AIDE) computer program [10]. This study is focused on the exposure of actinon decay products (^{211}Pb and ^{211}Bi).

1.2.2   Bateman equations

The Bateman equation is a mathematical model describing abundances and activities in a decay chain as a function of time based on the decay rates and initial abundances. Bateman work out a method which set up differential equations describing the decay chain based on its known properties. Let considering the simplest case with a radioactive parent which decay to a single progeny. The variation of parameters such as decay rates and relative initial radioactive population atoms describes the chain evolution as a function of time. Let $N_1(0)$ and $N_2(0)$ be the initial numbers of parent and progeny atoms respectively. The atom numbers of parent and progeny in time t, are denoted by $N_1(t)$ and $N_2(t)$ respectively. λ_1 and λ_2 represent the decay rates of parent and progeny respectively. The equation for the time evolution of the parent is given by equation 1.1. The equation for the time evolution of the progeny, however includes a term describing progeny decay but also progeny feeding by the parent. This equation is given by [25]:

$$\frac{dN_2(t)}{dt} = -\lambda_2 N_2(t) + \lambda_1 N_1 t \tag{1.8}$$

The equation (1.8) could be written as:

$$\frac{dN_2(t)}{dt} = \lambda_1 N_1(0) exp(-\lambda_1 t) - \lambda_2 N_2(t) \tag{1.9}$$

The solution of the differential equation (1.9) is given by:

$$N_2(t) = \frac{\lambda_1}{(\lambda_2 - \lambda_1)} N_1(0)[exp(-\lambda_1 t) - exp(-\lambda_2 t)] + N_2(0)exp(-\lambda_2 t) \tag{1.10}$$

The activity of the progeny is given by:

$$A_2(t) = \lambda_2 N_2(0) exp(-\lambda_2 t) - N_1(0) \frac{\lambda_1 \lambda_2}{(\lambda_2 - \lambda_1)} (exp(-\lambda_2 t) - exp(-\lambda_1 t)) \qquad (1.11)$$

In the case of a decay chain with n radioactive atoms (considering at $t = 0$ the radioactive chain is represent by $N_1(0)$; all other radionuclides of the chain do not occur yet), the expression of the general solution for the nth radioactive atom is given by:

$$N_n(t) = N_1(0) \sum_{i=0}^{n} [\frac{exp(-\lambda_i t)}{\prod_{j=0, j \neq i}^{n} (\lambda_j - \lambda_i)}] \prod_{i=0}^{n-1} \lambda_i \qquad (1.12)$$

The general form of activity for the nth atom of a radioactive chain is given by:

$$A_n(t) = N_1(0) \sum_{i=0}^{n} [\frac{exp(-\lambda_i t)}{\prod_{j=0, j \neq i}^{n} (\lambda_j - \lambda_i)}] \prod_{i=0}^{n-1} \lambda_i \qquad (1.13)$$

1.3   Interactions of radiation with matter

Some radiations occur during nuclear phenomenona. These radiations would cause damages on the matter as they produce interactions. Those interactions are differents and depend on the type of particles or radiations released. Ionizing radiation is classified into two groups (charged particles and uncharged particles). This classification is justified by the fact that the interactions, due to their mechanisms, are fundamentally different even if the consequences are substantially the same.

1.3.1   Interaction of charged particles with matter

The interaction of charged paricles with matter concerns the impart of energy from the charged particles to the material which they pass through. The charged particles are alpha particles (+ 2 charge), beta particles (+ or - charge) or electrons. The charged particles continuonously interact through the coulomb force with the electrons and nuclei of the surrounding atoms in the medium which they pass through. In other words alpha and beta particles are continually slowing down as they travel through the matter [26]. The colomb force involve the electromagnetic forces of attraction or repulsion between the alpha or beta particles and the surrounding electrons and nuclei. The Colomb force associated with these interactions can be described by Colomb's

equation given by [15]:

$$F = \frac{kq_1q_2}{r^2} \qquad (1.14)$$

where k is a constant = $9 \times 10^9 \, N.m^2/C^2$, q_1 is the charge on the incident particle in Colombs, q_2 is the charge on the "struck" particle and r is the distance between the particles in meters. There are four types of interactions of charged particles: ionization, excitation, bremsstrahlung and Cerenkov radiation. The main phenomenon of loss energy is almost always ionization.

1.3.1.1   Ionization

A charged particle mostly alpha or beta particle applies enough force of attraction or repulsion to remove completely one or more electron from an atom. The energy transfered to the electron must exceed the binding energy of the electron. Ionization is most likely to involve atoms near the charged particle's trajectory. The velocity of the charged particles is decreased with the number of ionization (the alpha or beta particles loses kinetic energy) [14]. After ionization a neutral atom turns into an ion pair. the electron removed from the atom is the negative member of the ion pair (second electron) and the vacancy on the electron shells of the atom is the positive member of the ion pair. The kinetic energy of the second electron is usually less than 100 eV. Sometimes it has sufficient energy to ionize additional atoms (delta ray) [15].

1.3.1.2   Excitation

The charged particle exerts just enough to promote one of the atom's electrons to a higher energy state (shell). Excitatiton usually occurs farther away from the charged particle's trajectory than ionization. The energy transferred to the atom is insufficient to ionize it, instead this energy excite the atom. The excited atom will de-excite by emitting a low energy ultraviolet photon. The decrease of the velocity for the charged particle depends on the number of excitation which occur during one particle travel [13].

1.3.1.3   Bremsstrahlung

Bremsstrahlung radiation is electromagnetic radiation that created when charged particles are deflected (decelerated) while moving near an atomic nucleus. Electrons (beta particles) are easily deflected. Therefore, bremsstrahlung is almost exclusively associated with electrons. As alpha particles travel in straight lines, they do not produce significant bremsstrahlung (bremsstrahlung production is inconsequential). The photons produced by bremsstrahlung may have any energy

up to the energy of the incident particle and their energy increase with the energy of incident particle (beta particles) [13, 14].

1.3.1.4   Cerenkov radiation

Cerenkov radiation is the blue light emitted by charged particles that move through a transparent medium (e.g. water) faster than the speed of light in that medium. A cone of light (Cerenkov radiation) is produced as a charged particle going faster than light. The production of Cerenkov radiation is essentially limited to high energy (i.e. fast) beta particles and electrons [26].

1.3.2   Interaction of uncharged particles with matter

In contrast to charged particles, photons interact differently in matter, because photons have no electrical charge. In addition photons do not continuosly lose energy when they travel through matter. Generally uncharged particles interact by transferring energy to charged particles (usually electron) then, the charged particles give up their energy via secondary interactions (mostly ionization). While the interaction of charged particles with matter is certain, the interaction of photons is probabilistic. The probability of a photon interacting depends on the photon energy and the atomic number, and density of material. The three principal types of photon interactions are photoelectric effect, compton scattering and pair production [13].

1.3.2.1   Photoelectric effect

The photoelectric interaction occurs when an inner shell electron (e.g. K shell) of an atom absorbs photon. Therefore, the photon disappears as all the photon energy is transferred to the electron. The latter is ejected from the atom by creating a vacancy in the shell that electron originally occupied.The energy of the incident photon is divided; some of this is used to overcome the binding energy of the electron and the rest is given to the electron as kinetic energy. Afterwards an electron from a higher energy shell falls to fill the vacancy created in the electron shell. While this happens, either a characteristic X-ray or an Auger electron is emitted. The photoelectric effect is most probable for low energy photons (photon energy higher than electron's binding energy), high atomic number and high density materials [13, 26].
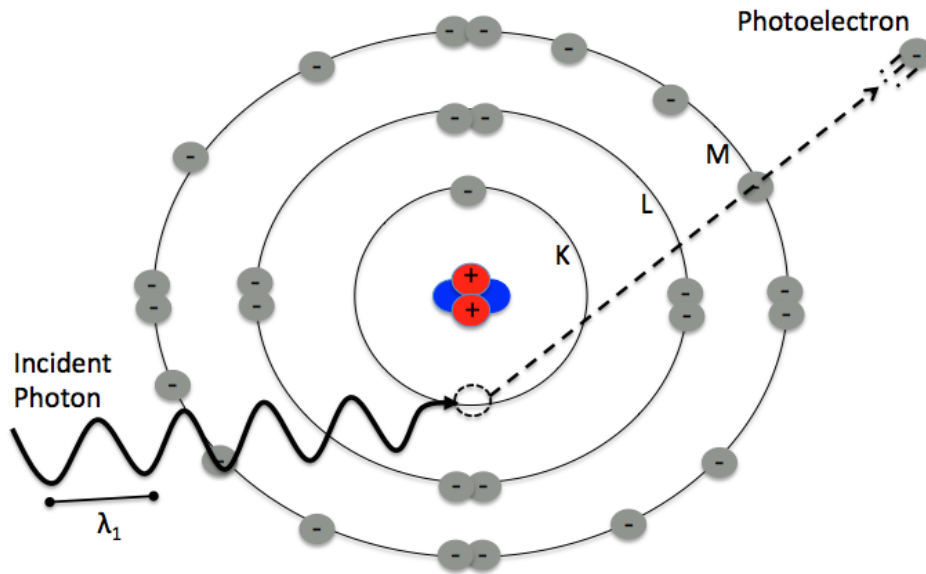
Figure 1.4: Photoelectric effect [27].

1.3.2.2   Compton scattering

In compton scattering, a photon transfers a portion of its energy to a loosely bound outer shell electron of an atom (the binding energy of the electron is considered negligible). The photon loses energy and changes direction. This is known as incoherent scattering. The energy of the scattered photon (E_γ') is given by [13]:

$$E_\gamma' = \frac{E_\gamma}{1 + (\frac{E_\gamma}{511keV})(1 - cos\theta)}$$

(1.15)

where E_γ is the energy of the incident photon. The equation of the scattered electron is given by:

$$E_e = E_\gamma - E_\gamma'$$

(1.16)

The energy is divided between the electron and the scattered photon. This energy divided depends on the angle of scatter denoted θ. The photon loses the least amount of its energy when θ is small and the largest when θ is 180 degrees. As the energy of the incident photons decrease, the energy of the scatterd photon decrease. Compton scattering occurs at all photon energies and in all materials. It is usually the most probable type of interaction.
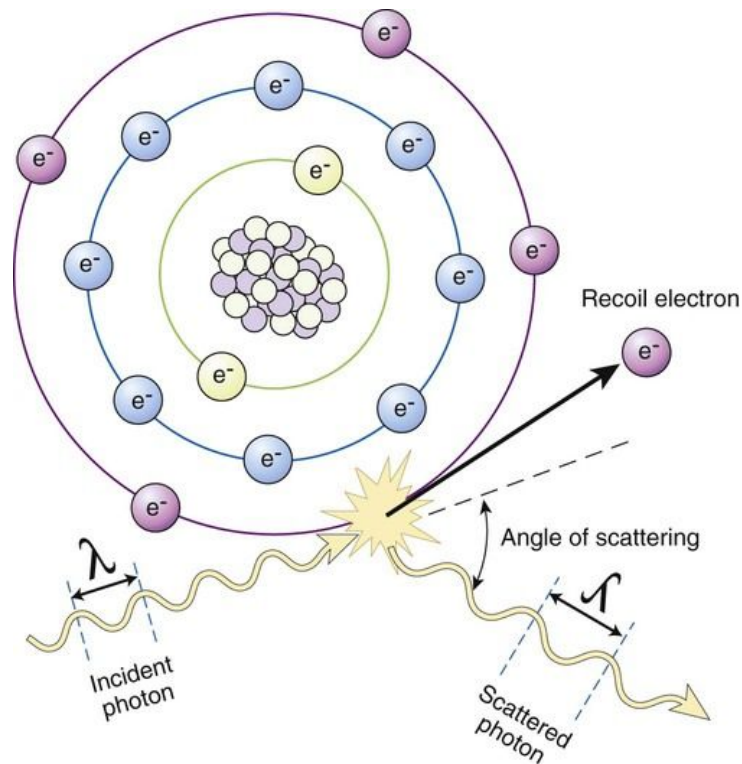
Figure 1.5: Compton scattering [28].

1.3.2.3   Pair production

Pair production occurs when a photon interacts with the electric field of the nucleus of an atom. While the photon disappears completely an electron and a positron are produced. Each of the electron and positron produced have an energy equivalence of 511 keV, the incident photon must have an energy of at least 1022 keV. The additional photon energy above 1022 keV is given to the positron and the electron as kinetic energy. This kinetic energy is lost via ionization, excitation and/or bremsstrahlung phenomenons. Ultimately the positron travels through the matter and annihilates with an electron in the material when it is nearly at rest. Then two photons of 511 keV are created in the annihilation process, which go in the opposite directions to each other [26].

There are other types of interactions of photon with matter which are less important than those described below. They are Raleigh scattering, Thomson scattering and photonuclear reactions. Raleigh and Thomson scattering are types of coherent scattering whereas Compton scattering is incoherent. In the Raleigh scattering process the photon changes direction but does not lose energy and its wavelength is unaffected. In contrast to Raleigh, Thomson scattering process involves only a single (free) electron instead of all the electrons of an atom. The photonuclear

reaction occurs when the photon is absorbed by a nucleus of an atom then a nuclear particle (alpha, neutron and proton) is ejected. All these interactions would cause damages on the human body depending on the type of radiation and whether exposure occurs external or internal of the human body.
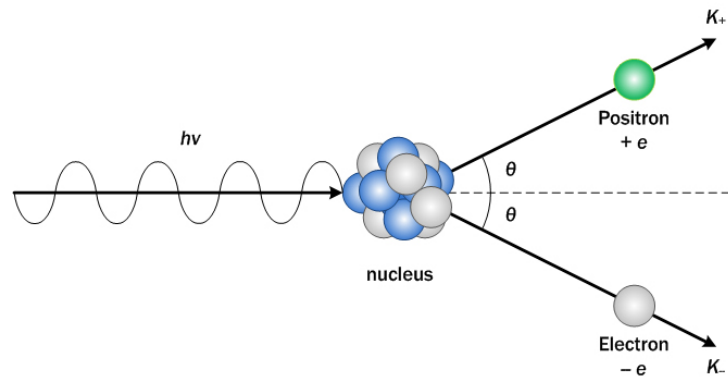
Figure 1.6: Pair production [29].

1.4   Radiation exposure

Humans are continously exposed to radiation. Radiation exposure refers to the situation where the body is in the presence of radiation. This exposure occurs generally in two ways, external exposure and internal exposure. External exposure means to receive radiation from a source (radioactive materials), which is outside causing external irradiation. This source usually exists on the ground, suspended in the air or attached to the clothes or the surface of the body. The external exposure stops as soon as the irradiated body is no longer in the path of radiation. However, internal exposure takes place when the source (radioactive substance) is incorporated in the body. The intake source will irradiate inside the body (organs and tissues) until it is excreted in the urine or feces (biological process) or as radioactivity weakens over time (physical process) [30]. The difference between internal exposure and external exposure depends on whether the source that emits radiation is inside or outside the body. The terms internal and external exposure do not depend on the types of radiation (naturally occuring radiation, accident- derived radiation or medical radiation). This study concerns internal exposure. The latter mentionned arises when a person breathes in radioactive materials in the air (inhalation), or when a person takes in radioactive materials in food or drink (ingestion) or when radioactive materials enter the body from a wound and when radiopharmaceuticals containing radioactive materials are administered for the purpose of medical treatment [31]. In the case of internal contamination,

the ICRP (International Commission on Radiological Protection) has set up a suite of models for describing the behaviour of radionuclides that have entered the body either by inhalation or ingestion. For other pathways of exposure, intakes are only likely to occur as a result of accidents that cannot be completely prevented or readily predicted [32].
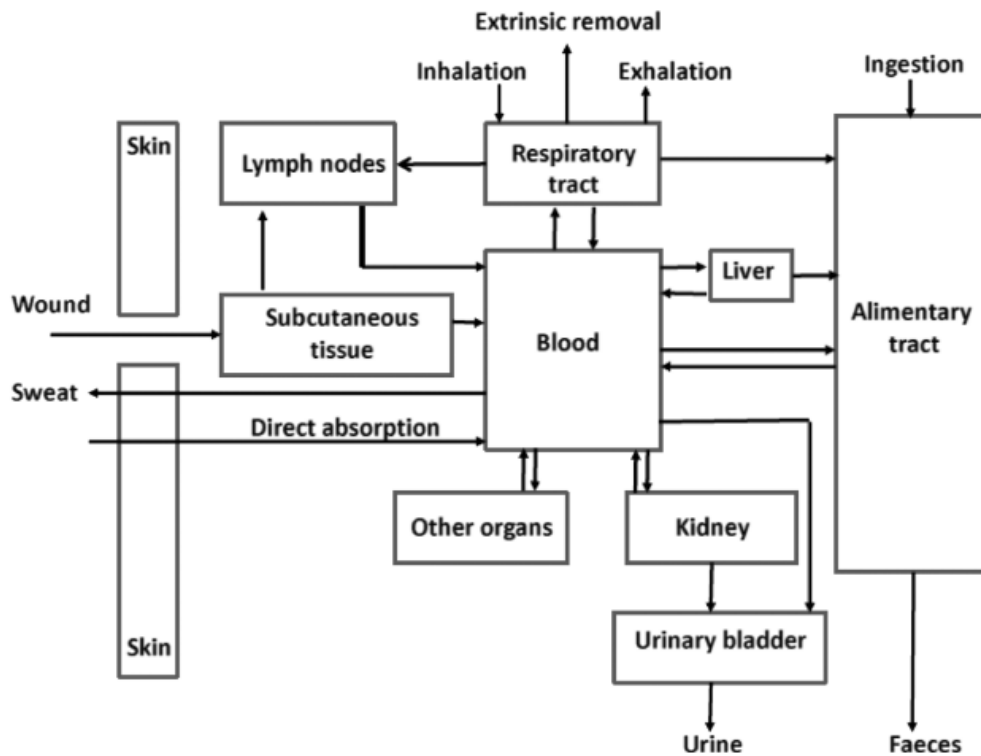
Figure 1.7: Summary of the main routes of intake, transfer, and excretion of radionuclides in the body [32].

1.4.1   Inhalation

Inhalation exposure can result from breathing air that is contaminated with particulate matters (e.g. radioactive materials) mainly aerosols. Individuals can be exposed via the inhalation route during a variety of oudoor and indoor activities. Evaluation of exposure from inhalation requires information on the concentrations of radionuclide in the air and the timeframe over which inhalation exposure occurs. In Radiological protection there are three situations of exposure: occupational exposure, public exposure and medical exposure. Inhalation is the main route of occupational and public exposure. According to UNSCEAR, radon, thoron and their decay products are responsible for natural source of internal exposure [17]. More than 50% of annual effective dose comes from inhalation of radon, thoron and their decay products. The
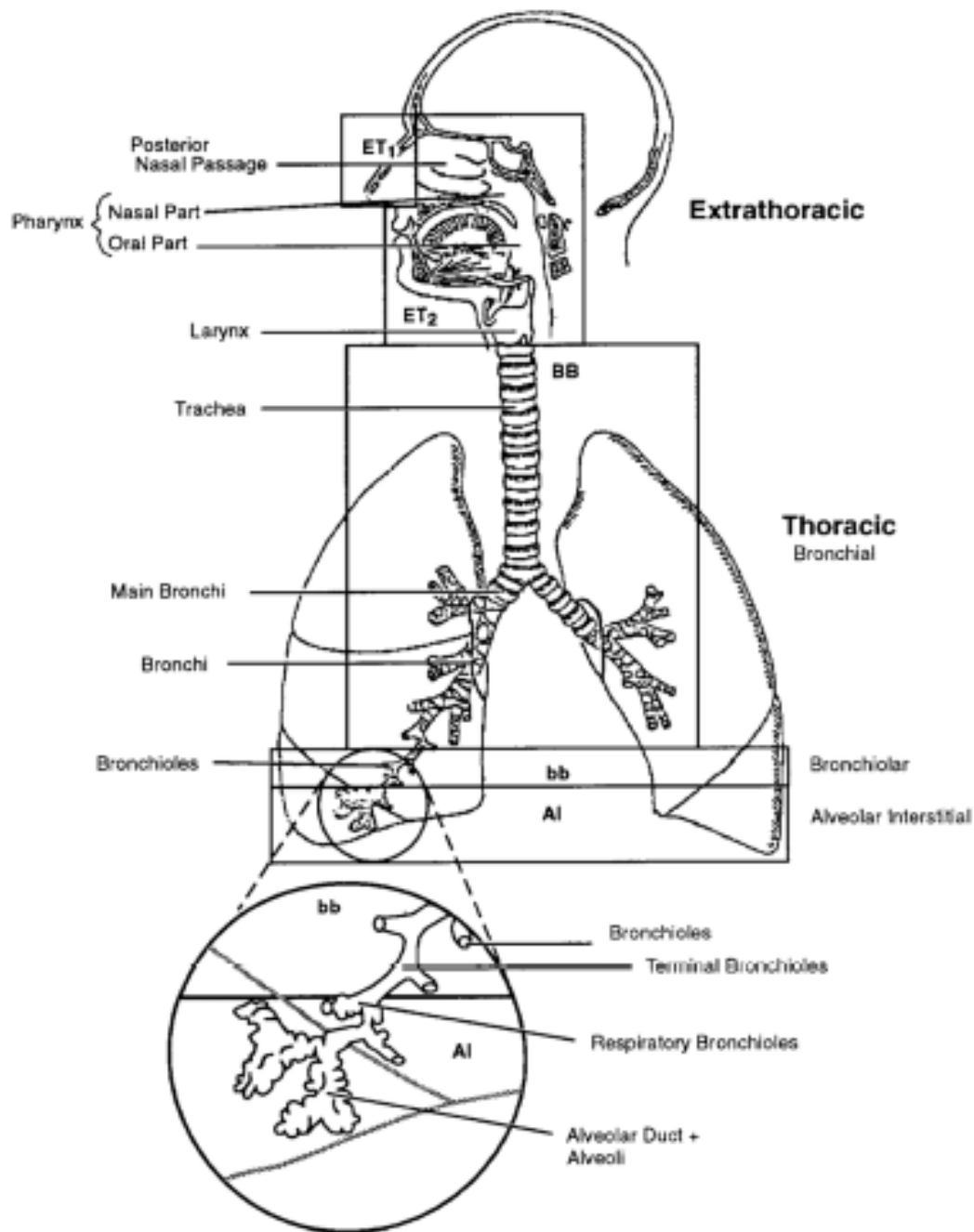
Figure 1.8: Respiratory tract regions defined in the new ICRP model [7]

inhaled and deposited radionuclides would emit α rays which can penetrate deep enough to reach lung cells (bronchioles sensitive to cancers). The β rays emitted would also reach the lungs but deposit less energy than alpha. The deposited energy within the body leads to dose, to assess the inhaled dose, inhalation rates, particle sizes and receptor body weights might be needed. The International Commission on Radiological Protection (ICRP) has set up a model called Human Respiratory Tract Model (HRTM) which describes the behaviour of inhaled ra-

dionuclides. In the HRTM, respiratory system is represented by five regions (Fig.1.8). The ET airways are divided into ET_1 which is the anterior nasal passage and ET_2 which consists of the posterior nasal and oral passages, the pharynx and larynx. The thoracic regions are bronchial (BB), bronchiolar (bb) and alveolar-interstitial (AI). Lymphatic tissue is coupled with ET and thoracic airways LN_{ET} and LN_{TH}, respectively. The deposition and clearence in the respiratory tract are treated separately. Calculations to assess dose from inhalation, are provided in this study for a particular exposure scenario. A fraction of material deposited in the respiratory system will be transferred to the throat and overwhelmed, giving the opportinuty for absorption in the alimentray system.

1.4.2   Ingestion

Ingestion exposure can result when radioactive materials enter the body through the food or drink. The ICRP has recently developped a new alimentary model called Human Alimentary Tract Model (HATM), which describes the behaviour of radionuclides incorporated in the body by ingestion. This model is applicable to children and adults under all circonstances of exposure and closely related to the anatomy of the alimentary system. It is divided into several regions; mouth region (oral cavity, teeth and oral mucosa), oesophagus, stomach, small intestine, colon divided into the left colon and right colon and the last region comprising the sigmoid colon and rectum. This model considers that the transfer to blood can be done at the level of mouth, stomach and the regions of intestine. The HATM represents the entry of a radionuclide into the oral cavity by ingestion, or into the oesophagus after particle transport from the respiratory tract. It describes the sequential transfer through the alimentary tract regions including the oral cavity, oesophagus, stomach, small intestine and segments of the colon followed by excretion in faeces [12].

1.4.3   Wounds intake

Wound intake can result when radionuclides enter the human body through wound. ICRP and NCRP have jointly developed a model describing the behaviour of radionuclides incorporated in the human body through the wound. Fig.1.9 shown the NCRP wound model which describes the transfer of radioactive materials within the body [33]. This model consists of seven compartments that comprise the wound site. These compartments are: fragment, soluble, colloid & intermediate state particles and aggregates. Additionally, blood and lymph-node compartments

receive radionuclides cleared from the wound site.
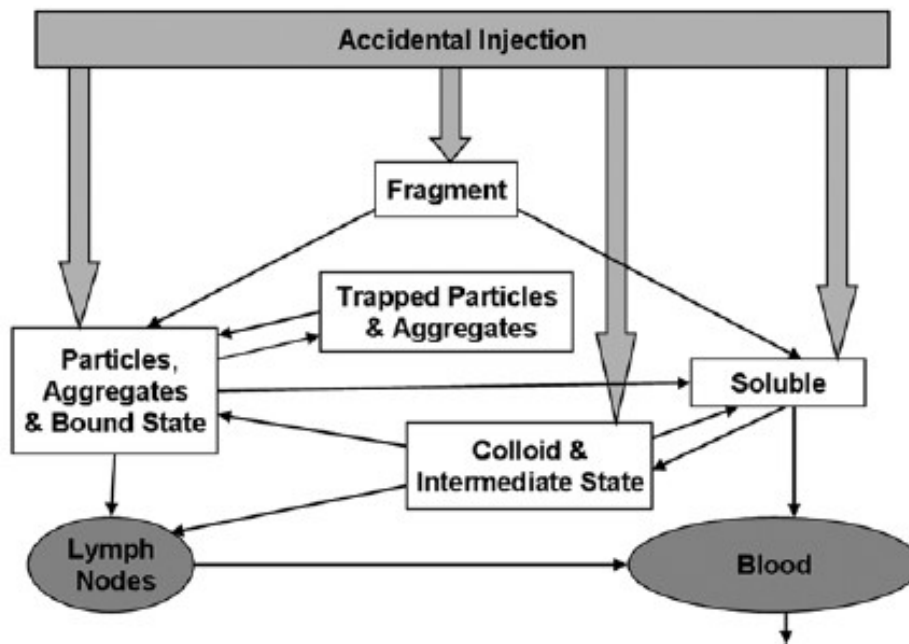
Figure 1.9: Wound model developed by NCRP and ICRP [12]

1.4.4 Clearence of intake materials

The clearence refers to the difference processes of removal for deposited material which occur in the respiratory and alimentary models. The clearence from the respiratory tract is described by several ways. Some deposited substance in the extrathoracic region (ET_1) is removed by extrinsic process such as nose blowing (ICRP 66). In other regions there is also a competitive process of clearence between the particle transport towards the alimentary tract and lymph nodes, and the absorption into blood from the deposited particles in the respiratory tract. The absorption into blood and particles transport are taken to be independent of each other [32]. In addition the deposited material is also removed by transformation to a decay product. Mostly the rates of clearence for deposited materials depend on the physicochemical form of the material, the location of the material in the respiratory tract and the time since deposition of the material. Conversely the absorption of ingested materials into blood occurs from all regions of the HATM depending on the element and its chemical form. The absorbed materials from the respiratory and alimentary regions are redistribued in other organs through the body fluids (mostly blood) [7].

1.5   Health effects of radiation

1.5.1   Biological effects

The incorporated radioactive material decays by emitting ionizing radiation within the body. Therefore, the radiation would affect the atoms in living cells and thereby damage their genetic material (DNA). Fortunately, the living cells are extremely efficient at healing this damage. However, if the damage is not fixed correctly, a cell may die or eventually become cancerous. Exposure of high level of radiation over a short period of time could lead to some symptoms such as nausea and vomiting within hours and could sometimes result in death over the following days or weeks. This is known as acute radiation syndrome. A low level of radiation exposure does not cause immediate health effects, it could increase the risk of cancer over a lifetime. Interaction of radiation with DNA could be a direct or indirect process [26]. In the direct process, radiation would break strands of DNA. However in the indirect process, radiation would break water molecules surrounding the DNA. Afterwards, the broken water molecules produce free radicals unstable oxygen molecules. The new created oxygen molecules would damage cells and organ. The cell damage would repairs itself and go back to normal or the cell damage is not repaired or is incorrectly repaired creating a changed cell which may eventually lead to cancer, or the cell is badly damage causing the death of this cell. When cells die there is two options: The body will recover and there is no risk of those cells potentially turn into cancer (a few radiation damaged), and the high radiation dose could cause widespread cell death which can lead to organ failure. All those effects described below are classified in two types; Deterministic effects and stochastic effects [30].

1.5.1.1   Deterministic effects

Deterministic effects or tissue reactions of ionising radiation are referred directly to the absorbed radiation dose and the severity of the effect increases as the dose increases. A deterministic effect typically has a threshold below which the effect does not occur [30].

1.5.1.2   Stochastic effects

Stochastic effects of ionising radiation are chance events, with the probability of the effect increasing with dose, but the severity of the effect is independent of the dose received. These type effects are assumed to have no threshold. Cancer risk and hereditary disorders are stochastic

effects [30].

1.6 Dosimetric quantities and units

In general dosimetric quantities are descriptions of methods for a quantitative determination of energy deposited in a given medium by directly or indirectly ionizing radiations. Therefore, there is a number of physical quantites and units which are definied for describing a beam of radiation and the dose of radiation. The quantitative concept of a dose of radiation is to predict associated radiation effects. The most commonly used dosimetric quantities and their units for internal exposure are briefly described in this section.

1.6.1 Absorbed dose

The absorbed dose denoted D is a quantity which describes a measure of the amount of radiation energy absorbed per unit mass (Joules / kilogram). The units of the absorbed dose is gray (Gy) 1 Gy = 1 J/kg. This quantity is applied to all types of radiation (Photons, alphas, betas and neutrons) and could be calculated for any material (air, water and tissue). Absorbed dose reflects the energy deposited per unit mass, not the total energy. As absorbed dose depends on the type of material, the absorbed dose to human tissue from gamma rays would be greater than the absorbed dose to air in the situation for example. The absorbed dose could also be definie as the quotient of $d\bar{\varepsilon}$ by dm as given below [34]:

$$D = \frac{d\bar{\varepsilon}}{dm} \tag{1.17}$$

where $d\bar{\varepsilon}$ is the mean energy imparted by ionizing radiation to matter of mass dm. The energy imparted (denoted ε in Joule), by ionizing radiation to matter in a volume is given by:

$$\varepsilon = R_{in} - R_{out} + \sum Q \tag{1.18}$$

where R_{in} is the radiant energy incident on the volume or it is the sum of the energies of all those charged and uncharged ionizing particles which enter the volume. R_{out} is the radiant energy emerging from the volume or it is the sum of the energies of all those charged and uncharged ionizing particles which leaves the volume. $\sum Q$ is the sum of all changes (decreases positive sign and increases negative sign) of the rest mass energy of nuclei and elementary

particles in any interactions which occur in the volume (ICRU 51).

1.6.1.1   Absorbed dose rate

The absorbed dose rate, $\dot{D}$ ($Gray/second : Gy/s$) is the quotient of dD by dt, where dD is the variation of absorbed dose in the time interval dt. The absorbed dose rate is given by:

$$\dot{D} = \frac{dD}{dt} \tag{1.19}$$

1.6.2   Kerma

Kerma is a measure of the energy released (lost) by the radiation rather than the energy absorbed by a material. In order words kerma is the energy transferred to charged particles per unit mass of material by indirectly ionizing radiation for insistance gamma rays and neutrons. There is no kerma definied for charged particle radiation (alpha and betas). Kerma means kinetic energy released in matter. This concept is widely used in medical radiology. In some situations, the absorbed dose equals the kerma (in air) [34].

1.6.3   Equivalent dose

The equivalent dose is the protection quantity which is used to specify exposure limits to ensure that occurence of stochastic health effect is kept below unacceptable levels and that tissue reactions are avoided (ICRP 103). It sets out to be a measurement for a long term biological consequence for humans due to some radiation exposure. Hence, the regulatory limits are expressed as an equivalent dose rather than absorbed dose. Equivalent dose can be calculated for any type of radiation and its general expression is given by [34]:

$$H_T = D_{R,T} \times w_R \tag{1.20}$$

where H_T represents the equivalent dose for a tissue/ organ T in Sievert (Sv), $D_{R,T}$ is the absorbed dose for radiation type R and tissue or organ T in Gray (Gy) and w_R is the radiation weighting factor for radiation type R. w_R for most common radiation encountered are given below in the Table.1.

The value of radiation weighting factor is based on the stopping power of the charged particles

Table 1.2: International Commission on Radiological Protection radiation weighting factor [30].

Radiation type	Radiation weighting factor w_R
Photons	1
Electrons and muons	1
Alpha particles, fission fragments and heavy ions	20

(in water), and the energy lost per unit of distance. According to the ICRP the radiation weighting factor is a dimensionless factor by which the organ or tissue absorbed dose component of radiation type R is multiplied to reflect the relative biological effectiveness of that radiation type. The ICRP and ICRU have defined many types of equivalent doses [30, 34]. Some of these include the directional dose equivalent, ambient dose equivalent, committed equivalent dose and committed effective dose.

1.6.3.1   Directional Dose Equivalent

The directional dose equivalent, H*(0.07) is an operational radiation protection quantity in all cases for the environmental monitoring. It has been defined for weakly penetrating radiation (betas) at the depth of 0.07 mm.

1.6.3.2   Ambient Dose Equivalent

The ambient dose equivalent, H*(10) is an operational radiation protection quantity in all cases for the environmental monitoring. It has been defined for penetrating radiation (photons and neutrons) at the depth of 10 mm.

1.6.3.3   Committed Equivalent Dose

The committed equivalent dose is calculated only for internal exposure, i.e. exposure resulting from inhalation, ingestion, injection or absorption through the skin or wound. It has been defined as the time integral of the equivalent dose rate in a particular tissue or organ that will be received by an individual following intake of radiactive material into the body. The committed equivalent dose is attributed to the year of intake. The time integral or commitment period is taken to be 50 years for adults and 70 years for children. The committed equivalent dose is the same as the equivalent dose delivered during the year of intake for a short half-life radionuclide or for the radionuclide rapidly excreted from the body. However, for the long lived radionuclide that remain within the body the committed equivalent dose is much higher than the equivalent

dose during the year of intake [30].

1.6.3.4   Effective Dose and Committed Effective Dose

Effective dose is always calculated for internal exposure, namely when a radionuclide is incorporated in the body via inhalation, ingestion or injection. This concept is defined for non-uniform radiation exposures. In contrast to external exposure, where the doses to the different organs or tissues of the body are almost the same, the different organs or tissues receive very different doses for internal exposure. The effective dose is the sum of the product of the equivalent dose H_T of a tissue/organ T and the tissue weighting factor for that tissue/organ (w_T). This is given by [30]:

$$E = w_T \times H_T \tag{1.21}$$

The w_T represents the risk of dying cancer per unit equivalent dose to that tissue. In other word is the factor by which the equivalent dose in a tissue T is weighted to represent the relative contribution of that tissue or organ to the total health detriment resulting from uniform irradiation of the body [30]. It is weighted as:

$$\sum_T w_T = 1 \tag{1.22}$$

When the equivalent dose to the tissue is a committed equivalent dose, the committed effective dose is calculated instead of effective dose. In more cases the calculations deal which committed effective dose rather effective dose. The effective dose is rarely calculated. The exception could be made on the calculation of effective dose for a non-uniform external exposure. The committed concept is only applies for internal exposure. The expression of the committed effective dose is given by [34]:

$$E_\tau = \sum_T w_T H_{\tau,T} \tag{1.23}$$

where τ represents the commitment period, E_τ the committed effective dose in Sievert (Sv), H_τ is the committed equivalent dose in Sievert (Sv) and w_T is the tissue weighting factors given in Table.2.

According to the ICRP the tissue weighting factors could be interpreted in several ways for example, the weighting factor of the lung is 0.12. [35] This could be interpreted as 12% of the deaths due to uniform whole body exposures are due to lung cancer [35].

Table 1.3: International Commission on Radiological Protection tissue weighting factors [30].

Tissue	w_T	$\sum w_T$
Active bone marrow, breast, colon, lung, stomach, remainder tissue*	0.12	0.72
Gonads	0.08	0.08
Urinary bladder, oesophagus, liver, thyroid	0.04	0.16
Bone endosteum, brain, salivary glands, skin	0.01	0.04

*Remainder tissues: adrenals, extrathoracic regions of the respiratory tract, gall bladder, heart, kidneys, lymphatic nodes, muscle, oral mucosa, pancreas, prostate (male), small intestine, spleen, thymus, and uterus/cervix (female).

1.6.4   Dose Coefficient

Dose coefficient could be defined as either the committed equivalent dose in tissue T per unit of activity intake, or the committed effective dose per unit of activity intake in the commitment period of 50 years for adults and 70 years for children which the dose is calculated. On internal exposure, there are three types of dose coefficient; inhalation for the activity intake by the nose or/and mouth, ingestion for the activity contained in the eaten food and injection for the activity intakes through the skin. Sometimes the term dose per unit of intake (DPUI) is used instead of dose coefficient. In contrast to the situation with external dosimetry, it is impossible to measure directly dose due to internal contamination. In order to compare the results of the routine monitoring of the workers or members of the public with the regulations, the retained or excreted activity is measured and then interpreted in terms of committed effective dose, using biokinetic models of radioelements and the radiation transport. In practice, the dosimetric interpretation of an activity measurements is broken down into two points: the assessment of intake activity I which is obtained by dividing the activity value M measured t days after intake by the m(t) value of the retention or excretion function m, then the calculation of the committed effective dose E or the committed equivalent dose for a particular tissue over 50 years for the adults or up to the age of 70 years for children, by multiplying the incorporated activity I value by the dose coefficient (DPUI). The incorporated activity and the committed effective dose is given by [32]:

$$I = \frac{M}{m(t)} \tag{1.24}$$

$$E_\tau = I \times \epsilon \tag{1.25}$$

where E_τ represents the committed effective dose for a commitment period τ, I represents the incorporated activity and ϵ the dose coefficient which depends on the type of intake (inhalation,

ingestion or injection), the contaminated subject and the condition of exposure (single or acute intakes). There are some special quantities and units to charaterise the inhalation exposure of radon, thoron and their short-lived decay products.

1.6.5   Dose conversion coefficient

In general, the lungs dose arises from the alpha particles emitted during the decay of the short-lived radon progenies that are incorporated in the body mainly by inhalation. The dose conversion coefficient of radon or thoron decay products depends on several parameters such as the potential alpha energy (PAE), the potential alpha energy concentration (PAEC), the intake activity of radon or thoron progeny and the unattached fraction [2].

1.6.5.1   The potential alpha energy (PAE)

The potential alpha energy denoted $\epsilon_{p,i}$ of an atom i in the decay chain of radon is the total alpha energy emitted during the decay of this atom to stable (^{210}Pb for a atom of ^{222}Rn decay chain). PAE per activity (Bq) of radionuclide i is $\frac{\epsilon_{p,i}}{\lambda_{r,i}}$, where λ_r is the decay radioactive constant [2].

1.6.5.2   The potential alpha energy concentration (PAEC)

The potential alpha energy concentration PAEC denoted c_p of any mixture of short lived radon or thoron progeny in air is the sum of PAE of these atoms present per volume of air. PAEC is given by [2]:

$$c_p = \sum_i c_i \left(\frac{\epsilon_{p,i}}{\lambda_{r,i}} \right) \tag{1.26}$$

where c_i represents the activity concentration of radionuclide i (Bq.m^{-3}). The SI unit of c_p is J.m^{-3} (1 J.m^{-3} = 6.242$\times$ 10^{12} MeV.m^{-3}).

1.6.5.3   The unattached fraction

The unattached fraction denoted f_p, is defined as the fraction of PAEC of the short-lived progeny (radon or thoron) that is not attached to the ambient aerosol.

The dose conversion coefficient or the effective dose per exposure to airborne short-lived radon (or thoron) progeny is calculated in terms of Sv per PAE exposure and is given by [2]:

$$E(SvperWLM) = \sum_j f_{p,j} \sum_i I_{j,i} e_{j,i} \tag{1.27}$$

where the unit of PAE is WLM (Working Level Month) or J.h m^{-3}. The relationship between WLM and J.h m^{-3} is given by 1WLM = 3.54 mJ.h m^{-3} and 1mJ.h m^{-3} = 0.282 WLM. The working level months is defined as the cumulative exposure from breathing an atmosphere at a concentration of 1 WL for a working month of 170 h.

$I_{j,i}$ in the equation (1.29) represents the intake activity of the radon progeny i and a mode j.

1.7 Softwares for internal dose calculation

The procedures introduced above can be programmed in a computer code which could speed up the calculations of the committed doses. This computer code takes into account some parameters such as biokintic data and computational phantoms (generally for reference person). In the following, several common used computer programs for biokinetic modeling and internal dose calculations are briefly introduced .

SAAM II, is a modeling simulation and analysis software package which supports the development and statistical calibration of compartmental models in biological, metabolic and pharmaceutical systems. In particular it could also defined as a user friendly commercial software for compartmental modeling. This software is initially developed by National Institues of Health (NIH) for pharmacokinetic investigation was later licenced to Washington University for further development and now is maintained by company [36]. SAAM II can be used for the calculation of the number of nuclear transformations [37].

SEECAL, is a computer program which was developed at Oak Ridge National Lab (ORNL). The program is used for the calculation of SEE values (Specific Energy Effective, now S_w coefficients) for many radionuclides based on the mathematical phantoms developed at ORNL. It is generally associated with SAAM II for internal dose calculations.

DCAL, is a free software for internal dosimetry calculation. It was also developed by ORLN and used for the assessment of dose coefficients according to the ICRP methodology [38].

IMBA, is a commercial software for professional internal dosimetry and monitoring program. The program is mainly designed for application in workplace and for occupational workers. It is implemented only for adult ICRP biokinetic models and phantoms. [39]

OLINDA/EXM, is a commercial software for internal dose assessment mainly used in nuclear medicine. It was implemented according to the MIRD methodology. This software is generally used for the estimation of organ doses of patients or provided dose report for new radiopharmaceuticals.

ICRPDOSE, is a free software for dose coefficients calculation developed by ICRP on the approach of publication [40]. The database contains committed equivalent doses per unit intake (dose coefficients) to various tissues and committed effective doses per unit intake (dose coefficients). Results are given for both workers and members of the public.

There are other internal dose programs such as DOSAGE and PLEIADES which generating ICRP dose coefficients; IDSS, AIDS, MONDAL and IDEA system for implementation of ICRP internal dose methodology and biokinetic models and reference S coefficient, for incorporation monitoring and internal dose calculation; IDAC for the assessment of patient doses from radio-pharmaceuticals [36].

1.8   Radiological protection

Radiological protection is a term applied to the protection of workers, patients, the public and the environement from harmful effects of exposure to ionising radiation, and the means for acheiving this. The radiological protection is based on three fundamentals principles:

1.8.1   Justification

Any decision that alters the radiation exposure situation should do more good than harm. This means that, by introducing a new radiation source, by reducing existing exposure, or by reducing the risk of potential exposure, one should achieve sufficient individual or societal benefit to offset the detriment it causes [30].

1.8.2   Optimisation

The probability of incurring exposures, the number of people exposed, and the magnitude of their individual doses should all be kept as low as reasonably achievable, taking into account economic and societal factors. This means that the level of protection should be the best under the prevailing circumstances, maximising the margin of benefit over harm. In order to avoid severely inequitable outcomes of this optimisation procedure, there should be restrictions on the doses or risks to individuals from a particular source (dose or risk constraints and reference levels) [30].

1.8.3 The principle of application of dose limits

The total dose to any individual from regulated sources in planned exposure situations other than medical exposure of patients should not exceed the appropriate limits recommended by the regulation agency or some commission. Regulatory dose limits are determined by the regulatory authority, taking account of international recommendations, and apply to workers and to members of the public in planned exposure situations [30].

Conclusion

In sum this chapter has presented briefly some generalities on radioactivity, the actinon and its progeny, the interaction of radiation with matter, internal exposure and some fundamental quantities and dosimetric units. In addition some results of dose conversion coefficients of inhaled radon and thoron progenies found in the literature were presented and the fundamental principles of radiation protection were also briefly defined. The next chapter will present material and methods used for the assessment of dose following inhalation of actinon progeny.

Chapter 2

Material and Methods

Introduction

This chapter introduces the internal dose assessment after inhalation of actinon decay products (^{211}Pb and ^{211}Bi). First, the mathematical model of Human Respiratory Tract Model (HRTM) is presented. Second, the deposition fractions in the HRTM depending on particles size distribution and the biokinetics models describing dissolution absorption and elimination of desposited material in the human body were implemented and third, activity occuring within the organs or tissues were calculated. Finally, the dosimetric model was applied to assess organ equivalent dose and effective dose coefficients with the calculation of radiation weigthed S coefficient values, denoted S_w for specified source and target organ which were derived from the new ICRP voxel computational phantoms for reference adult [18].

2.1   The Human Respiratory Tract Model (HRTM)

The most important route for radionuclides and other hazardous airbone materials to enter the body is the intake by inhalation. Therefore, the International Commission on Radiological Protection (ICRP) has developed and updated a model describing the entrance, deposition, clearence and absorption of intake materials in the human body through its publications [31, 7, 32]. The most recent updated version of the Human Respiratory Tract Model is used in this study [32]. As the consequences of the inhaled radionuclides which irradiate tissues and cells of the respiratory tract as well as those of many other organs, the HRTM was created to facilitate calculation of biologically meaningful doses, which depend on morphological, physiological and radiobiological characteristics of the respiratory tissues. This model is applicable to all

33
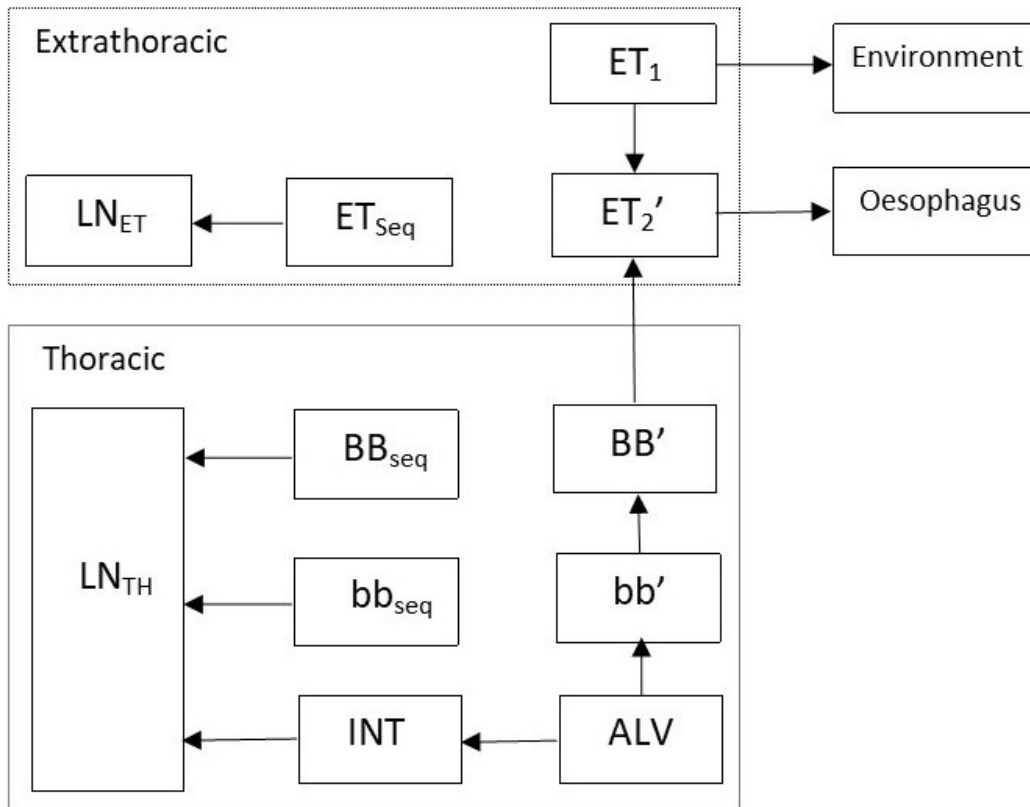
Figure 2.1: Compartment model representing time-dependent particle transport from each respiratory tract region. Each arrow describes the transfer rate depending on time of the deposited material. ET_1: extrathoracic region including the anterior nasal passage; ET_2: extrathoracic region including posterior nasal passage, pharynx and larynx; BB: bronchial region; bb: bronchiolar region; AI: alveolar interstitial region.[32]

members of the world's population including specific individuals. It is assumed that particle transport rates are independent of age and sex, and these rates are common for all materials. However, the information on the deposition and clearence is specific to each material. For dosimetric purposes a common compartment model is therefore provided and described particle transport of inhaled material. The most recently update particle transport model used in this study is shown in Fig.2.1. The respiratory model consists of 13 compartments (including environment compartment and oesophagus) which represent a part of tissues. There are alveolo interstitial (AI) divided in two compartments ALV (alveolo) and INT intertitial compartment. The deposited materials in ALV are cleared either to the ciliated airways (bb') or to the INT with a biological half-time of approximately 250 days. In the INT, deposited particles are cleared very slowly to the lymph nodes. BB' is a compartment of bronchial region which describes the retention of particles with a biological half-time of approximately 100 minutes and transport of these particles to ET_2'. The bronchiolar region with a main compartment bb' that describes re-

tention (half-time of approximately 3.5 days) and transport (to BB') and transport of particles. bb_{seq} and BB_{seq} describe the long term retention in bronchiolar airways walls and bronchiol airways walls respectively, all of them with half time of approximately 700 days. The region ET_1 is considered as a compartment and therefore not subdivided. This compartment includes exhalation of the deposition particles. ET_2' represents a part of the posterior passage nasal, with a short term retention (half time approximately 10 minutes). However, ET_{seq} describes a compartment with a long term retention in airways tissue of a small fraction of particle. The compartments denoted LN_{ET} and LN_{TH} represents lymphatics and lymph nodes that drain the ET regions and thoracic regions respectively. The rates of change between compartments are given in table 2.1. The deposition and clearance of this model depend on several parameters.

Table 2.1: Reference values of transfer rates for compartment model of the human respiratory tract [7]

From compartment	To compartment	Transfer rate (d^{-1})
ALV	bb'	0.002
ALV	INT	0.001
INT	LN_{TH}	0.00003
bb'	BB'	0.2
bb_{seq}	LN_{TH}	0.001
BB'	ET'$_2$	10
BB_{seq}	LN_{TH}	0.001
ET'$_2$	Oesophagus	100
ET_{seq}	LN_{ET}	0.001
ET_1	Environment	0.6
ET_1	ET'$_2$	1.5

2.1.1   Aerosol fractional deposition in HRTM

The fractional deposition in respiratory tract regions depend on several parameters such as, the volume and rate of air inhaled, the proportions entering through the nose and mouth which determine the quantity of radionuclide inspired and their penetration into the respiratory tract, the respiratory parameters which vary with the body size, the level of activity and sometimes the respiratory diseases, the fraction of an airbone material present in a person's breathing environment that is deposited in each region and determined by particle parameters including size shape and density. The particles deposition within the respiratory tract could occur through five mechanisms: interception, impaction, sedimentation, diffusion and electrostatic precipitation. In the most case, only impaction, sedimentation and diffusion are important. The appropriate

unit in terms of particle deposition by sedimentation and impaction is aerodynamic diameter [7]. However, the dominant mechanism for particle size less than 0.5 μm is the diffusion which depends only on size and not on density or shape (thermodynamic diameter) [7]. For a particular case of actinon (^{219}Rn) and its progeny there are no concentration and activity size measurements up to now. ^{219}Rn due to its short half-life (3.96 s) will probably not be able to escape from point where it is formed. Therefore, actinon and its progeny (^{211}Pb and ^{211}Bi) are very rare in the ambient air. As the lead (^{211}Pb) decay product of actinon has a half-life of 36.1 min, which is much closer to that of the lead (^{214}Pb) progeny of radon (^{222}Rn) with a half-life of 26.8 min, the activity size for radon progeny was used as the deposition fraction in the respiratory tract region, as displayed in Table 2.2. Table 2.3 gives the partition of deposit in each region of the respiratory tract between compartments (Fig.2.1).

Table 2.2: Deposition fraction in the HRTM [2]. A breathing rate of 1.2 m^3.h^{-1} is assumed. Geometric standard deviation (GSD) of 1.3 and 2.0 for unattached and attached particles, respectively a unit of density and a shape factor are used for all modes [2]

	Deposition fraction (%)		
Region^a	AMTD (1 nm)	AMAD (60 nm)	AMAD (500 nm)
ET$_1$	51.91	3.85	10.68
ET$_2$	27.96	2.08	5.75
BB	7.93	0.93	0.60
bb	10.05	6.53	1.42
AI	0.59	27.90	9.05
Total	**98.43**	**41.29**	**27.51**

^{a}ET$_1$ anterior nasal passage; ET$_2$ posterior nasal passage, pharynx and larynx; BB bronchial; bb bronchiolar. AI alveolar interstitial.

2.1.2   Clearence: Absorption into blood

Absorption into blood (or body fluids) depends on the physical and chemical forms of the deposited material. This absorption occurs at the same rate in all regions of the HRTM, except ET$_1$ region where no absorption takes place. The process of clearence from the respiratory tract to blood is treated as a two stages process. Dissociation of particles into material which could be absorbed easily into blood (dissolution) and then absorption of soluble material and the dissociated one into blood from particles. Both stages are associated to some clearence rates which could be time dependent. A simple compartment models are used to represent the time

Table 2.3: Partition of deposit in each region between compartments [32]

Region or deposition site	Compartment	Fraction of deposition in assigned to compartment
ET_1	ET_1	1
ET_2	ET'_2	0.998
	ET_{seq}	0.002
BB	BB'	0.998
	BB_{seq}	0.002
bb	bb'	0.998
	bb_{seq}	0.002
AI	ALV	1

dependent dissolution and absorption of the deposited material. Fig. 2.2 and 2.3 show two differents methods descrbing the clearence of deposited material from the respiratory tract regions to body fluids. The first presented system (Fig 2.2) can only represent an overall dissolution rate that decreases with time (decribing the majority of material). To overcome the limitation of the first system, a second system (Fig 2.3) is developed [7, 32]. According to the recent ICRP publication (Occupational Intake of Radionuclides series), the first system is adopted as the default system. The relation between parameters of those two systems is given below[32]:

$$s_p = s_s + f_r(s_r - s_s) \tag{2.1}$$

$$s_{pt} = (1 - f_r)(s_r - s_s) \tag{2.2}$$

$$s_t = s_s \tag{2.3}$$

The compartment labelled bound material (Fig. 2.2 and Fig. 2.3) represents regions where a fraction of dissolved material (bound fraction f_b) is retained. While the remaining fraction (1-f_b) enters body fluids immediately, the material from bound material compartment goes into blood by uptake instead of particles transport processes. The first system described in Fig. 2.2 is used for the inhalation of [211]Pb and [211]Bi decay products of actinon. Table 2.3 displays dissolution and absorption parameters (rapid, slow and bound) used in this study, following inhalation of actinon decay products.

The details about dissolution and absorption of inhaled actinon progeny are presented in the biokinetic section. The behavior of intake material within the body including dissolution, absorption and blood distribution represents biokinetic model.
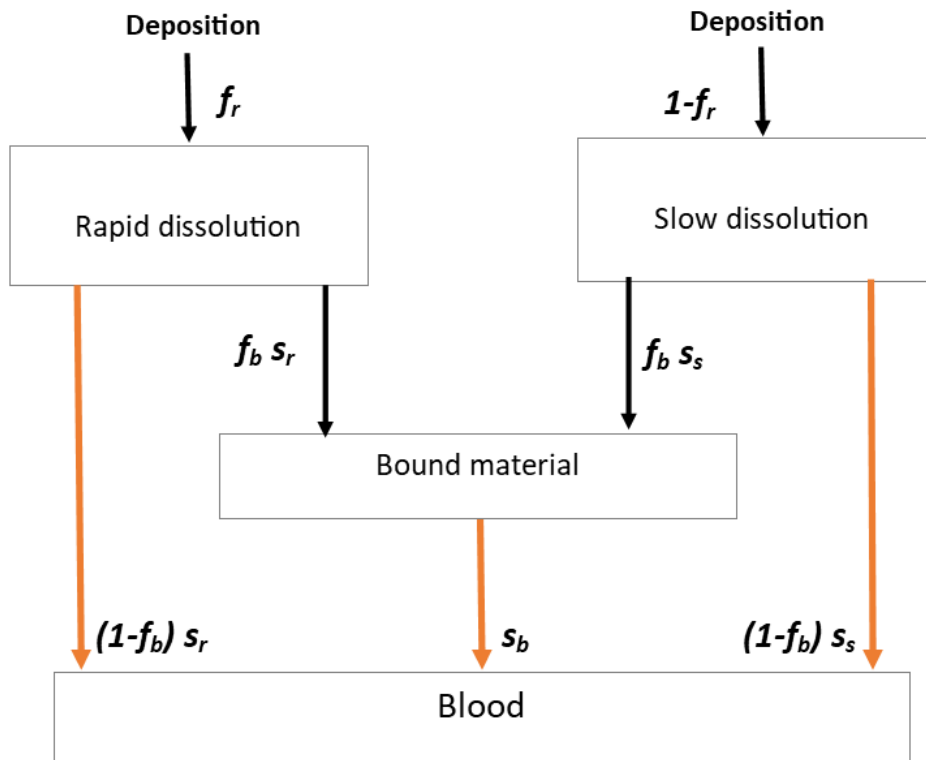
Figure 2.2: Compartment models representing time-dependent absorption into blood (dissolution and uptake). f_r is a fraction of deposited material which dissolves relatively rapidly at a rate s_r and (1-f_r) represents the remaining fraction of the deposited material that dissolves more slowly at a rate s_s.[32]

2.1.3 Progeny radionuclides formed in the respiratory tract

In general, progeny radionuclides formed before inhalation and inhaled with its parent are treated as separate intakes. However, the treatment of progeny radionuclides formed in the respiratory tract after radioactive decay of its parent are based on some assumptions. Those assumptions concern the clearence (dissolution and absorption parameters) of a progeny radionuclides from respiratory tract to body fluids. It is assumed that, the particle matrix determined the rate at which a particle dissociates. Therefore the dissolution parameter values of the inhaled material would be applied to progeny radionuclides formed within particles in the respiratory tract. This is called "shared kinetics". It is also assumed that, the behaviour of dissociated material would depend on its elemental form. For instance, the bound parameter values for a progeny radionuclide would not be those of its parent. This is called "independent kinetics". In the present study, the shared kinetics is used on ^{211}Bi formed in the respiratory tract after inhalation of ^{211}Pb progeny of ^{219}Rn. The dissolution and absorption parameter values of ^{211}Pb
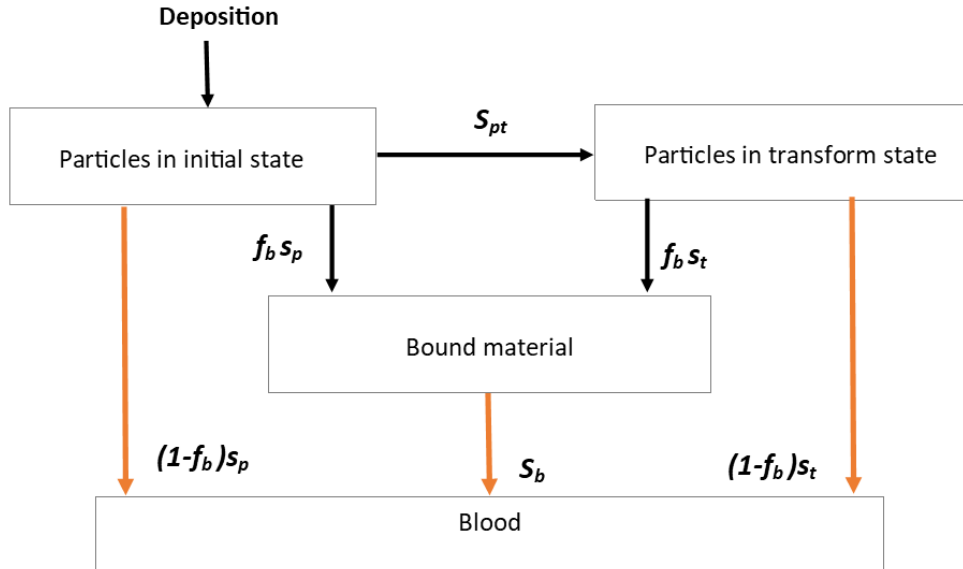
Figure 2.3: Compartment models representing time-dependent absorption into blood (dissolution and uptake).The deposited material in the respiratory tract is assigned to a compartment labelled "particles in initial state" which dissolves at a constant rate s_p and transferred simulataneously with a constant rate s_{pt} to a compartment labelled "particles in transform state". The new deposited material in the PTS has its own dissolution rate s_t. The initial dissolution rate denoted s_p and the final dissolution rate denoted s_t [32].

Table 2.4: Absorption parameter values for inhaled and ingested lead and bismuth [2].

Radon progeny	Dissolution parameter			Uptake parameter		Absorption from HATM
	f_r	s_r (d^{-1})	s_s (d^{-1})	f_b	s_b (d^{-1})	f_A
Lead	0.1	100	1.7	0.5	1.7	0.20
Bismuth	1	1	-	0	-	0.05

are used for ^{211}Bi formed in the respiratory regions. The absorbed material in blood reaches systemic circulation which is described by the systemic model.

2.2 The Human Alimentary Tract Model (HATM)

The Human Alimentary Tract Model has been developed by the ICRP to describe mainly the intake of radionuclides by ingestion[12]. It is also used with the HRTM in the case of inhalation. The particle deposited in the extrathoracic compartement denoted ET'$_2$ is moved to the oesophagus (oesophagus slow compartment) [32]. The HATM is applicable to all situations of radionuclide intake by children and adults. It consists of several organs such as oral cavity, oesophagus, stomach, small intestine and colon. All these organs are divided in compartments
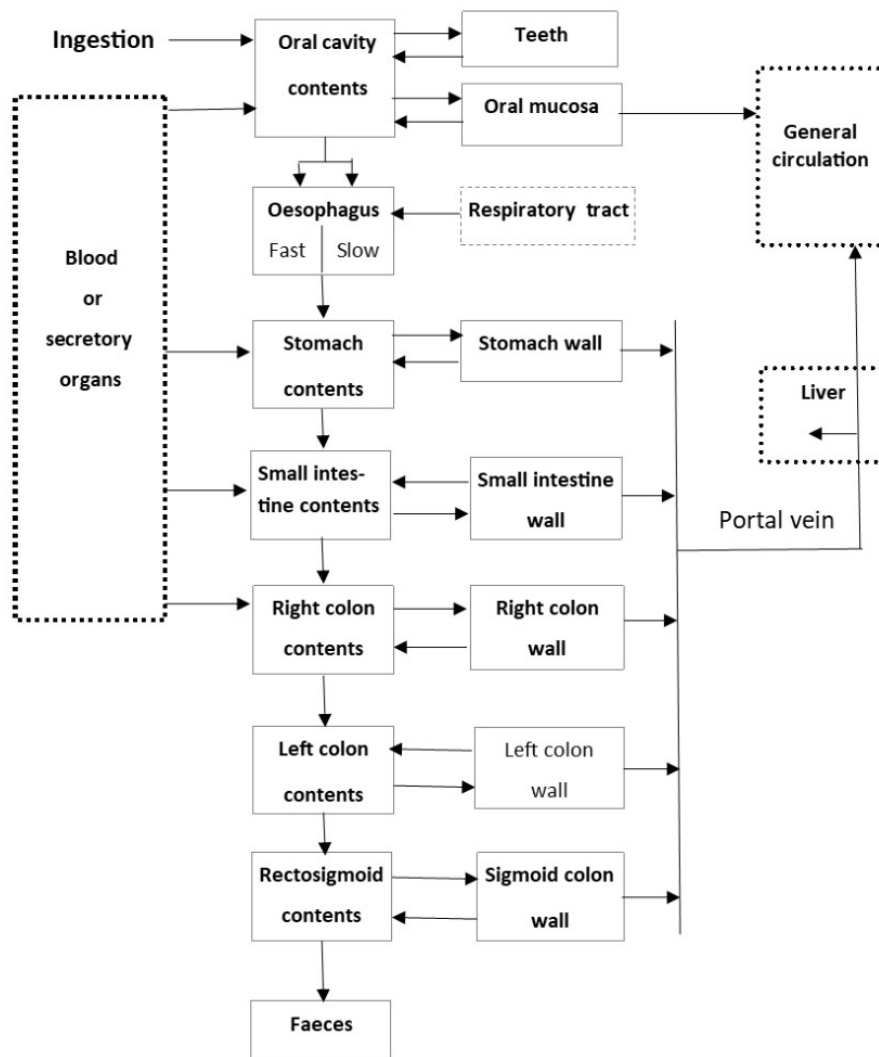
Figure 2.4: Structure of the Human Alimentary Tract Model (HATM). The dashed boxes are included to show connections between the HATM and the Human Respiratory Tract Model and systemic biokinetic models [12].

which describe the flow and retention of radionuclide. Fig.2.4 shows the update of HATM [12]. The default assumption is that radionuclide absorption takes place in the small intestine, but when some information is available the model allows absorption from other regions (stomach, right colon, left colon, etc...). In the particular case of actinon progeny, the absorption takes place in the small intestine and the transfer coefficient describing the uptake from small intestine to plasma is given by[12]:

$$\lambda_{SI,P} = \frac{f_A \lambda_{SI,RC}}{1 - f_A} \tag{2.4}$$

2.3 Biokinetic models of actinon progeny

A systemic model describes a time dependent distribution and excretion of an incorporated radionuclide in the body after it reaches systemic circulation. However, a biokinetic model describes the behaviour of radionuclides in the respiratory tract, alimentary tract and systemic model. To set up the biokinetics of inhaled radionuclides in human lungs and retention in other tissues and organs, the systemic models, the HRTM and the HATM are coupled to one comparmental model. To predict the retention and excretion of the inhaled aerosols, the inhalation biokinetic model is also used. In general a compartmental approach is used for those models. The body is divided in many pools of incorporated radionuclides between which radionuclide is exchanged. A uniform kinetic behaviour describes each pool. These pools could be identified as organs, tissues or a group of organs and linked to anatomical structures. The model takes into account the behaviour of the radionuclide (biokinetic model is common to each radioisotope) which depends on many factors, such as element, pathway of intake, chemical form and aerosol size (for inhalation). The reference models set up by ICRP describe the behaviour of the incorporated radionuclides in a reference person [7, 12, 2]. The biokinetic models describing inhalation of each actinon progeny are represented in Fig. 2.5 for ^{211}Pb and Fig. 2.6 for ^{211}Bi. In these figures arrows describe radionuclide distribution between compartments with the constant transfer rate values are given in Tables 2.5 and 2.6. The so called "Other soft tissues" compartemnts (Fig. 2.5 and 2.6) are defined to represent a group of soft tissues (source organs) that are not explicitly considered in the systemic model of the applied radioisotope. Note that each actinon progeny (^{211}Pb and ^{211}Bi) has its own systemic model and the structure and parameters of biokinetic models for different progeny are therefore different.

2.3.0.1 Systemic model for bismuth form within the body by the decay of lead

The characteristic model for bismuth applied in the OIR series publications of the ICRP, is used to build the systemic model for bismuth as a progeny of lead form within the body [2]. The systemic model of bismuth is modified by the addition of some compartements, which represent red marrow, spleen, skin, testes and ovaries. These compartments are explicitly identified in models for some other decay products of lead (e.g. polonium)[2]. Each of these compartments exchanges bismuth with plasma. Transfer coefficients for the added compartments are selected for reasonable consistency with the retention database underlying the characteristic model for bismuth and the retention curve for total soft tissues based on that original model [2]. The trans-
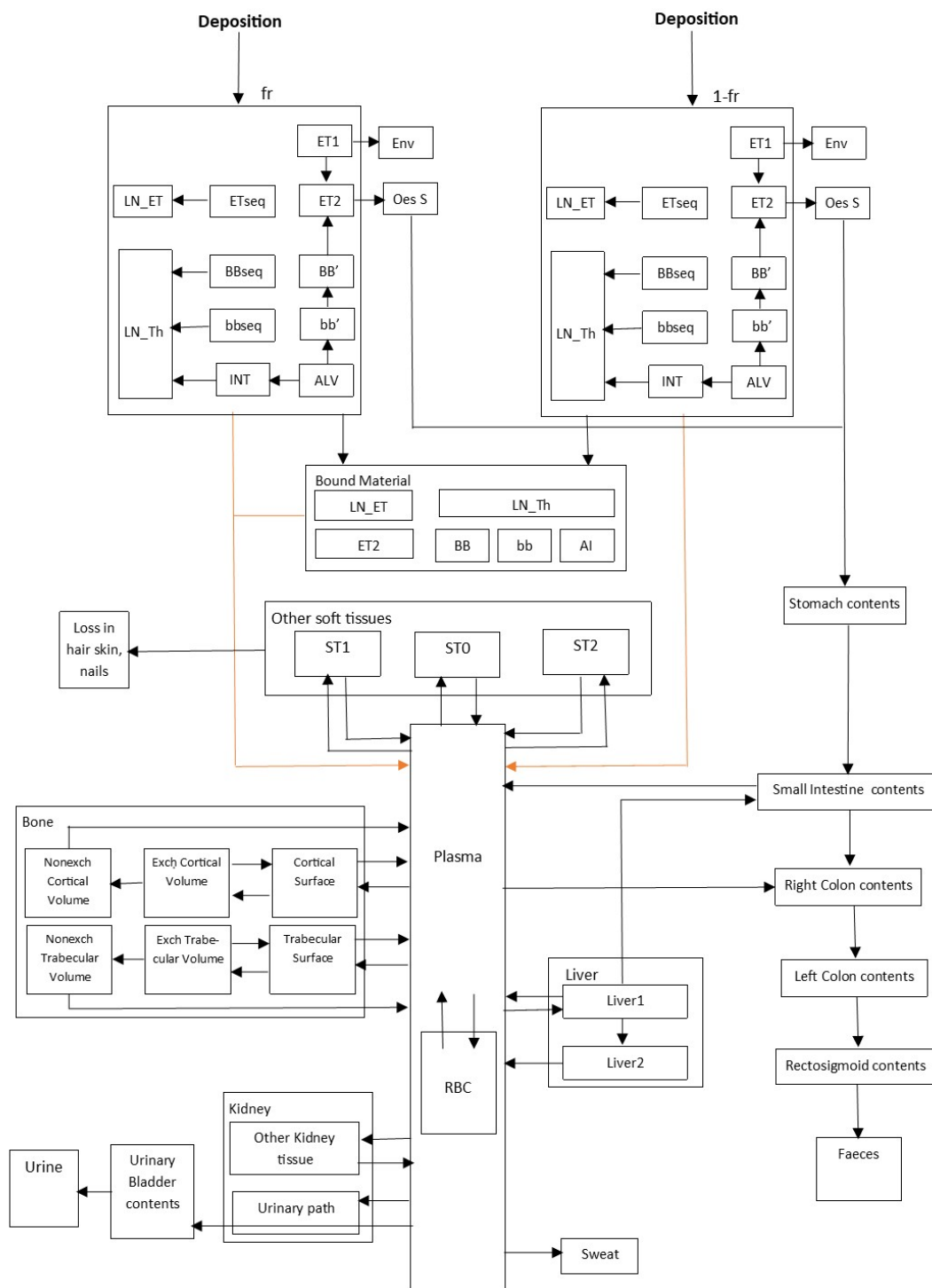
Figure 2.5: **Inhalation biokinetic compartmental model for lead.** It combines the HATM [12]. The systemic model of lead [2] and the HRTM [7, 32]. Extrathoracic region: ET_1 = anterior nose), ET_2 = posterior nasal passages, larynx, pharynx andmouth. LN_{ET} = lymph nodes. Thoracic region: BB = bronchial, bb = bronchiolar, AI = alveolar-interstitial, LN_{TH} = lymph nodes) [36]. ALV and INT = alveolar-interstitial. Other soft tissues: ST0 = soft tissue (fast turnover), ST1 = soft tissue (intermediate turnover), ST2 = soft tissue (slow turnover). Other compartments: Oes S = oesophagus slow, RBC = red blood cells. Bone: cortical surface, Exch Cortical Volume = exchangeable cortical volume, Nonexch Cortical Volume = Nonexchangeable cortical volume, Trabecular Surface. Exch Trabecular Volume = exchangeable trabecular volume, Nonexch Trabecular Volume = nonexchangeable trabecular volume

Table 2.5: Transfer coefficients in the biokinetic model for systemic lead [2].

From	To	Transfer coefficient (d^{-1})
Plasma	Urinary bladder contents	1.75
Plasma	Right colon contents	0.7
Plasma	Trabecular bone surface	4.86
Plasma	Cortical bone surface	3.89
Plasma	ST0	22.16
Plasma	ST1	0.7
Plasma	ST2	0.14
Plasma	Liver1	4.9
Plasma	Urinary path	2.45
Plasma	Other kidney tissue	0.0245
Plasma	RBC	28
Plasma	Excreta (sweat)	0.42
RBC	Plasma	0.139
Trabecular bone surface	Plasma	0.5
Trabecular bone surface	Exch trabecular bone volume	0.5
Cortical bone surface	Plasma	0.5
Cortical bone surface	Exch cortical bone volume	0.5
Exch trabecular bone volume	Trabecular bone surface	0.0185
Exch trabecular bone volume	Nonexch trabecular bone volume	0.0046
Exch cortical bone volume	Cortical bone surface	0.0185
Exch cortical bone volume	Nonexch cortical bone volume	0.0046
Nonexch trabecular bone volume	Plasma	0.000493
Nonexch cortical bone volume	Plasma	0.0000821
Liver1	Plasma	0.0312
Liver1	SI contents	0.0312
Liver1	Liver2	0.00693
Liver2	Plasma	0.0019
Urinary path	Urinary bladder contents	0.139
Other kidney tissue	Plasma	0.0019
ST0	Plasma	7.39
ST1	Plasma	0.00416
ST2	Plasma	0.00038
ST1	Excreta (hair, skin, nails)	0.00277
Urinary bladder contents	Urine	12

RBC, Red Blood Cells; exch, exchangeable; nonexch, non-exchangeable; SI, small intestine. ST0, ST1, and ST2 represent soft tissues with fast, intermediate, and slow turnover, respectively
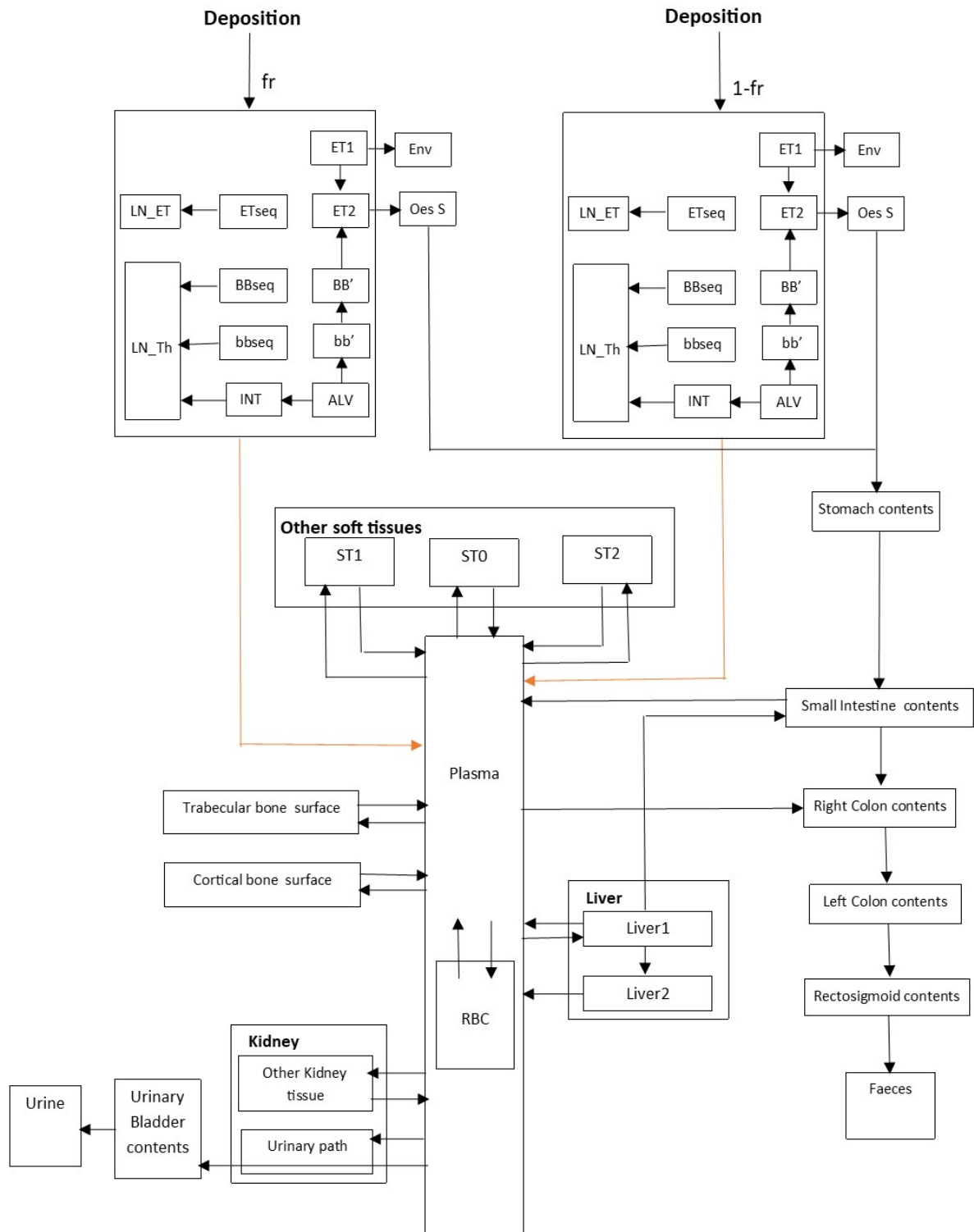
Figure 2.6: Inhalation biokinetic compartmental model for bismuth. It combines the HATM [12]. The systemic model of bismuth [2] and the HRTM [7, 32]. Extrathoracic region: ET_1 = anterior nose, ET_2 =posterior nasal passages, larynx, pharynx andmouth. LN_{ET} =lymph nodes. Thoracic region: BB = bronchial, bb = bronchiolar, AI = alveolar-interstitial, LN_{TH} = lymph nodes [36]. Other soft tissues: ST0 = soft tissue (fast turnover), ST1 = soft tissue (intermediate turnover), ST2 = soft tissue (slow turnover).

Table 2.6: Transfer coefficients in the biokinetic model for systemic bismuth [2]

From	To	Transfer coefficient (d^{-1})
Plasma	Urinary bladder contents	20
Plasma	Right colon contents	4.0
Plasma	RBC	0.5
Plasma	ST0	300
Plasma	ST1	4.2
Plasma	ST2	1.3
Plasma	Liver1	30
Plasma	Urinary path (kidneys)	30
Plasma	Other kidney tissue	5.0
Plasma	Cortical bone surface	2.5
Plasma	Trabecular bone surface	2.5
RBC	Plasma	0.173
ST0	Plasma	66.54
ST1	Plasma	0.0347
ST2	Plasma	0.00116
Liver1	Small intestine contents	0.208
Liver1	Liver2	0.139
Liver2	Plasma	0.0693
Urinary path (Kidneys)	Urinary bladder contents	0.693
Other kidney tissue	Plasma	0.139
Cortical bone surface	Plasma	0.0347
Trabecular bone surface	Plasma	0.0347
Urinary bladder contents	Urine	12

RBC, Red Blood Cells; SI, small intestine. ST0, ST1, and ST2 represent soft tissues with fast, intermediate, and slow turnover, respectively

fer coefficient rates from plasma to the added compartments are 0.3 d^{-1} for red marrow, 0.3 d^{-1} for skin, 0.02 d^{-1} for spleen, 0.003 d^{-1} for testes and 0.001 d^{-1} for ovaries. The transfer coefficients from each of the added compartment to plasma is 0.0347 d^{-1}. The bismuth is exchanged from plasma to other soft tissue compartment with a moderate turnover rate of 3.576 d^{-1} instead of 4.2 d^{-1}. The bismuth produced in a trabecular or cortical bone volume compartment is transferred to plasma with the reference turnover rate for that bone type.

The dynamic behavior of decay products of actinon in the organism is represented by a number of interconnected compartments with transfer coefficients describing the exchange of material. These interconnected compartments are called biokinetic models and are built by using the recent updated HRTM, HATM and systemic models for lead and bismuth (progeny of actinon)[32, 12, 2]. These biokinetic models are used for dose assessment by applying dosimetric models.

2.4 Dosimetric models

In this section, the different methods describing the calculations of the number of nuclear transformations, the radiation weighting S coefficient, the committed equivalent doses in each organ/tissue within the body and the effective doses of the inhaled actinon progeny are presented.

2.4.1 Number of nuclear transformations

In order to determine the number of nuclear transformations occurring in the body, the biokinetic models of inhaled actinon progeny are identified as compartmental models. A compartmental model is defined as a network where the nodes are compartments connected by arrows designing the flow of a deposited substance (radionuclide) from one compartment to another [41]. The complete biokinetic behaviour of inhaled actinon progeny in the lungs and other relevant organs, is described by systems of first order linear differential equations. These systems represent the rate of change of the radionuclide concentration, between compartments of the biokinetic models. The general form of those equations can be written as in [18, 11].

$$\frac{dA_i(t)}{dt} = \sum_r k_{r,i} A_r(t) - \sum_j k_{i,j} A_i(t) - \lambda A_i(t) + b_i(t) \tag{2.5}$$

where A_i(t) is the retention of the activity for a radionuclide in compartment i at time t, $k_{r,i}$ is the rate of change of the activity form compartment r to compartment i ($k_{i,j}$ is the rate of change of the activity from compartment i to compartment j), A_r(t) is the retention of the activity for a radionuclide in compartment r at time t. λ is the physical decay constant and b_i(t) is the input activity coming from the environment to compartment i at time t. The term on the left-hand side of Eq.2.5 represents the variation of the retention of the activity in compartment i at time t. The first term on the right-hand side of Eq.2.5 represents the inputs to the compartment i from the rest of compartments r $\neq$i and the second term represents the outputs from the compartment i to other compartments j $\neq$i. As mentionned above (section 2.2) there are initial compartments where the intake (deposition in respiratory tract regions) of the radionuclide takes place and final compartments form which the radionuclide is eliminated such as urine and faeces compartments. In this work a single input is considered. In general, a so called dummy compartment denoted n+1, is considered as the environement, receiving flow but not giving

input again to the system. The total rate of outputs form compartment i is defined as [41]:

$$k_i = \sum_{j=1, j\neq i}^{n+1} k_{i,j} \tag{2.6}$$

with i = 1, 2, 3, ..., n+1. In the case of $k_i = 0$ the compartment is a trap compartment (compartment which receives flow and does not transfer). This is always the case of the dummy compartment. The compartments such as faeces, urine and sweat represent dummy compartments for the inhaled actinon progeny exchanged within the body. The rewriting eq.2.5 as system of differential equations is given below [41]:

$$\frac{dA_1(t)}{dt} = \sum_r k_{r,1} A_r(t) - \sum_j k_{1,j} A_1(t) + b_1 \tag{2.7}$$

$$= \sum_r k_{r,1} A_r(t) - k_1 A_1(t) + b_1(t) \tag{2.8}$$

$$\dots \quad \dots \quad \dots\dots\dots\dots \tag{2.9}$$

$$\tag{2.10}$$

$$\frac{dA_n(t)}{dt} = \sum_r k_{r,n} A_r(t) - \sum_j k_{n,j} A_n(t) + b_n(t) \tag{2.11}$$

$$= \sum_r k_{r,n} A_r(t) - k_n A_n(t) + b_n(t) \tag{2.12}$$

The variation of quantity eliminated at time t for the whole system is given by[41]:

$$\frac{dA_{n+1}(t)}{dt} = \sum_r k_{r,n+1} A_r(t). \tag{2.13}$$

The above differential equations can also be written as:

$$\frac{dA(t)}{dt} = \Omega A(t) + b(t) \tag{2.14}$$

where A(t), Ω and b(t) are matrices and the general form of each matrix is given below:

$$A(t) = \begin{pmatrix} A_1(t) \\ A_2(t) \\ A_3(t) \\ \vdots \\ A_n(t) \\ A_{n+1}(t) \end{pmatrix}$$

the matrix Ω have non-positive elements in the diagonal and non-negative elements elsewhere:

$$\Omega = \begin{pmatrix} -k_1 & k_{2,1} & \dots & k_{n,1} & 0 \\ k_{1,2} & -k_2 & \dots & k_{n,2} & 0 \\ k_{1,3} & k_{2,3} & -k_3 & \dots & 0 \\ \dots & \dots & \dots & \dots & \dots \\ k_{1,n} & k_{2,n} & \dots & -k_n & 0 \\ k_{1,n+1} & k_{2,n+1} & \dots & k_{n,n+1} & 0 \end{pmatrix}$$

$$b(t) = \begin{pmatrix} b_1(t) \\ b_2(t) \\ b_3(t) \\ \vdots \\ b_n(t) \\ 0 \end{pmatrix}$$

The last column of the Ω matrix represents the dummy compartment as there is no output from this compartment. Therefore, it is zero column. Other columns are sum up to zero if there is no exchange between compartments. b(t) is a function which describes the kind of input from the environment (acute, chronic), and it is considered separately in the equation (eq.2.14). The general solution of the eq.2.13 is given as [41]:

$$A(t) = e^{t\Omega}A_0 + \int_0^t e^{(t-\tau)\Omega}b(\tau)d\tau \tag{2.15}$$

where A_0 is the initial condition which represents the initial deposition (deposition in the regions of the respiratory tract in case of inhalation). The solution depends on the matrix Ω. To get a simple solution some assumptions will be made on Ω: Ω is diagonalizable and the eigenvalues are real, etc...

The biokinetic models for actinon progeny are large compartmental systems, with about 50 compartments for each progeny. It would be quite complicated to solve those systems using common mathematical methods. In order to solve general models of inhaled actinon progeny (^{211}Pb and ^{211}Bi), the network is decomposed in subsystems. Those biokinetic models are divided in four subsystems for lead and three subsystems for bismuth. It is assumed that each subsystem is formed with compartments denoted by numbers, i = 1, 2, 3, ..., n+1. Fig.2.7 shows the biokinetic model of inhaled lead (^{211}Pb), which is divided in four subsystems. The

blue compartments are dummy compartments where excretions take place, and the orange compartments are pseudotrap compartments, which are the ending compartments for subsystems. The main idea to divide a compartmental system in subsystems, is the concept of pseudotrap compartments. They are built on the following conditions [41]:

- Pseudotrap compartments are the only compartments in the subsystem which have flow to another subsystem;

- There is no flow from pseudotrap compartments to other compartments in their own subsystem;

- Each of them has flow to one or more compartements in just one other subsystem;

- Recycling involving compartments of differents subsystems is not allowed.

The recycling occurs when the flow returns to the original compartment throughout others. In this case the rate of changed $k_{i,j} \neq 0$ (for the system forming cycle). A subsystem is solved independently by considering pseudotrap compartments as trap compartments (which do not flow to any other compartments). Once a subsystem is solved, afterwards the pseudotrap compartment becomes a compartment for another subsystem. The subsystems 1, 2 and 3 represent the respiratory tract which have been described (Fig. 2.7). The ending compartments of these subsystems are plasma and oesophagus slow. Both of them are considered trap compartments. The subsystem 4 represents the systemic model including some compartments of gastro intestinal tract (Fig. 2.7). In this case, because plasma and oesophagus slow in subsystems 1, 2 and 3 were assumed pseudotrap compartments, they are replaced with an input flow to oesophagus slow and to plasma (subsystem 4) given respectively by:

$$b_{Oes}(t) = \frac{dA_{OesS}(t)}{dt} \tag{2.16}$$

$$b_{plasma}(t) = \frac{dA_{plasma}(t)}{dt} \tag{2.17}$$

where $A_{OesS}(t)$ is the sum of the retention in compartments "Oes S" of subsystems 1 and 2, and $A_{Plama}(t)$ is also the sum of the retention in compartment "plasma" (solution of retention for pseudotrap compartment of subsystems 1, 2 and 3). Therefore, numbering plasma as compartment 1 and Oes S as 19, in subsystem 4 and the input function b(t) for the subsystem 4 is given by b(t) = (b_{plasma} (t), 0, 0...., 0.., ..., b_{Oes}(t), 0, 0,.....).
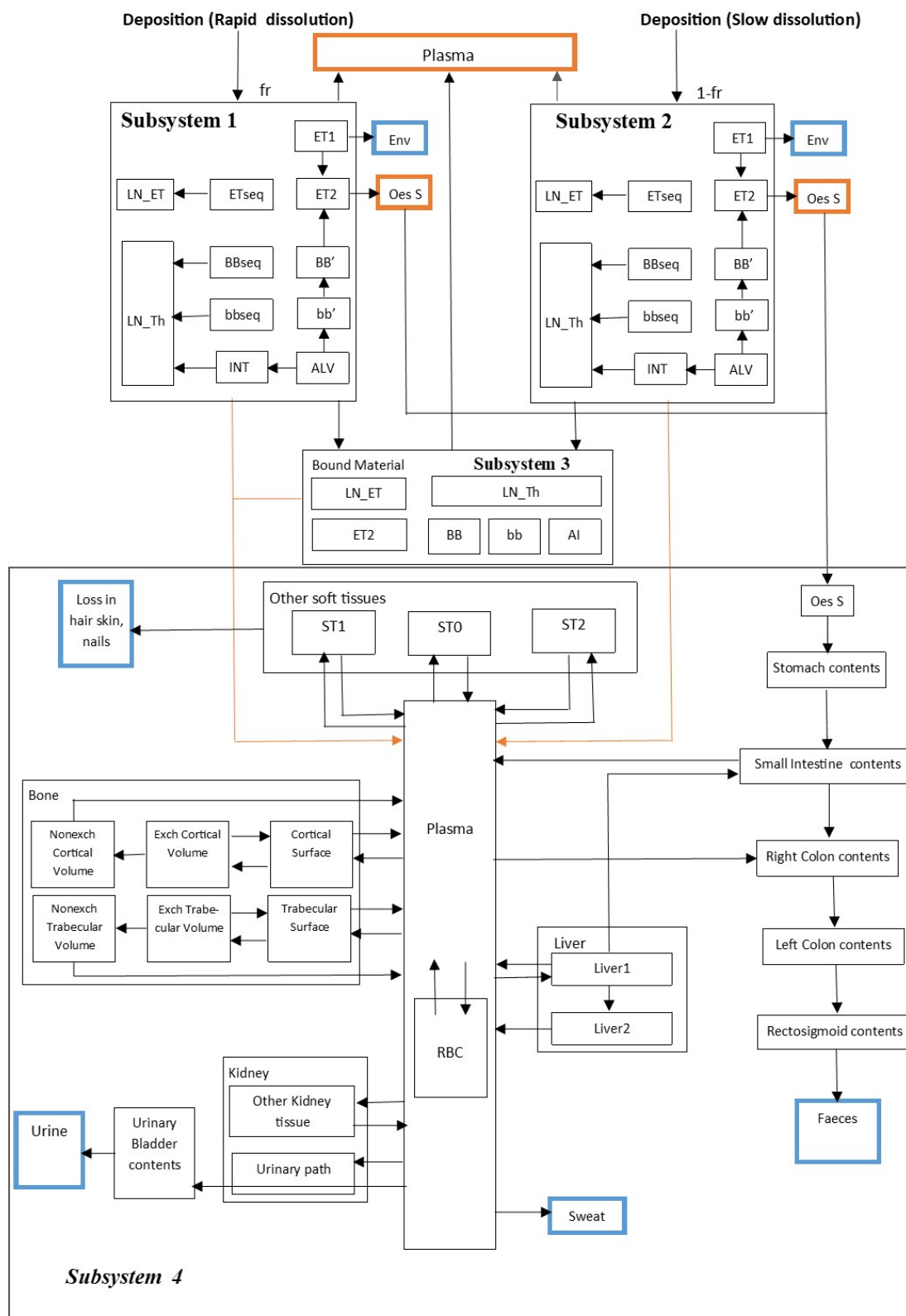
Figure 2.7: Biokinetic model of inhaled lead divided in four subsystems. The blue compartments represent dummy compartments and the orange compartments represent pseudotrap compartments. Plasma and Oes S (orange compartments) are the pseudotrap compartments which are common to three subsystems (1, 2 and 3).

The described subsystems have been mathematically implemented using a free package ICRP130-Models on the recent version of BIOKMOD (version 5.4). BIOKMOD (Biokinetic Modeling) is a computer tool developed by G. Sanchez using the Wolfram Mathematica programming language [42, 43]. The function **CompartMatrix** is used to build all Ω matrices for each subsystem, then adding the appropriate initial conditions and input function b(t), and finally the function **SystemDSolve** has been used to solve the the system of equations. Solutions of retention for some compartments of the inhaled unattached ^{211}Pb are given in Appendix. The number of nuclear transformations occurring in source region r_S during the commitment period (18250 days for adults) denoted $\tilde{A}_i(r_S)$ is given as follows:

$$\tilde{A}_i(r_S) = \sum_i \int_0^{18250} A_i(t)dt \tag{2.18}$$

where 18 250 (50 years) represents the number of days which is the commitment period for an adult. The summation in the equation above is over the association of kinetic compartments i forming source regions r_S. These numbers of nuclear transformations for actinon progeny were calculated by using Wolfram Mathematica software. The number of nuclear transformations per activity intake in the source region r_S is given in the following equation [18]:

$$\tilde{a}(r_S) = \frac{\tilde{A}(r_S)}{\sum_i A_i(0)} \tag{2.19}$$

where $A_i(0)$ represents the initial deposition fraction in each compartment i. The summation in the denominator is over the compartments contents at t= 0. In the case of inhalation, the denominator considers only the activity intakes and deposited in the compartments of the HRTM. The exhaled activity is included.

2.4.2   Radiation weighted S coefficient

The radiation weighted S coefficient denoted $S_w(r_T \leftarrow r_S)$ represents the time-dependent equivalent dose rate in the target tissue r_T per unit activity present in source tissue r_S. $S_w(r_T \leftarrow r_S)$ was calculated for each radiation type emitted by the actinon progeny. The general form of the S_w coefficient is given by [18].

$$S_w(r_T \leftarrow r_S) = \sum_R w_R \sum_i E_{Ri} Y_{Ri} \phi(r_T \leftarrow r_S, E_{Ri}) \tag{2.20}$$

where w_R is the radiation weighting factor for radiation type R, E_{Ri} is the energy of the ith radiation of type R emitted in the nuclear transformations of the radionuclide in joules (J); Y_{Ri} is the yield of the ith radiation of type R per nuclear transformations (Bq.s^{-1}); ϕ ($r_T \leftarrow r_S$, E_{Ri}) is the specific absorbed fraction denoted as SAF which is defined as the fraction of energy E_{Ri} of radiation type R emitted within the source tissue/organ r_S that is absorbed per mass in the target tissue r_T (kg^{-1}). Table 2.7 displays the energies and yields for actinon progeny used in this study. In beta decay process, the neutrino emitted carries off a portion of the available energy. However, this energy does not contribute to dose, due to the negligible interaction of neutrino with matter. As mentioned in the ICRP, the spectral data are used in the calculation of Sw rather than mean energy [18]. Therefore, the inner summation (Eq. 2.20) is replaced by the integral over the beta particle spectrum. The expression of S_w for beta decay process is given by:

$$S_w(r_T \leftarrow r_S) = w_\beta \int_0^{E_{max}} P(E)dE\phi(r_T \leftarrow r_S, E) \qquad (2.21)$$

where $P(E)$ replaced Y_R (yield) of the Eq.2.20 and is proportional to the probability that beta particle will be emitted with kinetic energy between E and $E+dE$, E represents the beta energy. $P(E)$ and E are taken from DECDATA software [44]. DECDATA means "Decay Data" for dosimetric calculation is a free software developed by the ICRP. The software enables viewing the radiological properties of radionuclides in a tabular and graphical manner. Data on the yields and energies of the radiations for radionuclides can be extracted into ASCII files for subsequent use [44]. The calculation of intergral over the beta particle spectrum is made by numerical methods. The values of $P(E)$ and E have been extracting from DECDATA software, then for each value of energy E, a specific absorbed fraction $\phi(r_T \leftarrow r_S, E)$ is determined by linear interpolation on Microsoft Excel. The specific absorbed fractions values are taken from the electronic data of ICRP [18]. ^{211}Pb decays to the nuclide ^{211}Bi through beta particle emission. In this case the spectral data are used for the calculation of S_w (Eq.2.21). However, ^{211}Bi decays to the nuclide of ^{207}Tl through alpha particle emission and to ^{211}Po through beta emission. The form of $S_w(r_T \leftarrow r_S)$ of alpha emission is given by:

$$S_w(r_T \leftarrow r_S) = w_\alpha E_\alpha Y_\alpha \phi(r_T \leftarrow r_S, E_\alpha) \qquad (2.22)$$

$w_{\alpha,\beta,\gamma}$ values (radiation weighting factor) are taken from ICRP publication [30]. For the compartment called "Other soft tissues" (ST0, ST1 and ST2) in the systemic models, including

several source regions r_S, the specific absorbed fraction $\phi(r_T \leftarrow r_S)$ was calculated as [18]:

$$\phi(r_T \leftarrow Other) = \frac{1}{M_{Other}} \sum_{r_S} M_{r_S} \phi(r_T \leftarrow r_S) \tag{2.23}$$

where M_{Other} is the sum of masses of all organs which are implicitly represented in the compartment denoted Other soft tissue, M_{r_S} is the mass of a specific source tissue. The calculation of the specific absorbed fractions for ?Other soft tissues? has been done using the following steps:

- The selection of Other soft tissues in the list of source organs given in the ICRP [18]. These source organs (on the table of source organs) which are not explicitly represent in the systemic model of lead (or bismuth) are identify as Other soft tissues with the exception made for mineral bone (cortical and trabecular form) and teeth.

- The specific absorbed fractions values are taken from the electronic data of ICRP 133. The linear interpolation was done on Microsoft excel to find each corresponding value of $\phi(r_T \leftarrow r_S)$ to E_{Ri}.

- The masses of source organs are taken in the ICRP publication [18]. M_{Other} represents the sum of masses for the selected source organs (Other).

Table 2.7: Decay properties (energies and yields) for actinon progeny [45]

| Radionuclide | Main radiation energies (E) and Yields (Y) | | | | | |
| | Alpha | | Beta | | Gamma | |
	E(MeV)	Y (/nt)	E(MeV)	Y (/nt)	E(MeV)	Y (/nt)
^{211}Pb	-	-	4.497E-01	1.00	5.86E-01	1.087E-01
^{211}Bi	6.567	9.972E-01	1.732E-01	2.760E-02	3.511E-01	1.288E-01

/nt= per nuclear transformations

2.4.3   Committed equivalent dose and committed effective dose

The committed equivalent dose $h(r_T)$ in the target region was calculated for reference adult male $h^M(r_T)$ and reference adult female $h^F(r_T)$ as [18]:

$$h^M(r_T) = \sum_{r_S} \tilde{a}(r_S) S_w^M(r_T \leftarrow r_S) \tag{2.24}$$

Table 2.8: Target region fractional weights, f (r_T, T) [18].

Tissue,T	r_T	Acronym	f (r_T, T)
Extrathoracic region	ET_1 basal cells	ET_1-bas	0.001
	ET_2 basal cells	ET_2-bas	0.999
Lung	Bronchi basal cells	Bronch-bas	1/6
	Bronchi secretory cells	Bronch-sec	1/6
	Bronchiolar secretory cells	Bchiol-sec	1/3
	Alveolar-interstitial	AI	1/3
Colon	Right colon	RC-stem	0.4
	Left colon	LC-stem	0.4
	Rectosigmoid colon	RS-stem	0.2
Lymphatic nodes	Extrathoracic lymph nodes	LN-ET	0.08
	Thoracic lymph nodes	LN-Th	0.08
	Systemic lymph nodes	LN-Sys	0.84

$$h^F(r_T) = \sum_{r_S} \tilde{a}(r_S) S_w^F(r_T \leftarrow r_S) \tag{2.25}$$

where $S_w^M(r_T \leftarrow r_S)$ and $S_w^F(r_T \leftarrow r_S)$ are the S coefficient for male and female respectively. There is an exception for target regions consisting of several target tissues: extrathoracic region, lung, colon and lymphatic nodes. For each target region in those tissues there is an associated fractional weighting factor. The committed equivalent dose for those particular regions was calculated as [18]:

$$h_T^M = \sum_{r_T} f(r_T, T) h^M(r_T) \tag{2.26}$$

$$h_T^F = \sum_{r_T} f(r_T, T) h^F(r_T) \tag{2.27}$$

where $f(r_T, T)$ is the fractional weight, the values are given in Table 2.8. The committed effective dose coefficient was calculated as [30]:

$$e(50) = \sum_T w_T \left(\frac{h_T^M + h_T^F}{2} \right) \tag{2.28}$$

where w_T is the weighting factor for tissue T taken from the ICRP publication and given in Table 1.3 [30]. Microsoft Excel was used to calculate the radiation weighting S coefficient, the committed equivalent dose coefficient and the committed effective dose coefficient after inhalation of the actinon progeny.

Conclusion

The purpose of this chapter was to present the material used for the deposition, dissolution and absorption of inhaled actinon progeny such as; HRTM, HATM and biokinetics models, as well as the methodology of the calculation of committed equivalent dose coefficients in each target tissues and dose coefficents following inhalation actinon progeny (^{211}Pb and ^{211}Bi). The next chapter will present and discuss the results found out after inhalation of actinon progeny.

Chapter 3

Results and discussion

Introduction

This chapter presents in detail the results obtained in this study. These results will be discussed and compared to those existing in the literature whenever the need arises. Any of shortcomings in the methods used will be addressed.

3.1 Aerosol fractional deposition in the human respiratory tract

The particle deposition fraction in the HRTM used in the study is interpreted using the general description made in the ICRP [7]. Due to the effect of Brownian motion, nearly 90% of small particles (around 1 nm) are deposited in the ET region. The increase of particle size reduces the effect of brownian motion and more particles could reach other part of respiratory tract (BB, bb and AI) and could be exhaled [7]. When particle size increase to hundereds of nanometers, gravitational sedimentation and inertial impaction become dominant, which lead to an increase in ET region [21]. The unattached particles are easily deposited (more than 95 %) that they could barely reach the AI area (0.59 % deposit for 1 nm). This means exhalation hardly takes away unattached particles [21]. However, the exhalation has an important effect on attached particles. It allows around or less than 40 % deposit in HRTM (41.29 % for 60 nm and 27.51 % for 500 nm), nearly half of which deposit in the AI region (27.90 % for the size of 60 nm and 9.05 % for 500 nm) [21].

3.2   Number of nuclear transformations per activity intake

Number of nuclear transformations per activity intake for actinon progeny were calculated using methods described in chapter 2 (section 2.4.1). Tables 3.1, 3.2 and 3.3 display number of nuclear transformations per activity intake for the inhaled ^{211}Pb, for ^{211}Bi formed within the body after inhalation of ^{211}Pb and for the inhaled ^{211}Bi respectively (Eq. 2.19). For all actinon progeny including ^{211}Bi formed within the body after inhalation of ^{211}Pb, the number of nuclear transformations per activity intake were the highest in ET1-sur for the unattached (1 nm) and accumulation (500 nm) modes. However, for nucleation mode (60 nm) "ALV" was the region with the highest number of nuclear transformations per activity intake. Those values strongly depend on the deposition fraction, e.g. the deposition fraction in ET1 region which represent more than 50% (unattached mode) of the inhaled material, has the higest number of nuclear transformations per activity intake for all actinon progeny deposited in the respiratory tract. In the same way "ALV" region with the deposition of 27.90% (nucleation mode) for inhaled material has the highest number of nuclear transformations per activity intake. Source organs such as ET1-sur, ALV, blood, Other, bronchiole, lungs, st-cont, RT-air and lungs-tissues were the organs with have relatively high number of nuclear transformations per activity intake for all modes (unattached, nucleation and accumulation) after inhalation actinon progeny (^{211}Pb and ^{211}Bi). ^{211}Bi formed within the body after inhalation of ^{211}Pb are more important than inhaled ^{211}Bi in terms of number of nuclear transformations per activity intake (see tables 3.2 and 3.3). Therefore, ^{211}Bi due to its short half-life (2.17 m), the decay process (disintergation) would start while the inhalation occurs. In general ã(r_S) values are closely depend on some factors such as; deposition fraction, input type (acute, chronic or single), decay constant (^{211}Pb = 27.649 d^{-1} and ^{211}Bi = 466.4167 d^{-1}) and transfer rate between compartments (describes by metabolism).ã(r_S) values depend on the capacity of retention of the concerned source region. This retention also depends on several factors, such as biological half-life which is linked to the source region, the physical-chemical properties (absorption and binding parameters) and the amount of the inhaled material. For each nuclear transformation an energy is released depending on the type of radionuclide. This energy would interact with organ/tissue (target tissue). The amount of energy reaches each target tissue is quantified with Absorbed Fractions (AF). Absorbed fractions were calculated using monte carlo simulation on voxel phantoms (reference adult).

Table 3.1: Values for the number of nuclear transformations per activity intake after inhalation of ^{211}Pb decay product of ^{219}Rn.

Source Organs	Number of nuclear transformations per activity intake $\tilde{a}(r_S)$		
	Unattached	Nucleation	Accumulation
Other	1.61E+01	2,16E+02	1,37E+02
Oesophag-s	9.63E+00	9.91E-01	3.99E+00
St-cont	4.32E+02	4.44E+01	1.79E+02
SI-cont	2.53E+02	2,60E+01	1,05E+02
RC-cont	5.17E+01	1.30E+01	2.60E+01
LC-cont	3.49E+00	8.75E-01	1.76E+00
RS-cont	2.36E-01	5.93E-02	1,19E-01
ET1-sur	1.53E+03	2.71E+02	1.13E+03
ET2-sur	1.20E+01	2.17E+01	8.72E+01
ET2-bnd	2.63E+01	3.70E+01	1.49E+02
ET2-seq	1.54E+00	6.82E-02	2.83E-01
LN-ET	5.36E-05	1.44E-06	5.99E-06
Bronchi	1.65E+02	1.85E+01	1.37E+01
Bronchi-b	1.33E+01	3.16E+01	2.34E+01
Bronchi-q	4.38E-01	3.05E-02	2.95E-02
Brchiole	2.75E+02	1.07E+02	3.48E+01
Brchiole-b	1.95E+01	1.82E+02	5.95E+01
Brchiole-q	5.55E-01	2.14E-01	6.99E-02
ALV	1.74E+01	1.24E+03	6.02E+02
LN-Th	3.45E-05	5.18E-06	2.11E-06
Lungs[a]	5.40E+02	2.23E+03	1.15E+03
Blood[b]	4.87E+01	6.56E+02	4.15E+02
C-bone-S	3.30E+00	4.43E+01	2.80E+01
C-bone-V	5.96E-02	8.01E-01	5.06E-01
T-bone-S	4.12E+00	5.54E+01	3.50E+01
T-bone-V	7.44E-02	1.00E+00	6.35E-01
Kidneys	2.16E+00	2.91E+01	1.84E+01
Liver	4.29E+00	5.77E+01	3.65E+01
UB-cont	1.08E+00	1.45E+01	9.18E+00
Lung-Tis[c]	4.92E+02	1.58E+03	7.34E+02
RT-air	1.57E+03	3.30E+02	1.36E+03

[a] It represents the sum of the number of nuclear transformations per activity intake for lung tissues (AI, bronchiolar and bronchiole) and blood. [b] represents the sum of the number of nuclear transformations per activity intake in the compartments RBC and plasma with form blood. [c] describes the sum of the number of nuclear transformations per activity intake in the lung tissues without blood.

Table 3.2: Values for the number of nuclear transformations per activity intake for ^{211}Bi produced within the body by the decay of inhaled ^{211}Pb .

Source Organs	Number of nuclear transformations per AI ã(r_S)		
	Unattached	Nucleation	Accumulation
Other	2.22E+01	2.75E+02	1.74E+02
Oesophag-s	8,50E+00	8.81E-01	3.51E+00
St-cont	4.51E+02	4.64E+01	1.87E+02
SI-cont	2.69E+02	2.77E+01	1.11E+02
RC-cont	5.50E+01	1.45E+01	2,81E+01
LC-cont	3.71E+00	9.33E-01	1,87E+00
RS-cont	2.51E-01	6.30E-02	1.26E-01
ET1-sur	1.52E+03	2.70E+02	1.12E+03
ET2-sur	1.78E+02	1.85E+01	7.37E+01
ET2-seq	1.53E+00	6.68E-02	2.77E-01
LN-ET	5.46E-05	6.64E-07	2.75E-06
Bronchi	1.61E+02	1.71E+01	1.32E+01
Bronchi-q	4.34E-01	2.99E-02	2.89E-02
Brchiole	2.73E+02	1.04E+02	3.41E+01
Brchiole-q	5.50E-01	2.10E-01	6.84E-02
ALV	1.62E+01	4.48E+02	2.18E+02
LN-Th	3.51E-05	2.38E-06	9.68E-07
Lungs	4.81E+02	9.41E+02	5.00E+02
Blood	3.06E+01	3.72E+02	2.34E+02
C-bone-S	3.37E+00	4.51E+01	2.85E+01
C-bone-V	9.79E-06	1.33E-04	8.41E-05
T-bone-S	4.19E+00	5.62E+01	3.55E+01
T-bone-V	1.23E-05	1.67E-04	1.05E-04
Kidneys	1.23E-05	4.01E+01	2.53E+01
Liver	5.19E+00	6.72E+01	4.25E+01
UB-cont	1.64E+00	2.04E+01	1.29E+01
Lung-Tis	4.50E+02	5.70E+02	2.65E+02
RT-air	1.70E+03	2.88E+02	1.20E+03
<-R-marrow	8.97E-03	9.48E-02	5.95E-02
Skin	8.97E-04	9.48E-02	5.95E-02
Spleen	5.97E-04	6.32E-03	3.97E-03
Ovaries	2.97E-05	3.16E-04	1.96E-04
Testes	8.92E-05	9.47E-04	5.94E-04

Oesophagus-s, oesophagus slow; St-cont, stomach contents; SI-cont, small intestine contents; RC-cont, Right colon content; LC-cont, Left colon content; RS-cont, Rectosigmoid colon content; ET1-sur, ET1 surface; ET2-sur, ET2 surface; ET2-bnd, ET2 bound region; ET2-seq, ET2 sequestered region; LN-ET, Extrathoracic lymph nodes; Bronchi, Bronchial surface; Bronchi-b, Bronchial bound region; Bronchi-q, Bronchial sequestered region; Brchiole, Bronchiolar surface; Brchiole-b, Bronchiolar bound region; Brchiole-q, Bronchiolar sequestered region; AI, Alveolar-interstitial; LN-Th, Thoracic lymph nodes; C-bone-S, Cortical bone surface; C-bone-V, Cortical bone; T-bone-S, Trabecular bone surface; T-bone-V, Trabecular bone; UB-cont, Urinary bladder content; Lung-Tis, Lung tissue; RT-air, Respiratory tract air; R-marrow, Red (active) marrow.

Table 3.3: Values for the number of nuclear transformations per activity intake after inhalation of^{211}Bi decay product of^{211}Rn.

Source Organs	Number of nuclear transformations per AI ã(r_S)		
	Unattached	Nucleation	Accumulation
Other	5.44E-02	1.15E-01	7.38E-02
Oesophag-s	1.66E+00	2.96E-01	1.22E+00
St-cont	7.38E+00	1.31E+00	5.41E+00
SI-cont	3.21E-01	5.71E-02	2.35E-01
RC-cont	4.92E-03	2.44E-03	4.11E-03
LC-cont	2.10E-05	1.04E-05	1.76E-05
RS-cont	1.22E-07	4.62E-08	7.91E-08
ET1-sur	9.72E+01	1.72E+01	7.16E+01
ET2-sur	4.37E+01	7.77E+00	3.20E+01
ET2-seq	1.05E-01	1.86E-02	7.73E-02
LN-ET	2.25E-07	3.98E-08	1.65E-07
Bronchi	1.46E+01	4.08E+00	3.94E+00
Brchiole	1.88E+01	2.92E+01	9.52E+00
Brchiole-q	3.77E-02	5.85E-02	1.91E-02
ALV	1.11E+00	1.25E+02	6.08E+01
LN-Th	1.44E-07	1.43E-07	5.81E-08
Lungs	3.47E+01	1.59E+02	7.45E+01
Blood	9.47E-02	2.00E-01	1.29E-01
C-bone-S	5.07E-04	1.07E-03	6.88E-04
T-bone-S	5.07E-04	1.07E-03	6.88E-04
Kidneys	7.09E-03	1.50E-02	9.63E-03
Liver	6.09E-03	1.29E-02	8.26E-03
UB-cont	3.96E-03	8.39E-03	5.38E-03
Lung-Tis	3.46E+01	1.59E+02	7.43E+01
RT-air	1.41E+02	2.50E+01	1.04E+02

Oesophagus-s, oesophagus slow; St-cont, stomach contents; SI-cont, small intestine contents; RC-cont, Right colon content; LC-cont, Left colon content; RS-cont, Rectosigmoid colon content; ET1-sur, ET1 surface; ET2-sur, ET2 surface; ET2-bnd, ET2 bound region; ET2-seq, ET2 sequestered region; LN-ET, Extrathoracic lymph nodes; Bronchi, Bronchial surface; Bronchi-b, Bronchial bound region; Bronchi-q, Bronchial sequestered region; Brchiole, Bronchiolar surface; Brchiole-b, Bronchiolar bound region; Brchiole-q, Bronchiolar sequestered region; AI, Alveolar-interstitial; LN-Th, Thoracic lymph nodes; C-bone-S, Cortical bone surface; C-bone-V, Cortical bone; T-bone-S, Trabecular bone surface; T-bone-V, Trabecular bone; UB-cont, Urinary bladder content; Lung-Tis, Lung tissue; RT-air, Respiratory tract air; R-marrow, Red (active) marrow.

3.3   Committed equivalent dose and committed effective dose

The committed equivalent dose coefficients (reference adult male and female) for inhaled ^{211}Pb and ^{211}Bi in each target organ/tissue were calculated using Eq.2.26 and 2.27 (chapter 2). The voxel phantoms are used for the calculations of Specific Absorbed Fractions (SAFs taken form the ICRP [18]) given in the Eq. 2.22, 2.23, 2.24 and 2.25 (Chapter 2). These phantoms for calculations of energy deposition in body organs and tissues (so called "target regions") should accommodate all organs and tissues which are important to the estimation of human exposure to ionising radiaton [46]. For the dose assessment purposes, the target regions are: active (red) bone marrow, adrenals, brain, breast, colon, endosteal tissue (bone surface), extrathoracic (ET) airways, eye (lens), gall bladder, heart, kidneys, liver, lungs, lymphatic nodes muscle, oesophagus, oral mucosa, ovaries, pancreas, prostate, salivary glands, skin, small intestine, spleen, stomach, testes, thymus, thyroid, urinary bladder, uterus and thoracic tissues [46]. SAFs are one of the most important factor for committed equivalent doses assessment. They are radiation type, amount of energy, volume, masse and distance (between target and source regions) depending. Monte Carlo simulations were used for the computation of those SAFs [18, 46]. The alpha, electron, photon and neutron SAF files for adult male and female are taken on the ICRP website. The calculated committed equivalent dose coefficients of the inhaled actinon progeny for all target regions are shown in Tables 3.4 and 3.5 (more details) . Due to the difference between masses of reference adult male and female, the committed equivalent dose for each target tissue following inhalation of actinon progeny by an adult reference female is higher than that of an adult reference male. This is explained by the fact that the absorbed dose by a tissue is inversely proportional to the mass of this tissue. In general, the equivalent dose coefficients in the lung and extrathoracic tissues were relatively larger than in other organs for the three particles sizes (radon and thoron progeny as well). For the progeny of ^{211}Pb, the equivalent doses in bronchi basal cells, bronchiole basal cells and ET_1 basal cells were the highest for each mode: unattached, nucleation and accumulation respectively. However, for the progeny of ^{211}Bi the ET_2 basal cells, bronchiole basal cells and ET_2 basal cells were the target regions where the equivalent dose coefficient was the highest for unattached (1 nm), nucleation (60 nm) and accumulation (500 nm) modes, respectively. The committed equivalent dose in each tissue/organ for actinon progeny in unattached and attached modes are given in Table 3.7 (including equivalent dose for remainder tissues and lung). For both actinon progeny the lung equivalent dose was the highest for unattached and nucleation modes. However, the ET airways (extrathoracic region)

equivalent dose was the highest for accumulation mode. The lung dose strongly depends on the percentage of the deposition fraction within the bronchial and bronchiolar tissues. The organs and effective doses (dose coefficients) after inhalation actinon (^{219}Rn) progeny. ^{211}Pb and ^{211}Bi in unattached and attached (nucleation and accumulation) modes are given in Table 3.6. The dose coefficient of short-lived actinon progeny was the highest for unattached mode (1 nm).

In this study, the lung equivalent dose for ^{211}Pb (4.65×10^{-7}Sv.Bq^{-1}) of the unattached was 4-9 times lager than the values (1.12×10^{-7} and 5.06×10^{-8}Sv.Bq^{-1}) of nucleation and accumulation. For ^{211}Bi, the lung equivalent dose (3.76×10^{-8} Sv.Bq^{-1}) of the unattached mode was 1-3 times larger than those (2.91×10^{-8} and 1.39×10^{-8}Sv.Bq^{-1}) of the other modes. For actinon progeny, organs such as kidneys, colon, stomach and oesophagus received relatively high doses compared to other organs. Equivalent doses following inhalation of ^{211}Pb are dominated by alpha radiations emitted by ^{211}Bi formed within the body after ^{211}Pb decays. More than 98% of each organ equivalent dose of inhaled ^{211}Pb come from alpha radiation emitted by ^{211}Bi within the body. In general others decay products of actinon progeny such as ^{207}Tl and ^{211}Po formed within the body are neglected in dose calculation (short half-lives and the low proportion of 0.276% for ^{211}Po).

The inhalation dose coefficients of ^{211}Pb and ^{211}Bi for adults are 5.78×10^{-8} and 4.48×10^{-9}Sv.Bq^{-1} for unattached particles (1 nm), and 1.41×10^{-8} and 3.55×10^{-9}Sv.Bq^{-1} for attached particles (nucleation mode 60 nm) and 7.43×10^{-9} and 1.91×10^{-9}Sv.Bq^{-1} for attached particles (accumulation mode 500 nm). Those effective dose coefficents are in comparison with the values of 6.6×10^{-8} and 4.8×10^{-9}Sv.Bq^{-1} in the unattached mode (1 nm), 2.2×10^{-8} and 1.5×10^{-9}Sv.Bq^{-1} in the nucleation mode (60 nm) and 7.4×10^{-9} and 5.3×10^{-10}Sv.Bq^{-1} in the accumulation mode (500 nm) for ^{211}Pb and ^{211}Bi respectively, calculated by ICRP 137 (ICRP 137). In table 3.6 effective dose coefficients of actinon progeny calculated in this study were compared to those of ICRP and the differences were found to be in the range -36 to 0.4% for ^{211}Pb and 0.8-260% for ^{211}Bi [2]. The calculations were made using assumptions of the Occupational Intakes of Radionuclides (OIR) publications series. The differences found between the dose coefficients would come from the calculation pattern such as, the numerical intergration of S$_W$ for beta spectrum (Eq.2.21), the calculation of specific absorbed fractions ϕ(r$_T \leftarrow$ Other) for the compartments denoted other soft tissues and the linear interpolation of specific absorbed fractions, and some details about the treatment of decay products formed in the respiratory tract. Apart of ^{211}Bi, all other progeny radionuclides formed in the respiratory tract (^{207}Tl and ^{211}Po) after inhalation of ^{211}Pb were neglected. In addition, the bound parameter values (transfer rate

from the bound-state compartments to the body fluids as shown in Fig.2.5) were also neglected for bismuth formed in the respiratory tract. Inhalation dose coefficients for actinon progeny were also calculated by Stabin and Siegel [10]. The dose coefficients were 3.46×10^{-11} and 1.76×10^{-9} Sv.Bq^{-1} for ^{211}Pb and ^{211}Bi, respectively. One should note that Stabin and Siegel assessed the dose coefficients for one particles size mode (AMAD 5 μm) with the aerosol type 'M' (moderate soluble) in a particular situation of exposure. The dose coefficients (inhalation) of actinon progeny of tissues other than the lungs are $\sim 5\%$ of the total effective dose in the unattached and nucleation modes, while for the accumulation the coefficient is $\sim 15\%$ of the total effective dose. Overall the effctive dose of inhaled actinon was dominated by the lung equivalent dose (shown in Fig.3.4-3.9). The extrathoracic equivalent dose was of the same order of magnetitude or lower than that to the lungs. However its contribution to the effective dose was quite low, because it is one of the 13 remainder organs (equivalent dose of remainder tissues is the arithmetic mean of the 13 equivalent doses of the remainder tissues) [30].
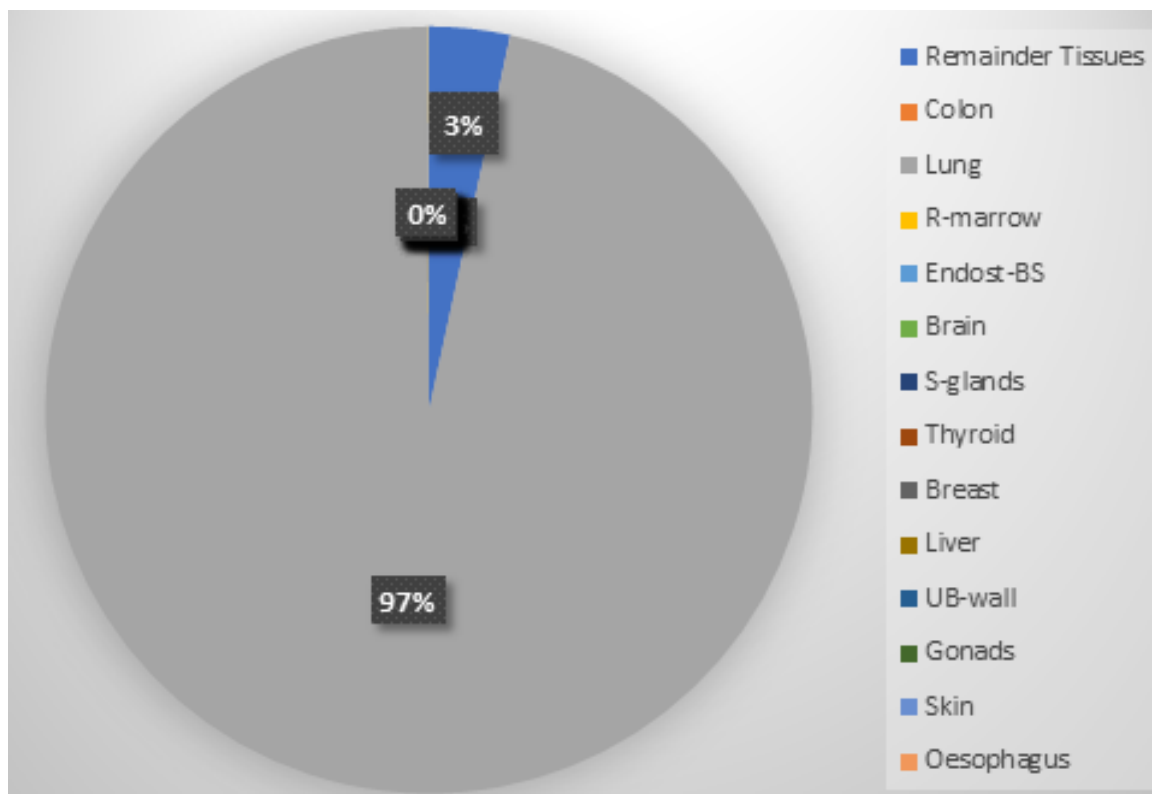
Figure 3.1: Contribution of dose coefficient for each target tissue to the committed effective dose coefficient after inhalation of ^{211}Pb for unattached mode (1 nm)

Table 3.4: Committed equivalent dose coefficients (Sv.Bq^{-1}) for target region after inhalation ^{211}Pb as decay product of actinon (reference adult male and female) $f(r_T, T)h^M(r_T)$ and $f(r_T, T)h^F(r_T)$ are committed equivalent dose coefficients for adult male and female respectively

Target tissues[a]	Unattached		Nucleation		Accumulation	
	$f(r_T, T)h^M(r_T)$	$f(r_T, T)h^F(r_T)$	$f(r_T, T)h^M(r_T)$	$f(r_T, T)h^F(r_T)$	$f(r_T, T)h^M(r_T)$	$f(r_T, T)h^F(r_T)$
O-mucosa	1.45E-11	1.62E-11	1.67E-10	1.82E-10	1.10E-10	1.21E-10
Oesophagus	1.16E-10	7.56E-11	4.15E-10	4.81E-10	2.91E-10	3.15E-10
St-stem	1.46E-10	1.61E-10	5.15E-10	6.01E-10	3.61E-10	4.18E-10
SI-stem	4.79E-11	6.95E-11	4.58E-10	7.04E-10	2.93E-10	4.48E-10
RC-stem	1.95E-11	1.68E-11	2.32E-10	1.97E-10	1.46E-10	1.24E-10
LC-stem	1.66E-11	1.88E-11	2.02E-10	2.30E-10	1.27E-10	1.45E-10
RS-stem	7.07E-12	9.41E-12	8.61E-11	1.15E-10	5.43E-11	7.24E-11
ET1-bas	8.19E-08	9.47E-08	1.45E-08	1.68E-08	6.03E-08	6.98E-08
ET2-bas	1.16E-07	1.34E-07	1.23E-08	1.43E-08	4.84E-08	5.61E-08
LN-ET	2.02E-12	1.14E-12	8.38E-12	8.94E-12	1.07E-11	7.23E-12
Bronch-bas	4.85E-08	5.40E-08	5.89E-09	6.61E-09	4.45E-09	4.99E-09
Bronch-sec	2.02E-07	2.24E-07	2.25E-08	2.51E-08	1.72E-08	1.92E-08
Bchiol-sec	1.97E-07	2.05E-07	7.67E-08	7.98E-08	2.53E-08	2.64E-08
AI	2.86E-10	3.61E-10	3.95E-09	4.86E-09	2.09E-09	2.58E-09
LN-Th	3.19E-12	1.20E-11	8.92E-12	1.60E-11	5.80E-12	1.10E-11
R-marrow	2.60E-11	3.36E-11	3.13E-10	3.94E-10	1.97E-10	2.49E-10
Endost-BS	2.21E-11	2.88E-11	2.79E-10	3.61E-10	1.76E-10	2.28E-10
Brain	1.31E-11	1.53E-11	1.61E-10	1.88E-10	1.01E-10	1.19E-10
Eye-lens	8.57E-12	9.85E-12	1.02E-10	1.22E-10	6.47E-11	7.67E-11
P-gland	8.44E-12	1.43E-11	7.00E-11	1.76E-10	5.56E-11	1.11E-10
Tongue	2.13E-11	1.50E-11	2.57E-10	1.77E-10	1.64E-10	1.14E-10
Tonsils	5.62E-12	1.45E-11	6.68E-11	1.76E-10	4.27E-11	1.12E-10
S-glands	1.31E-11	1.43E-11	1.61E-10	1.76E-10	1.02E-10	1.11E-10
Thyroid	2.44E-11	3.01E-11	2.94E-10	3.54E-10	1.85E-10	2.24E-10
Breast	1.31E-11	5.09E-12	1.61E-10	6.15E-11	1.02E-10	3.88E-11

continued

Target tissues[a]	Unattached		Nucleation		Accumulation	
	$f(r_T, T)h^M(r_T)$	$f(r_T, T)h^F(r_T)$	$f(r_T, T)h^M(r_T)$	$f(r_T, T)h^F(r_T)$	$f(r_T, T)h^M(r_T)$	$f(r_T, T)h^F(r_T)$
Thymus	1.61E-11	1.91E-11	1.67E-10	1.85E-10	1.06E-10	1.18E-10
Ht-wall	2.79E-11	4.27E-11	3.05E-10	4.07E-10	1.93E-10	2.58E-10
Adrenals	2.95E-11	3.40E-11	3.60E-10	4.15E-10	2.27E-10	2.61E-10
Liver	2.89E-11	3.81E-11	3.45E-10	4.52E-10	2.18E-10	2.85E-10
Pancreas	2.99E-11	3.62E-11	3.60E-10	4.35E-10	2.27E-10	2.74E-10
Kidneys	2.45E-10	2.89E-10	3.24E-09	3.83E-09	2.05E-09	2.42E-09
Spleen	4.70E-11	5.75E-11	5.62E-10	6.88E-10	3.55E-10	4.34E-10
GB-wall	1.33E-11	1.45E-11	1.62E-10	1.78E-10	1.03E-10	1.12E-10
Ureters	5.62E-12	1.43E-11	6.66E-11	1.76E-10	4.21E-11	1.11E-10
UB-wall	1.07E-11	1.30E-11	1.43E-10	1.73E-10	9.02E-11	1.09E-10
Ovaries	0.00E+00	3.02E-11	0.00E+00	3.68E-10	0.00E+00	2.32E-10
Testes	1.48E-11	0.00E+00	1.82E-10	0.00E+00	1.15E-10	0.00E+00
Prostate	1.31E-11	0.00E+00	1.61E-10	0.00E+00	1.02E-10	0.00E+00
Uterus	0.00E+00	5.31E-12	0.00E+00	6.15E-11	5.97E-11	3.89E-11
LN-Sys	1.47E-11	1.80E-11	1.57E-10	1.92E-10	9.96E-11	1.21E-10
Skin	1.43E-11	1.77E-11	1.67E-10	2.15E-10	1.06E-10	1.36E-10
Adipose	1.14E-11	1.43E-11	1.24E-10	1.52E-10	7.91E-11	9.69E-11
Muscle	1.12E-11	1.37E-11	1.37E-10	1.66E-10	8.64E-11	1.05E-10

O-mucosa, oral mucosa; St-stem, stomach; RC-stem, right colon; RC-stem, rectosigmoid colon; ET2-bas, ET2 basal cells; Bronch-bas, bronchi basal cells; Bchiol-sec, bronchiolar secretory cells; LN-Sys, lymph nodes thoracic; Endost-BS, endosteal cells; eye-lens, lens of eye; S-glands, salivary glands; Ht-wall, heart wall; GB-wall, gall bladder; UB-wall, urinary bladder.

Table 3.5: Committed equivalent dose coefficients (Sv.Bq^{-1}) for target region after inhalation ^{211}Bi as decay product of actinon (reference adult male and female) $f(r_T, T)h^M(r_T)$ and $f(r_T, T)h^F(r_T)$ are committed equivalent dose coefficients for adult male and female respectively

Target tissues[a]	Unattached		Nucleation		Accumulation	
	$f(r_T, T)h^F(r_T)$	$f(r_T, T)h^M(r_T)$	$f(r_T, T)h^F(r_T)$	$f(r_T, T)h^M(r_T)$	$f(r_T, T)h^F(r_T)$	$f(r_T, T)h^M(r_T)$
O-mucosa	3.96E-14	3.68E-14	8.19E-14	7.66E-14	5.31E-14	4.96E-14
Oesophagus	1.51E-13	1.32E-13	2.46E-13	2.13E-13	1.81E-13	1.58E-13
St-stem	1.39E-13	1.20E-13	2.89E-13	2.49E-13	1.87E-13	1.61E-13
SI-stem	1.61E-13	1.09E-13	3.40E-13	2.32E-13	2.18E-13	1.49E-13
RC-stem	4.74E-14	5.36E-14	1.00E-13	1.13E-13	6.43E-14	7.27E-14
LC-stem	5.38E-14	4.77E-14	1.14E-13	1.01E-13	7.31E-14	6.48E-14
RS-stem	2.69E-14	2.09E-14	5.70E-14	4.43E-14	3.65E-14	2.84E-14
ET1-bas	6.02E-09	5.20E-09	1.06E-09	9.20E-10	4.43E-09	3.83E-09
ET2-bas	3.09E-08	2.67E-08	5.50E-09	4.75E-09	2.27E-08	1.96E-08
LN-ET	2.42E-15	2.81E-15	4.59E-15	3.82E-15	3.12E-15	3.13E-15
Bronch-bas	4.84E-09	4.34E-09	1.36E-09	1.22E-09	1.31E-09	1.18E-09
Bronch-sec	2.03E-08	1.82E-08	5.68E-09	5.11E-09	5.49E-09	4.94E-09
Bchiol-sec	1.41E-08	1.36E-08	2.19E-08	2.11E-08	7.18E-09	6.91E-09
AI	8.98E-12	7.34E-12	9.93E-10	8.12E-10	4.82E-10	3.94E-10
LN-Th	2.96E-15	1.91E-15	5.11E-15	3.79E-15	3.37E-15	2.44E-15
R-marrow	9.31E-14	7.37E-14	1.97E-13	1.56E-13	1.26E-13	1.00E-13
Endost-BS	4.57E-14	3.62E-14	9.67E-14	7.66E-14	6.21E-14	4.92E-14
Brain	4.09E-14	3.51E-14	8.67E-14	7.43E-14	5.56E-14	4.77E-14
Eye-lens	2.38E-14	2.00E-14	5.04E-14	4.22E-14	3.23E-14	2.71E-14
P-gland	3.79E-14	1.82E-14	8.01E-14	3.53E-14	5.14E-14	2.37E-14
Tongue	3.82E-14	5.43E-14	8.02E-14	1.14E-13	5.17E-14	7.35E-14
Tonsils	3.79E-14	1.66E-14	8.01E-14	3.50E-14	5.14E-14	2.25E-14
S-glands	3.78E-14	3.52E-14	8.01E-14	7.46E-14	5.14E-14	4.79E-14
Thyroid	8.33E-14	6.92E-14	1.76E-13	1.46E-13	1.13E-13	9.39E-14
Breast	1.52E-14	3.53E-14	3.21E-14	7.46E-14	2.06E-14	4.79E-14

[a] .

continued

Target tissues[a]	Unattached		Nucleation		Accumulation	
	$f(r_T, T)h^F(r_T)$	$f(r_T, T)h^M(r_T)$	$f(r_T, T)h^F(r_T)$	$f(r_T, T)h^M(r_T)$	$f(r_T, T)h^F(r_T)$	$f(r_T, T)h^M(r_T)$
Thymus	3.82E-14	3.55E-14	8.08E-14	7.50E-14	5.18E-14	4.81E-14
Ht-wall	9.08E-14	6.97E-14	1.92E-13	1.48E-13	1.23E-13	9.47E-14
Adrenals	9.86E-14	8.61E-14	2.09E-13	1.82E-13	1.34E-13	1.17E-13
Liver	1.12E-13	8.58E-14	2.37E-13	1.82E-13	1.52E-13	1.17E-13
Pancreas	1.04E-13	8.61E-14	2.20E-13	1.82E-13	1.41E-13	1.17E-13
Kidneys	1.44E-13	1.22E-13	3.05E-13	2.57E-13	1.95E-13	1.65E-13
Spleen	1.68E-13	1.37E-13	3.55E-13	2.91E-13	2.28E-13	1.87E-13
GB-wall	3.80E-14	3.54E-14	8.04E-14	7.49E-14	5.16E-14	4.81E-14
Ureters	3.78E-14	1.66E-14	8.01E-14	3.50E-14	5.14E-14	2.25E-14
UB-wall	3.58E-14	2.95E-14	7.57E-14	6.24E-14	4.86E-14	4.00E-14
Ovaries	8.62E-14	0.00E+00	1.83E-13	0.00E+00	1.17E-13	0.00E+00
Testes	0.00E+00	4.05E-14	0.00E+00	8.57E-14	0.00E+00	5.50E-14
Prostate	0.00E+00	3.53E-14	0.00E+00	7.46E-14	0.00E+00	4.79E-14
Uterus	1.52E-14	0.00E+00	3.21E-14	0.00E+00	2.06E-14	0.00E+00
LN-Sys	4.16E-14	3.39E-14	8.80E-14	7.17E-14	5.65E-14	4.60E-14
Skin	4.77E-14	3.66E-14	1.01E-13	7.73E-14	6.47E-14	4.96E-14
Adipose	3.15E-14	2.55E-14	6.64E-14	5.39E-14	4.27E-14	3.46E-14
Muscle	3.51E-14	2.90E-14	7.43E-14	6.13E-14	4.77E-14	3.93E-14

O-mucosa, oral mucosa; St-stem, stomach; RC-stem, right colon; RS-stem, rectosigmoid colon; ET2-bas, ET2 basal cells; Bronch-bas, bronchi basal cells; Bchiol-sec, bronchiolar secretory cells; LN-Sys, lymph nodes thoracic; Endost-BS, endosteal cells; Eye-lens, lens of eye; RS-stem, rectosigmoid colon; S-glands, salivary glands; Ht-wall, heart wall; GB-wall, gall bladder; UB-wall, urinary bladder.

Figure 3.2: Contribution of dose coefficient for each target tissue to the committed effective dose coefficient after inhalation of ^{211}Pb for nucleation mode (60 nm)

Table 3.6: Inhalation dose coefficients (Sv Bq^{-1}) calculated in the present work and comparison to the results of ICRP 137

Mode	Dose coefficients (Sv/Bq)					
	Present study		ICRP-137		Differences (%)	
	^{211}Pb	^{211}Bi	^{211}Pb	^{211}Bi	^{211}Pb	^{211}Bi
Unattached	5.78E-08	4.84E-09	6.6E-08	4.8E-09	-12	0.8
Nucleation	1.41E-08	3.55E-09	2.2E-08	1.5E-09	-36	136
Accumulation	7.43E-09	1.91E-09	7.4E-09	5.3E-10	0.4	260

Lung dose is sensitive to the absorption rates of the radon progeny (including actinon progeny) if the assumed absorption half-times are less than or comparable with their radioactive half-lives [19]. The high contribution of lung dose to the committed effective dose coefficient could be explain by the sensitive of lung tissue to alpha and beta radiations. Due to the short distance travelled by alpha and beta particles in the air, these particles emitted within the lung tissues are almost absorbed by these tissues (high specific absorbed fraction). However, some organs such as stomach, small intestine and colon (gastrointestinal organs) are too thick there-fore, they are insensitive to alpha and beta radiations (with low specific absorbed fraction).The

committed dose coefficients of inhaled actinon progeny are strongly depend on the alpha and beta energies (produced by the decay of ^{211}Pb and ^{211}Bi) absorbed by organs and tissues.
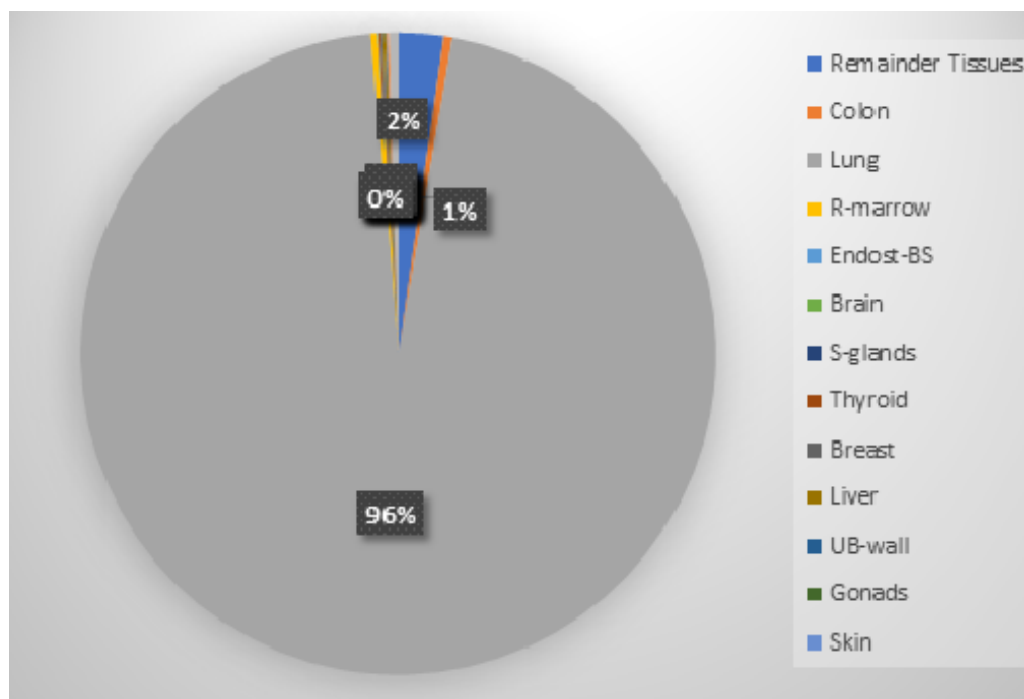

Figure 3.3: Contribution of dose coefficient for each target tissue to the committed effective dose coefficient after inhalation of ^{211}Pb for accumulation mode (500 nm)

Figure 3.4: Contribution of dose coefficient for each target tissue to the committed effective dose coefficient after inhalation of ^{211}Bi for unattached mode (1 nm)

Figure 3.5: Contribution of dose coefficient for each target tissue to the committed effective dose coefficient after inhalation of ^{211}Bi for nucleation mode (60 nm)
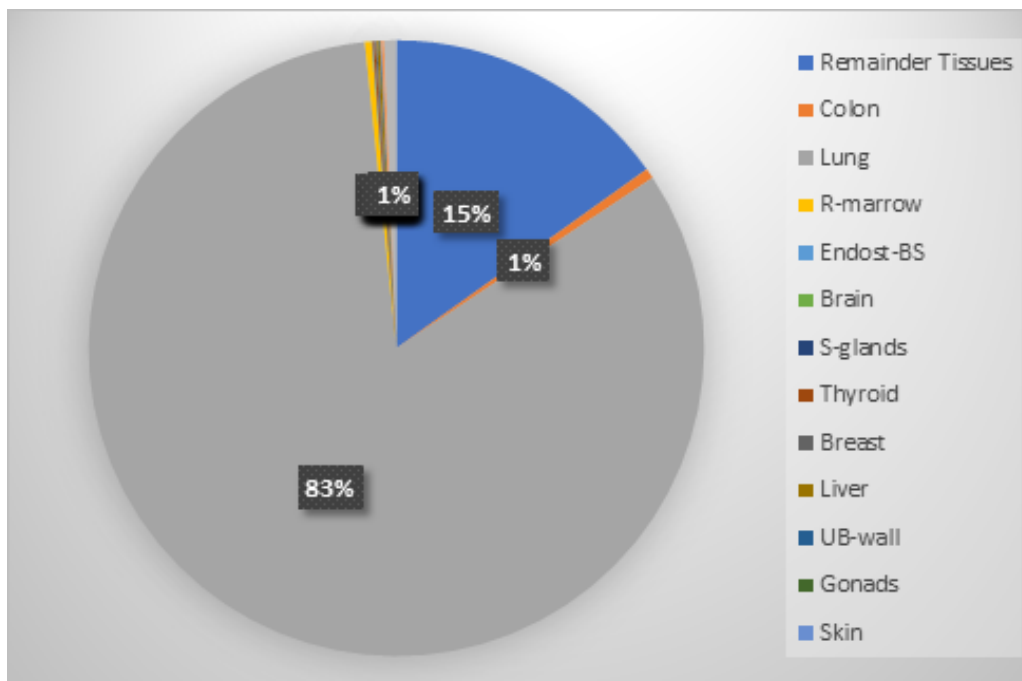

Figure 3.6: Contribution of dose coefficient for each target tissue to the committed effective dose coefficient after inhalation of ^{211}Bi for accumulation mode (500 nm)
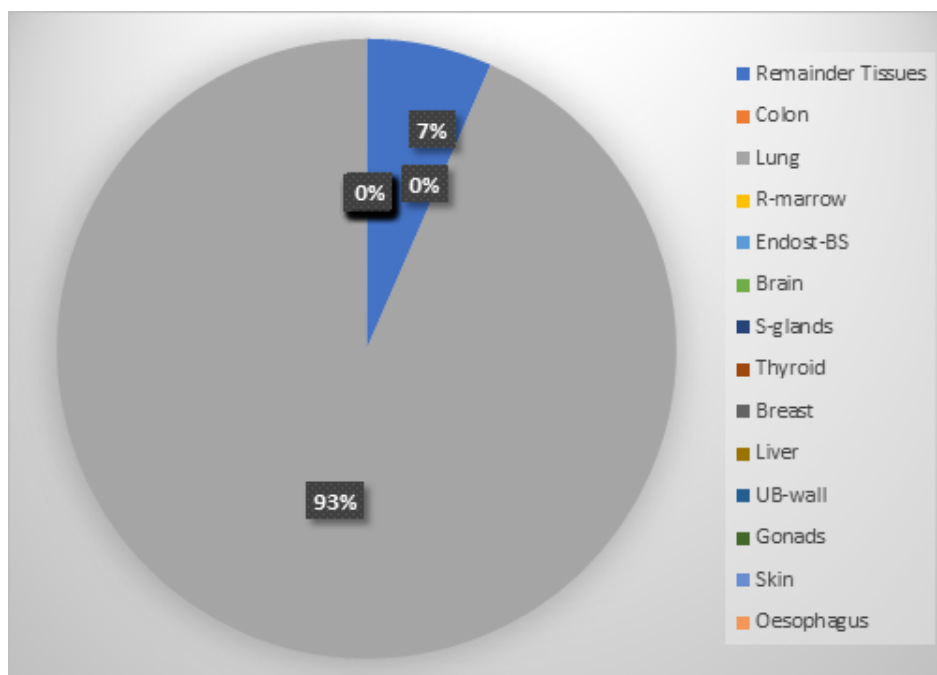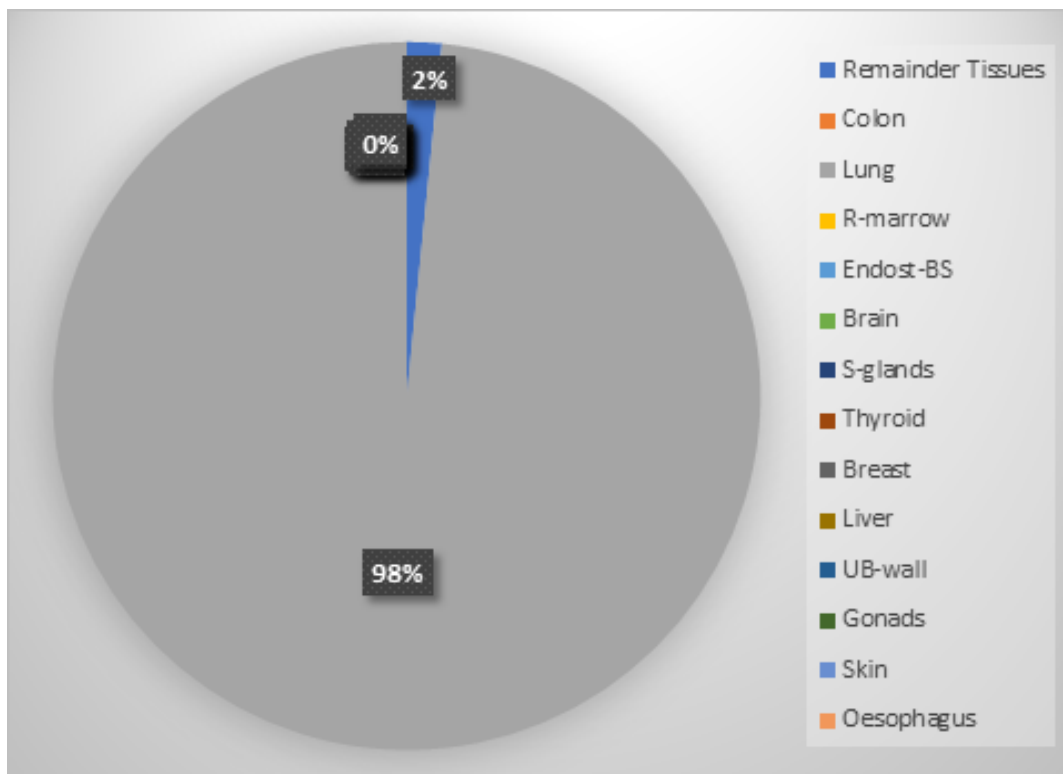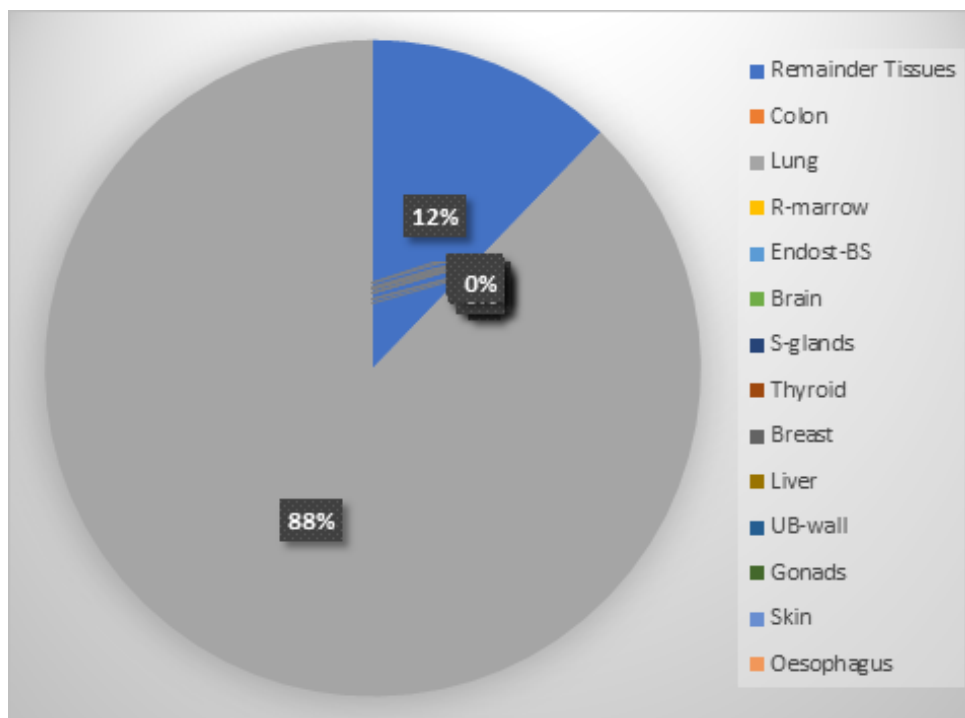
Table 3.7: Inhalation dose coefficients (Sv.Bq^{-1})of ^{211}Pb and ^{211}Bi as a function of particles size in unattached (1 nm) and attached (60 nmand 500 nm)

Organ	^{211}Pb			^{211}Bi		
	AMTD (1 nm)	AMAD (60 nm)	AMAD (500 nm)	AMTD (1 nm)	AMAD (60 nm)	AMAD (500 nm)
Remainder tissues[a,b]	1.64E-08	2.74E-09	9.35E-09	2.64E-09	4.70E-10	1.94E-09
Colon	4.41E-11	5.30E-10	3.35E-10	1.25E-13	2.64E-13	1.69E-13
Lungs	4.65E-07	1.12E-07	5.11E-08	3.76E-08	2.91E-08	1.39E-08
R-Marrow	2.98E-11	3.53E-10	2.23E-10	8.34E-14	1.76E-13	1.13E-13
Endost-BS	2.54E-11	3.19E-10	2.02E-10	4.09E-14	8.66E-14	5.56E-14
Brain	1.41E-11	1.74E-10	1.10E-10	3.80E-14	8.04E-14	5.16E-14
S-Glands	1.36E-11	1.68E-10	1.06E-10	3.65E-14	7.73E-13	4.96E-14
Thyroid	2.72E-11	3.24E-10	2.04E-10	7.62E-14	1.61E-13	1.03E-13
Breast	9.10E-12	1.11E-10	7.02E-11	2.52E-14	5.35E-14	3.43E-14
Liver	3.35E-11	3.98E-10	2.51E-10	9.89E-14	2.09E-13	1.34E-13
UB-Wall	1.18E-11	1.58E-10	9.98E-11	3.26E-14	6.90E-14	4.43E-14
Gonads	2.25.E-11	2.75E-10	1.73E-10	6.33E-14	1.34E-13	8.60E-14
Skin	1.59E-11	1.90E-10	1.20E-10	4.21E-14	8.91E-14	5.71E-14
Oesophagus	9.55E-11	4.48E-10	3.03E-10	1.41E-13	2.29E-13	1.69E-13
St-stem	1.53E-10	5.57E-10	3.89E-10	1.29E-13	2.68E-13	1.74E-13
ET airways	2.13E-07	2.89E-08	1.17E-07	3.44E-08	6.11E-09	2.52E-08
Kidneys	2.66E-10	3.53E-10	2.23E-09	1.32EáLŠ13	2.81E-13	1.80E-13
Adrenals	3.17E-11	3.87E-10	2.44E-10	9.23E-14	1.95E-13	1.25E-13
O mucosa	1.53E-11	1.74E-10	1.15E-10	3.82E-14	7.93E-13	5.13 E-14
SI-stem	5.86E-11	5.80E-10	3.70E-10	1.35EáLŠ13	2.85E-13	1.83E-13
Lymphatic N	1.63E-11	1.74E-10	1.10E-10	4.51E-14	9.91E-14	6.22E-14
Heart-wall	3.53E-11	3.56E-10	2.25E-10	8.01E-14	1.69E-13	1.08E-13
Thymus	1.76E-11	1.76E-10	1.11E-10	3.68E-14	7.80E-14	5.00E-14

continued

Organ	^{211}Pb			^{211}Bi		
	AMTD (1 nm)	AMAD (60 nm)	AMAD (500 nm)	AMTD (1 nm)	AMAD (60 nm)	AMAD (500 nm)
Spleen	5.22E-11	1.70E-10	3.94E-10	1.52E-13	3.23E-13	2.07E-13
Pancreas	3.30E-11	3.97E-10	2.50E-10	9.49E-14	2.01E-13	1.28E-13
Prostate/uterus	9.20E-12	1.11E-11	1.00E-11	3.45E-14	7.32E-14	4.69E-14
GB-wall	1.39E-11	1.69E-10	1.07E-10	3.66E-14	7.76E-13	4.98E-14
Muscle	1.24E-11	1.51E-10	9.55E-11	3.20E-14	6.77E-14	4.35E-14
Effective dose	5.78E-08	1.41E-08	7.43E-09	4.84E-09	3.55E-09	1.91E-09

[a]Remainder tissues: adrenals, extrathoracic regions of the respiratory tract, gall bladder, heart, kidneys, lymphatic nodes, muscle, oral mucosa, pancreas, prostate (male), small intestine, spleen, thymus and uterus/cervix (female)

[b]Lymphatic N = lymphatic nodes, O mucosa = oral mucosa, R-marrow = red marrow, St-stem = stomach, SI-stem = small intestine, UB-wall = urinary bladder wall, GB-wall = gall bladder wall, ET airways = extra thoracic airways, Endost-BS = endosteal cells, S Glands = Salivary Glands.

3.4   Committed dose coefficient of ^{211}Pb using ICRPDOSE software

The ICRPDOSE was implemented using the ICRP HRTM of publication 66, the gastrointestinal tract and systemic models of the publication 30 [7, 31]. The inhalation dose coefficient of ^{211}Pb was calculated using ICRPDOSE, for particle size of 1 nm (unattached mode) and for absorption parameters types: F (fast soluble), M (Moderate soluble) and S (Slow soluble). Table 3.8 displays committed dose coefficients for each target tissues and committed effective dose after inhalation ^{211}Pb for three absorption type (F, M and S). The calculation indicated that the committed equivalent dose coefficient in the lung and ET airways were relatively larger than in other organ for all absorption types. The equivalent dose coefficient was the highest in the ET airways for absorption type F. However, the lung equivalent dose coefficient was the highest for absorption types M and S. The calculations indicate that the committed dose coefficients strongly depend on the absorption type. The lung equivalent dose coefficient and committed effective dose coefficient increase when the absorption type decrease (the absorption type F has a high absorption parameters and the absorption type S has the low absorption parameters). This mean the retention in the HRTM tissues is more important for the low absorption parameters. The inhalation dose coefficients of unattached ^{211}Pb (1 nm) for three absorption types (F, M and S) calculated using ICRPDOSE software are 1.30×10^{-08} Sv.Bq^{-1} for absorption type F, 4.10×10^{-08} Sv.Bq^{-1} for absorption type M and 4.50×10^{-08} Sv.Bq^{-1} for absorption type S. The inhalation dose coefficient of inhaled unattached ^{211}Pb (5.78×10^{-08} Sv.Bq^{-1}), decay product of actinon given in table 3.7 was compared with those calculated with ICRPDOSE. The differences are 344%, 41% and 28% with the absorption types F, M and S respectively. The differences found between those committed dose coefficients would come from the biokinetic models used such as, HRTM (deposition, dissolution and absorption pattern), gastrointestinal tract (instead of HATM) and systemic model of lead. In addition the methodology of internal dose calculation is updated. The use of voxel phantoms for the calculation of Specific Absorbed Fraction is adopted instead of antropomorphic phantoms (the antropomorphic phantoms were used in the implementation of ICRPDOSE software).

Table 3.8: Inhalation dose coefficients (Sv.Bq^{-1}) of ^{211}Pb for unattached mode (1 nm) and three absorption types (F, M and S) using ICRPDOSE software

	Committed dose coefficients 1 nm (Sv.Bq^{-1})		
Organ^a	type F	type M	type S
Adrenals	2.30E-10	2.60E-11	7.00E-13
Bladder wall	2.60E-10	2.90E-01	6.30E-13
Bone surface	3.80E-09	4.20E-10	7.90E-12
Brain	2.30E-10	2.60E-11	6.60E-13
Breast	2.30E-10	2.60E-11	6.10E-13
Oesophagus	2.30E-10	2.60E-11	7.50E-13
St-wall	4.80E-10	4.50E-10	4.50E-10
SI-wall	3.20E-10	2.20E-10	2.10E-10
ULI-wall	2.80E-10	9.90E-11	7.80E-11
LLI-wall	2.40E-10	3.30E-11	8.60E-11
Colon	2.60E-10	7.10E-11	4.80E-11
Kidneys	2.50E-09	2.80E-10	5.40E-12
Liver	7.50E-10	8.20E-11	1.70E-12
Muscle	2.30E-10	2.60E-11	7.30E-13
Ovaries	2.30E-10	2.60E-11	8,40E-12
Pancreas	2.30E-10	2.60E-11	1.10E-12
Red Marrow	5.50E-10	6.00E-11	1.30E-12
ET airways	1.50E-07	2.20E-07	2.30E-07
Lungs	7.10E-08	3.40E-07	3,70E-07
Skin	2.30E-10	2.60E-11	5.80E-13
Spleen	2.30E-10	2.50E-11	8.70E-13
Testes	2.30E-10	2.50E-11	5.00E-13
Thymus	2.30E-10	2.60E-11	7.50E-13
Thyroid	2.30E-10	2.60E-11	6.80E-13
Uterus	2.30E-10	2.60E-11	7.70E-13
Remainder*	7.30E-08	1.40E-10	1.20E-10
Effective dose	1.30E-08	4.10E-08	4.50E-08

^{a}St-wall, Stomach wall; SI-wall, Small Intestine wall; ULI-wall, Upper large intestine wall; LLI-wall, Lower Large intestine wall; ET airways, Extrathoracic airways.
*Remainder: Muscle, Brain, Small intestine, Kidneys, Pancreas, Spleen, Uterus, Adrenals, Extrathoracic airways

Conclusion

This chapter has presented results of the current work. The comparision between committed dose coefficients calculated in this study and those given in the ICRP-137 were presented. The dose coefficients of actinon progeny have just been presented in the ICRP publication [2]. Due to the lack of calculation details, (form ICRP publication) the differences would not be state properly. In general the methodology of internal dose assessment implemented in this study is in agreement with the one found in the ICRP publications, since the results found are much closer to those of the published ICRP-137.

General conclusion

This work presents internal dose calculations of inhaled actinon progeny. Throughout this study the essential elements for dose assessment due to inhalation of actinon progeny were presented. The first chapter has briefly described some generalities on the radioactivity, the actinon and its progeny, the interaction of radiation with matter, the internal exposure and some fundamental quantities and dosimetric units. In addition the fundamental principles of radiation protection were also briefly defined. The second chapter has described the behavior of inhaled radioactive particles using the HRTM, HATM and systemic models of lead and bismuth. The methodology of the number of nuclear transformations, committed equivalent dose coefficients and committed effective dose calculations were also described. The third chapter has presented results found out in this study. The effective dose coefficients were calculated separately for three modes, using biokinetic and dosimetric models developed in the recent OIR publications series of ICRP. The biokinetic models of ^{211}Pb and ^{211}Bi have been implemented and solved in BIOKMOD using the approach developed by Sanchez is described in references [11, 41, 42]. Number of nuclear transformations per activity intake were calculated using compartmental systems. The calculations have shown that number of nuclear transformations per activity intake were the highest in ET1-sur for the unattached (1 nm) and accumulation (500 nm) modes for actinon progeny, including ^{211}Bi formed within the body after inhalation of ^{211}Pb. However, for nucleation mode (60 nm) "ALV" was the region with the highest number of nuclear transformations per activity intake. Those values strongly depend on the deposition fraction. The inhalation actinon progeny provided the highest dose to the lungs and ET airways. The calculations indicated that the most exposed region of the lung tissues for ^{211}Pb was the bronchial tissue for the unattached and attached fractions respectively for particle sizes of 1 nm and 500 nm and the bronchiolar tissue for the attached fraction of 60 nm. However, the most exposed region of the lung tissues for ^{211}Bi was the bronchiolar tissue for unattached fraction (1 nm) and bronchioles for attached fractions (60 nm and 500 nm particles size). The dose coefficients of ^{211}Pb and ^{211}Bi calculated are 5.78×10^{-8} Sv.Bq^{-1} and 4.84×10^{-9} Sv.Bq^{-1} for unattached

particles (AMTD=1nm) and, 1.4×10^{-8} Sv.Bq^{-1} and 3.55×10^{-9}Sv.Bq^{-1} for attached particles (AMAD=60 nm), and 7.37×10^{-9}Sv.Bq^{-1} and 1.91×10^{-9}Sv.Bq^{-1} for attached particles (AMAD=500 nm). These values are much closer to those published by the ICRP [2]. In sum the methodology of internal dose assessment set up in this study could be used for dose coefficients (inhalation) calculation of other radionuclides. Furthermore, in order to work out the dose conversion coefficient for actinon (^{219}Rn) decay products, a study of activity size distributions and measurement of activity concentration of actinon progeny is recommended to be conducted in hospitals during the treatment of prostate cancer metastasis with ^{223}Ra. The biokinetic modelling and dosimetry of ^{223}Ra as targeted radiopharmaceutical in treatment of prostate cancer metastasis will be developed. The calculation of Sw values for specified source and target organs by using the mesh-type reference computational phantoms for adults will be performed [47].

Appendix

Analytical solution of the retention for some compartments of biokinetic models following inhalation of unattached (1 nm) ^{211}Pb

$A_{AI}(t) = 0.00059 \exp(-127.652\ t) + 0.005310 \exp(-29.352\ t)$.

$A_{bb'}(t) = 0.0902 \exp(-29.549\ t) + 0.000054 \exp(-29.352\ t) + 0.010023 \exp(-127.849\ t) + 5.9898 \times 10^{-6} \exp(-125.652t)$

$A_{bb_{seq}}(t) = 0.0000201 \exp(-127.65\ t) + 0.000181 \exp(-29.35\ t)$.

$A_{BB'}(t) = 0.00771 \exp(-137.649\ t) + 0.0002045 \exp(-127.849\ t) + 1.1983 \times 10^{-7} \exp(-127.652\ t) + 0.069385 \exp(-39.3490\ t) + 0.001841 \exp(-29.549\ t) + 1.0785 \times 10^{-6} \exp(-29.352\ t)$.

$A_{BB_{seq}}(t) = 0.0001427 \exp(-29.35\ t) + 0.000016 \exp(-127.65\ t)$.

$A_{ET_2'}(t) = .02663 \exp(-227.649\ t) + 0.00086 \exp(-137.649\ t) + 0.0000205 \exp(-127.849\ t) + 1.1984 \times 10^{-8} \exp(-127.652\ t) + 0.000393 \exp(-29.7490\ t)$.

$A_{ET_{seq}}(t) = 0.00005592 \exp(-127.65\ t) + 0.000503280 \exp(-29.35\ t)$.

$A_{ET_1}(t) = 0.46719 \exp(-29.749\ t) + 0.05191 \exp(-29.749\ t)$.

$A_{LN_{ET}}(t) = -0.00005592 \exp(-127.65\ t) + 0.00005592 \exp(-127.649\ t) - 0.00050328 \exp(-29.35\ t) + 0.0005033 \exp(-29.349\ t)$.

$A_{INT}(t) = -0.00179 \exp(-29.352\ t) + 0.00179 \exp(-29.34903\ t) - 0.000190 \exp(-127.652\ t) + 0.000199 \exp(-127.649\ t)$.

$A_{LN_{TH}}(t) = 1.99 \times 10^{-6} \exp(-127.652\ t) - 0.000036 \exp(-127.65\ t) - 0.000199 \exp(-127.64903\ t) + 0.000232627 \exp(-127.649\ t) + 0.000018 \exp(-29.352\ t) - 0.0003237 \exp(-29.35\ t) - 0.00179 \exp(-29.34903\ t) + 0.0020936 \exp(-29.349\ t)$.

$A_{AIbound}(t) = -0.000199 \exp(-127.652\ t) - 0.00010104 \exp(-127.64903\ t) - 0.998 \exp(-29.352\ t) - 50.656 \exp(-29.349\ t) + 51.6548 \exp(-29.349\ t)$.

$A_{bb_{bnd}}(t)$ = -0.00509 exp(-127.849 t) - 3.046625 $\times 10^{-6}$ exp(-127.652 t) - 0.0000102 exp(-127.65 t) - 0.3834 exp(-29.549 t) - 0.015274 exp(-29.352 t) - 0.15377 exp(-29.35 t) + 0.55755 exp(-29.349 t).

$A_{BB_{bnd}}(t)$ = -0.00356 exp(-137.649 t) - 0.0001039 exp(-127.849 t) - 6.09508$\times 10^{-8}$ exp(-127.652 t) - 8.06706$\times 10^{-6}$ exp(-127.65 t) - 0.00589 exp(-39.349 t) - 0.007824 exp(-29.549 t) - 0.000305 exp(-29.352 t) - 0.121329 exp(-29.350 t) + 0.139028 exp(-29.349 t).

$A_{ET_{bnd}}(t)$ = -0.00671 exp(-227.649 t) - 0.0003954 exp(-137.649 t) - 0.002008 exp(-129.349 t) - 0.0000104 exp(-127.849 t) - 6.09526$\times 10^{-9}$ exp(-127.652 t) - 0.0000284432508316 29388 exp(-127.65 t) - 0.000655 exp(-39.349 t) - 0.049182 exp(-29.749 t) - 0.01495 exp(-29.749 t) - 0.000784 exp(-29.549 t) - 0.00003055 exp(-29.352 t) - 0.42779 exp(-29.35 t) + 0.4958335 exp(-29.349 t) + 0.00671545 exp(-29.349 t).

$A_{LT_{THbnd}}(t)$ = -1.0104127$\times 10^{-6}$ exp(-127.652 t) + 0.0000183 exp(-127.65 t) + 0.00010104 exp(-127.64903 t) - 0.000118325 exp(-127.649 t) - 0.005065 exp(-29.352 t) + 0.27509 exp(-29.350 t) + 50.65 exp(-29.34903 t) - 50.9266 exp(-29.349 t) + 0.0017796 exp(-29.349 t) t.

$A_{LT_{ETbnd}}(t)$ = 0.0000284 exp(-127.65 t) - 0.0000284 exp(-127.649 t) + 0.4278 exp(-29.350 t) - 0.427788 exp(-29.3490 t) + 0.0004278 exp(-29.349 t) t.

$A_{plasma}(t)$ = 9.41021$\times 10^{-8}$ exp(-2187.649 t) - 0.010246 exp(-227.649 t) - 0.01100 exp(-137.649 t) - 0.009952 exp(-129.3489 t) - 0.01776 exp(-127.849 t) - 0.0006971 exp(-127.652 t) - 0.0005036 exp(-127.649 t) + 0.05055 exp(-100.270847 t) + 0.0049032 exp(-48.219 t) - 0.0117486 exp(-48.219 t) - 0.006055 exp(-39.349 t) + 0.000065 exp(-35.1490199 t) + 0.000405 exp(-35.14902 t) + 0.002515 exp(-32.595411 t) + 0.0001908 exp(-32.59541 t) - 0.001203 exp(-29.749 t) + 0.0046134 exp(-29.749 t) - 0.012812 exp(-29.549 t) - 0.035732 exp(-29.352 t) + 0.015022 exp(-29.35 t) - 0.01502262 exp(-29.35 t) + 0.052405 exp(-29.349 t) + 0.0002544 exp(-29.349 t) + 0.001156 exp(-28.5699 t) + 2.758836$\times 10^{-6}$ exp(-27.7273 t) + 0.000088924 exp(-27.72724 t) + 0.000454776 exp(-27.688018 t) + 0.000077345 exp(-27.659108 t) + 2.49032$\times 10^{-6}$ exp(-27.659107 t) + 7.01241$\times 10^{-7}$ exp(-27.65543 t) + 0.00002173 exp(-27.65544 t) + 3.611969$\times 10^{-6}$ exp(-27.65078 t) + 1.168103$\times 10^{-7}$ exp(-27.6508 t) + 1.28029$\times 10^{-6}$ exp(-27.64945 t) + 1.558113$\times 10^{-8}$ exp(-27.64937 t) + 4.81434$\times 10^{-7}$ exp(-27.649 t) + 2.604908$\times 10^{-7}$ exp(-27.64907 t) + 0.000077489 exp(-29.349 t) t.

$A_{RBC}(t)$ = -1.22$\times 10^{-9}$ exp(-2187.65 t) + 0.001435 exp(-227.649 t) + 0.002805 exp(-137.649 t) + 0.002744 exp(-129.348 t) + 0.00497 exp(-127.849 t) + 0.0001954 exp(-127.652 t) + 0.0001412 exp(-127.649 t) - 0.01953 exp(-100.27085 t) - 0.006719 exp(-48.219 t) + 0.01610 exp(-48.219 t) + 0.014665 exp(-39.349 t) - 0.00024795 exp(-35.14902 t) - 0.00154 exp(-35.149 t) - 0.014651

exp(-32.59541 t) - 0.0011 exp(-32.5954 t) + 0.01717954 exp(-29.749 t) - 0.06587 exp(-29.749 t) + 0.2037 exp(-29.549 t) + 0.6397 exp(-29.352 t) - 0.26929 exp(-29.35 t) + 0.26929 exp(-29.35 t) - 0.940 exp(-29.349 t) - 0.00545 exp(-29.3489 t) - 0.04139 exp(-28.5699 t) + 0.001271 exp(-27.72724 t) + 0.040982 exp(-27.72724 t) + 0.12736 exp(-27.688 t) + 0.0168 exp(-27.6591 t) + 0.00054 exp(-27.659 t) + 0.000148 exp(-27.655 t) + 0.00459 exp(-27.655 t) + 0.000737 exp(-27.65 t) + 0.0000238 exp(-27.6508 t) + 0.000258 exp(-27.649 t) + 3.147×10^{-6} exp(-27.6493 t) + 0.0000972 exp(-27.6493 t) + 0.0000525 exp(-27.649 t) - 0.00139 exp(-29.349 t) t.

$A_{ST1}(t) = $ 0.0000359 exp(-227.649 t) + 0.000070041 exp(-137.649 t) + 0.0000685 exp(-129.349 t) + 0.00012408 exp(-127.849 t) + 4.87992×10^{-6} exp(-127.652 t) + 3.52550×10^{-6} exp(-127.649 t) - 0.0004873 exp(-100.270847 t) - 0.0001669 exp(-48.219 t) + 0.000399 exp(-48.219 t) + 0.000362482 exp(-39.349 t) - 0.0000419 exp(-35.149019 t) - 1.972973×10^{-6} exp(-35.149 t) + 0.00066383 exp(-32.5954 t) - 0.001047352 exp(-32.5954 t) + 0.00040238 exp(-29.749 t) - 0.0015429 exp(-29.749 t) + 0.0047376 exp(-29.549 t) + 0.0147473 exp(-29.352 t) - 0.0062074 exp(-29.350 t) + 0.006207 exp(-29.350 t) - 0.02167 exp(-29.3490 t) - 0.0001241 exp(-29.349 t) - 0.0000133 exp(-28.57 t) - 0.000872 exp(-28.57 t) - 0.0008728 exp(-27.727 t) - 0.00002708 exp(-27.727246 t) - 0.0099207 exp(-27.68801 t) - 0.0175897 exp(-27.659107 t) + 0.00100098 exp(-27.6554 t) + 0.0310284 exp(-27.6554 t) + 0.0005075 exp(-27.6508 t) + 0.00013395 exp(-27.6494 t) + 4.335205×10^{-6} exp(-27.6494 t) + 1.66269×10^{-6} exp(-27.6493 t) + 0.000051 exp(-27.64937 t) + 0.0000266 exp(-27.649 t) - 0.000032 exp(-29.349 t) t.

References

[1] Alavanja MC et al. "Residential radon exposure and risk of lung cancer in Missouri." In: *American Journal of Public Health* 89.7 (1999).

[2] ICRP. "ICRP publication 137: Occupational intakes of radionuclides: part 3". In: *Annals of the ICRP* 46.3-4 (2017).

[3] International Commission on Radiation Units and Measurements. "Measurement and reporting of radon exposures. ICRU Report 88." In: *J. ICRU* 12.2 (2012).

[4] Parker C et al. "Alpha emitter radium-223 and survival in metastatic prostate cancer." In: *New England Journal of Medicine* 369.3 (2013).

[5] Hosono M et al. "Introduction of the targeted alpha therapy (with Radium-223) into clinical practice in Japan: learnings and implementation." In: *Annals of nuclear medicine* 33.3 (2019).

[6] ICRP. "ICRP publication 115: Lung cancer risk from radon progeny and statement on radon". In: *Annals of the ICRP* 40.1 (2010).

[7] ICRP. "ICRP publication 66: Human respiratory tract model for radiological protection." In: *Annals of the ICRP* 66.1 (1995).

[8] Knaapen Ad M et al. "DNA damage in lung epithelial cells isolated from rats exposed to quartz: role of surface reactivity and neutrophilic inflammation." In: *Carcinogenesis* 23.7 (2002).

[9] Paquet F et al. "Assessment and interpretation of internal doses: uncertainty and variability." In: *Annals of the ICRP* 45.1 (2016).

[10] Stabin MG and Siegel AJ. "Radiation dose and hazard assessment of potential contamination events during use of ^{223}Ra dichloride in radionuclide therapy." In: *Health physics* 109.3 (2015).

[11] Montse M, Sanchez G, and Lopez MA. "Internal dosimetry tool for the implementation and use of new ICRP/OIR models: a caesium study." In: *Radiation protection dosimetry* 188.4 (2020).

[12]   ICRP. "ICRP publication 100: Human alimentary tract model." In: *Annals of the ICRP* 36.1-2 (2006).

[13]   Evans RD. "The atomic nucleus." In: *McGraw-Hill New York* 582.992 (1955).

[14]   Sech LC and Ngo C. "Physique nucléaire. Des quarks aux applications." In: *DUNOD* (2010).

[15]   Takigawa N and Washiyama K. "Fundamentals of nuclear physics." In: *Springer* (2017).

[16]   Ekström SYF and Firestone LP. "WWW Table of Radioactive Isotopes. database version 2-28-1999." In: *http://nucleardata.nuclear.lu.se/nucleardata/toi/* (1999).

[17]   UNSCEAR Annex B. "Exposures of the public and workers from various sources of radiation." In: *Sources and effects of ionizing radiation* (2010).

[18]   ICRP. "ICRP publication 133: The ICRP computational framework for internal dose assessment for reference adults: specific absorbed fractions". In: *Annals of the ICRP* 45.2 (2016).

[19]   Marsh JW and Bailey MR. "A review of lung-to-blood absorption rates for radon progeny." In: *Radiation protection dosimetry* 157.4 (2013).

[20]   James AC, Birchall A, and Akabani G. "Comparative dosimetry of BEIR VI revisited." In: *Radiat. Prot. Dosim.* 108 (2004).

[21]   Bi L et al. "Age and Sex Dependent Inhalation Doses to Members of the Public from Indoor Thoron Progeny." In: *Journal of Radiological Protection* 30.639-658 (2010).

[22]   Ishikawa T, Tokonami S, and Nemeth C. "Comparative dosimetry of BEIR VI revisited." In: *J. Radiol. Prot.* 27 (2007).

[23]   Kendall GM and Phipps AW. "Effective and organ doses from thoron decay products at different ages." In: *J. Radiol. Prot.* 27 (2007).

[24]   Li WB et al. "Lung Dosimetry of Inhaled Thoron Decay Products." In: *12th international congress of IRPA. Buenos Aires.* (2008).

[25]   Bateman. H. "Solution of a System of Differential Equations Occurring in the Theory of Radioactive Transformations, Proceedings." In: *Cambridge Philosophical Society* 15 (1910).

[26]   Metivier H. "Radiation protection and nuclear engineering; Radioprotection et ingenierie nucléaire." In: *EDP sciences* (2006).

[27] http://electrons.wikidot.com/Photoelectric effect. "Electronic properties of materials". In: (2020).

[28] http://electrons.wikidot.com/Compton scattering. "Electronic properties of materials". In: (2020).

[29] http://electrons.wikidot.com/Pair production and annihilation. "Electronic properties of materials". In: (2020).

[30] ICRP. "ICRP publication 103: The 2007 recommendations of the international commission on radiological protection." In: *Annals of the ICRP* 37.2.4 (2008).

[31] ICRP. "Limits of Intakes of Radionuclides by Workers". In: *Annals of the ICRP* 2.3/4 (1979).

[32] ICRP. "ICRP publication 130: Occupational intakes of radionuclides: Part 1". In: *Annals of the ICRP* 44.2 (2015).

[33] NCRP. "Development of a biokinetic model for radionuclide-contaminated wounds and procedures for their assessment, dosimetry and treatment." In: *NCRP Report* 156 (2006).

[34] International Commission on Radiation Units and Measurements. "Quantities and Units in Radiation Protection Dosimetry. ICRU Report 51." In: *J. ICRU* os26.2 (1993).

[35] ICRP. "ICRP publication 26: the recommendations on radiological protection." In: *Journal of Radiation Protection and Research* 8.1 (1983).

[36] Wei BL. "Internal Dosimetry-A Review of Progress." In: *Jpn. J. Health Phys* 53.2 (2018).

[37] Barrett PHR et al. "SAAM II: simulation, analysis and modeling software for tracer and pharmacokinetic studies. Metabolism,." In: 47 (1998).

[38] KF Eckerman et al. "User?s guide to the DCAL system." In: *ORNL/TM-2001 Oak Ridge National Laboratory, Oak Ridge, TN.* 190 (2008).

[39] Birchall A et al. "IMBAEXPERTTM: Internal dosimetry made simple." In: *Radiat. Prot. Dosim.* 105 (2003).

[40] ICRP. "ICRP publication 72: Age-dependent Doses to Members of the Public from Intake of Radionuclides: Part 5 compilation of ingestion and inhalation dose coefficients." In: *Annals of ICRP* 26.1 (1996).

[41] Sanchez G and Jesus L-F. "Mathematical techniques for solving analytically large compartmental systems." In: *Health Physics* 85.2 (2003).

[42]   Sanchez G. "Biokmod: A mathematica toolbox for modelling biokinetic systems." In: *Math Educ Res* 10.184 (2005).

[43]   Inc. Wolfram Research. "Mathematica. Version 10.3". In: *Champaign Illinois Wolfram Research Inc* (2015).

[44]   ICRP. "ICRP publication 107: Nuclear decay data for dosimetric calculations." In: *Annals of the ICRP* 38.3 (2008).

[45]   Eckerman KF and Endo A. "Use guide to the ICRP CD and the DECDATA software". In: *Annals of the ICRP* 38.3 (2008).

[46]   ICRP. "ICRP Publication 110: Adult Reference computational phantoms". In: *Annals of the ICRP* 39.2 (2009).

[47]   ICRP. "ICRP Publication 145: Adult Mesh-Type Reference computational phantoms". In: *Annals of the ICRP* 49.3 (2020).